

GAE/AE/76D-4

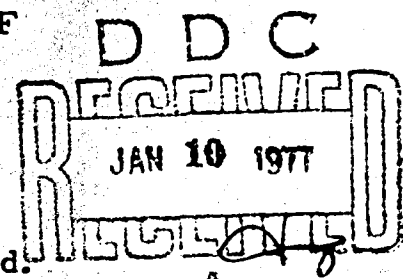
ADA 034271

PERFORMANCE AND EVALUATION OF AN  
X HOT WIRE SENSOR IN A TWO  
DIMENSIONAL FREE JET IN THE  
PRESENCE OF CROSS FLOW COMPONENT

THESIS

GAE/AE/76D-4v

Fazal B. Kauser  
Flt Lt PAF



Approved for public release; distribution unlimited.

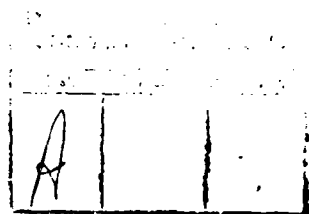
PERFORMANCE AND EVALUATION OF AN X  
HOT WIRE SENSOR IN A TWO DIMENSIONAL  
FREE JET IN THE PRESENCE OF  
CROSS FLOW COMPONENT

THESIS

Presented to the Faculty of the School of Engineering  
of the Air Force Institute of Technology  
Air University  
in Partial Fulfillment of the  
Requirements for the Degree of  
Master of Science

by

Fazal B. Kauser  
Flight Lieutenant, PAF  
Graduate Aeronautical Engineering  
December 1976



Approved for public release; distribution unlimited.

## Preface

The X hot wire probe is commonly used in anemometry for determining the mean flow direction of a generalized flow field. The problem frequently faced by the experimenters is the accurate alignment of the X sensor relative to the mean flow direction which is normally not known. In this report, I have investigated the performance of two typical cross wire arrangements--one having the sensor "X" lying normal to the probe plane and the other having "X" lying in the probe plane. The two dimensional free jet facility existing in the Aero-Mechanical Engineering Department of the Air Force Institute of Technology (AFIT) was used to conduct this study. A Thermo Systems, Inc. constant temperature Anemometer system and the related accessories were used as the primary instrumentation.

I have attempted to make the report as comprehensive as possible so that it could be useful, I hope, for further research in this area. All the calibration data is tabulated in the appendix and typical example calculations are outlined wherever necessary.

I am grateful to my thesis advisors, Dr. Harold E. Wright, Dr. William C. Elrod and Dr. Andrew J. Shine for providing me the opportunity to work on the anemometer and for invaluable guidance, support and encouragement throughout the course of study.

Mr. William Baker and Mr. John Flahive were very helpful in setting up the laboratory equipment and I am thankful for their valuable assistance.

I am also grateful to Mrs. Joyce Clark for her moral support and for the typing of this thesis.

Fazal B. Kauser

## Contents

	<b>Page</b>
Preface . . . . .	ii
List of Figures . . . . .	vii
List of Tables . . . . .	xiii
List of Symbols . . . . .	xvii
Abstract . . . . .	xx
I. Introduction . . . . .	1
Background . . . . .	1
Objectives . . . . .	4
II. Theoretical Considerations . . . . .	6
Sensor Response Equation . . . . .	8
Determining Mean Velocity Components with X-Sensor . . . . .	10
Determination of Fluctuating Velocity Components . . . . .	11
Effect of Fluid Temperature Variations . . . . .	13
III. Test Apparatus . . . . .	15
Free Jet Facility . . . . .	15
Cathodometer . . . . .	15
Sensors . . . . .	18
Instrumentation . . . . .	19
Calibrator . . . . .	19
Signal Processing by Anemometer . . . . .	19
Correlator . . . . .	25
Oscilloscope . . . . .	25
Voltmeters . . . . .	25
Manometer . . . . .	26
Thermocouple . . . . .	26
DC Power Supply . . . . .	26
Variac . . . . .	26

## Contents

	<b>Page</b>
IV. Data Reduction . . . . .	27
CDC 6600 Computer . . . . .	27
V. Experimental Procedures . . . . .	28
Control of Test Conditions . . . . .	28
Calibration . . . . .	28
Single Sensor . . . . .	28
X Wire Sensor . . . . .	29
Optimizing Frequency Response . . . . .	31
Linearization . . . . .	31
Experimental Measurements . . . . .	34
Experimental Arrangement . . . . .	34
Flow Direction Measurements . . . . .	36
Measurements in Potential Core . . . . .	36
Measurements in Shear Flow Region . . . . .	39
Measurement of the Influence of Fluid Temperature Variations on the Linearized System . . . . .	39
VI. Discussion of Results . . . . .	41
Measurements in the Potential Core with the X Sensor Model 1240 . . . . .	41
Rotation in Yaw . . . . .	41
Rotation Tests in Pitch . . . . .	58
Rotation Tests With the X Sensor Model 1241 . . . . .	62
Influence of the Air Temperature Variations on the Linearized Response . . . . .	74
Secondary Tests . . . . .	77
Rotation Tests in Shear Flow Region . . . . .	82
Rotation Tests in Pitch . . . . .	90
VII. Conclusions and Recommendations . . . . .	91
Conclusions . . . . .	91
Recommendations . . . . .	94
Bibliography . . . . .	96

## Contents

	Page
Appendix A: Experimental Data of Rotation Tests . . . . .	99
Appendix B: Influence of Air Temperature Variations on Linearized Sensor Response. . . . .	121
Appendix C: Calibration--Set Up . . . . .	124
Appendix D: Computer Programs . . . . .	183
Vita . . . . .	187

List of Figures

<u>Figure</u>		<u>Page</u>
1	Orientation of the X Sensor Model 1240 Relative to the Mean Flow Direction . . . . .	2
2	Determination of Velocity Components . . . . .	10
3	Flow Field Schematic . . . . .	16
4	Sensor Attachment on Cathodometer . . . . .	17
5a	Sensor Configuration . . . . .	20
5b	Sensor Configuration . . . . .	20
5c	Sensor Configuration . . . . .	21
5d	Sensor Configuration . . . . .	21
6a	TSI Model 1125 Calibrator . . . . .	22
6b	TSI Model 1125 Calibrator Flow Diagram . . . .	22
7	TSI Model 1050 Dual Constant Temperature Hot Wire Anemometer with Linearizer . . . . .	23
8	TSI Model 1015C Correlator . . . . .	23
9	Block Diagram Showing Signal Processing . . . .	24
10	Square Wave Test Signal on a 3.8 Micron Tungsten Hot Wire. . . . .	32
11	Fourth Order Least Square Polynomial Curve Fit for Evaluation of Linearized Coefficients . . . .	33
12a	Definition of Yaw Angle . . . . .	35
12b	Definition of Pitch Angle . . . . .	35

List of Figures

<u>Figure</u>		<u>Page</u>
13	Pitch Movement of the Sensor . . . . .	36
14	Error in $\bar{u}$ Due to Misalignment in Yaw (Re. No. = 7.2) . . . . .	43
15	Error in Mean Velocity Component $\bar{u}$ Due to Misalignment in Yaw (Re. No. = 14.54) . . . . .	44
16	Error in $\bar{u}$ Due to Misalignment in Yaw (Re. No. = 21.8) . . . . .	45
17	Error in $\bar{v}$ Due to Misalignment in Yaw (Re. No. = 7.2) . . . . .	46
18	Error in $\bar{v}$ Due to Misalignment in Yaw (Re. No. = 14.54) . . . . .	47
19	Error in $\bar{v}$ Due to Misalignment in Yaw (Re. No. = 21.8) . . . . .	48
20	Comparison of Yaw Response Curves (Re. No. = 7.2) . . . . .	51
21	Comparison of Yaw Response Curves (Re. No. = 14.54) . . . . .	52
22	Comparison of Yaw Response Curves (Re. No. = 21.8) . . . . .	53
23	Error in Mean Flow Direction Due to Misalignment in Yaw (Re. No. = 7.2) . . . . .	54
24	Error in Mean Flow Direction Due to Misalignment in Yaw (Re. No. = 14.54) . . . . .	55
25	Error in Mean Flow Direction Due to Misalignment in Yaw (Re. No. = 21.8) . . . . .	56
26	Error in Mean Flow Direction Due to Misalignment in Pitch (Re. No. = 7.2) . . . . .	59
27	Error in Mean Flow Direction Due to Misalignment in Pitch (Re. No. = 14.54) . . . . .	60

List of Figures

<u>Figure</u>		<u>Page</u>
28	Error in Mean Flow Direction Due to Misalignment in Pitch (Re. No. = 21.8) . . . . .	61
29	Error in $\bar{u}$ Due to Misalignment in Yaw (Re. No. = 7.2) . . . . .	63
30	Error in $\bar{u}$ Due to Misalignment in Yaw (Re. No. = 14.54) . . . . .	64
31	Error in $\bar{u}$ Due to Misalignment in Yaw (Re. No. = 21.8) . . . . .	65
32	Error in $\bar{w}$ Due to Misalignment in Yaw (Re. No. = 7.2) . . . . .	66
33	Error in $\bar{w}$ Due to Misalignment in Yaw (Re. No. = 14.54) . . . . .	67
34	Error in $\bar{w}$ Due to Misalignment in Yaw (Re. No. = 21.8) . . . . .	68
35	Error in Mean Flow Direction Due to Misalignment in Yaw (Re. No. = 7.2) . . . . .	70
36	Error in Mean Flow Direction Due to Misalignment in Yaw (Re. No. = 14.54) . . . . .	71
37	Error in Mean Flow Direction Due to Misalignment in Yaw (Re. No. = 21.8) . . . . .	72
38	Influence of Fluid Temperature Variations on Linearized Constant Temperature Anemometer System . . . . .	75
39	Comparison of Linearized Bridge Output With and Without Cosine Law Cooling Assumption . . . . .	78
40	Linearized Response Curve at Different Overheat Ratios . . . . .	80
41	Error in Mean Flow Direction Due to Misalignment in Yaw (Re. No. = 7.2) . . . . .	83

List of Figures

<u>Figure</u>		<u>Page</u>
42	Error in Mean Flow Direction Due to Misalignment in Yaw (Re. No. = 14.54) . . . . .	84
43	Error in Mean Flow Direction Due to Misalignment in Yaw (Re. No. = 21.8) . . . . .	85
44	Error in Mean Flow Direction Due to Misalignment in Pitch (Re. No. = 7.2) . . . . .	86
45	Error in the Mean Flow Direction Due to Misalign- ment in Pitch (Re. No. = 14.54) . . . . .	87
46	Error in the Mean Flow Direction Due to Misalign- ment in Pitch (Re. No. = 21.8) . . . . .	88
47	Non Linear Bridge Output Variations With Velocity .	157
48	Fourth Order Least Square Polynomial Curve Fit for Evaluation of Linearizer Coefficients. . . . .	158
49	Linearized Bridge Voltage Output for 0.00015 Inch (0.000381 cm) Dia. Hot Wire Sensor in Atmospheric Air. . . . .	159
50	Influence of Overheat Ratio on Non-Linear Sensor Response . . . . .	160
51	Non Linear Bridge Output Variations With Velocity .	161
52	Fourth Order Least Square Polynomial Curve Fit for Evaluation of Linearizer Coefficients. . . . .	162
53	Fourth Order Least Square Polynomial Curve Fit for Evaluation of Linearized Coefficients. . . . .	163
55	Linearized Bridge Output for 0.00015 Inch (0.000381 cm) Dia. Hot Wire Sensor in Atmospheric Air. . . . .	164
56	Linearized Bridge Output for 0.00015 Inch (0.000381 cm) Dia. Hot Wire Sensor in Atmospheric Air. . . . .	165

List of Figures

<u>Figure</u>		<u>Page</u>
57	Linearized Bridge Output for 0.00015 Inch Dia. (0.000381 cm) Hot Wire Sensor in Atmospheric Air . . . . .	166
58	Non Linear Bridge Output Variations With Velocity . . . . .	167
59	Fourth Order Least Square Polynomial Curve Fit for Evaluation of Linearizer Coefficients . . . . .	168
60	Linearized Bridge Output for 0.00015 Inch Dia. (0.000381 cm) Hot Wire Sensor in Atmospheric Air . . . . .	169
61	Non Linear Bridge Output Variations With Velocity . . . . .	170
62	Fourth Order Least Square Curve Fit for Evalu- ation of Linearizer Coefficients . . . . .	171
63	Linearized Bridge Output for 0.00015 Inch Dia. (0.000381 cm) Hot Wire Sensor in Atmospheric Air . . . . .	172
64	Non Linear Bridge Output Variations With Velocity . . . . .	173
65	Fourth Order Least Square Polynomial Curve Fit for Evaluation of Linearizer Coefficients . . . . .	174
66	Linearized Bridge Output for 0.00015 Inch Dia. (0.000381 cm) Hot Wire Sensor in Atmospheric Air . . . . .	175
67	Fourth Order Least Square Polynomial Curve Fit for Evaluation of Linearizer Coefficients . . . . .	176
68	Fourth Order Least Square Polynomial Curve Fit for Evaluation of Linearizer Coefficients . . . . .	177
69	Linearized Bridge Output for 0.00015 Inch Dia. (0.000381 cm) Hot Wire Sensor in Atmospheric Air . . . . .	178

List of Figures

<u>Figure</u>		<u>Page</u>
70	Non Linear Bridge Output Variations With Velocity . . . . .	179
71	Fourth Order Least Square Polynomial Curve Fit for Evaluation of Linearizer Coefficients . . . . .	180
72	Linearized Bridge Output for 0.00015 Inch (0.000381 cm) Dia. Hot Wire Sensor in Atmospheric Air . . . . .	181
73	The Cross Wire Arrangement of Model 1240 Sensor Viewed Under Microscope (Magnification 50:1) . . . . .	182

List of Tables

<u>Table</u>		<u>Page</u>
I	Rotation in Yaw (Potential Core) (Reference Orientation 48 deg) Error in $\bar{u}$ and $\bar{v}$ . . . . .	42
II	Rotation in Yaw (Potential Core) (Reference Orientation 48 deg) Error in Mean Flow Direction . . . . .	57
III	Rotation in Pitch (Potential Core) (Reference Orientation 48 deg) Error in Mean Flow Direction . . . . .	62
IVa	Rotation in Yaw (Potential Core) (Reference Orientation 48 deg) Error in $\bar{u}$ and $\bar{w}$ . . . . .	69
IVb	Rotation in Yaw (Potential Core) (Reference Orientation 48 deg) Error in Mean Flow Direction . . . . .	73
V	Influence of Fluid Temperature Variations on Linearized Response . . . . .	76
VI	Value of King's Law Exponent n . . . . .	81
VII	Rotation in Yaw (Shear Flow Region) (Reference Orientation 48 deg) Error in Mean Flow Direction . . . . .	89
VIII	Rotation in Yaw (Potential Core, Ref. Orientation 48 Deg. Re = 7.2) . . . . .	100
IX	Rotation in Yaw (Potential Core, Ref. Orientation 48 Deg. Re = 7.2) . . . . .	101
X	Rotation in Yaw (Potential Core, Ref. Orientation 48 Deg. Re = 14.54) . . . . .	102
XI	Rotation in Yaw (Potential Core, Ref. Orientation 48 Deg. Re = 14.54) . . . . .	103

List of Tables

<u>Table</u>		<u>Page</u>
XII	Rotation in Yaw (Potential Core, Ref. Orientation 48 Deg. Re = 21.8 . . . . .	104
XIII	Rotation in Yaw (Potential Core, Ref. Orientation 48 Deg. Re = 21.8 . . . . .	105
XIV	Rotation in Yaw (Potential Core, Ref. Orientation 135 Deg. Re = 7.2 . . . . .	106
XV	Rotation in Yaw (Potential Core, Ref. Orientation 135 Deg. Re = 7.2). . . . .	107
XVI	Rotation in Yaw (Potential Core, Ref. Orientation 135 Deg. Re = -14.54). . . . .	108
XVII	Rotation in Yaw (Potential Core, Ref. Orientation 135 Deg. Re = 14.54) . . . . .	109
XVIII	Rotation in Yaw (Potential Core, Ref. Orientation 135 Deg. Re = 21.8) . . . . .	110
XIX	Rotation in Yaw (Potential Core, Ref. Orientation 135 Deg. Re = 21.8) . . . . .	111
XX	Rotation in Pitch (Potential Core, Re = 7.2) . . .	112
XXI	Rotation in Pitch (Potential Core, Re = 14.54) . .	113
XXII	Rotation in Pitch (Potential Core, Re = 21.8) . .	114
XXIII	Rotation in Yaw (Model 1241, Potential Core, Re = 7.2). . . . .	115
XXIV	Rotation in Yaw (Model 1241, Potential Core, Re = 14.54). . . . .	116
XXV	Rotation in Yaw (Model 1241, Potential Core, Re = 21.8) . . . . .	117
XXVI	Rotation in Pitch (Model 1241, Potential Core, Re = 7.2). . . . .	118

List of Tables

<u>Table</u>		<u>Page</u>
XXVII	Rotation in Pitch (Model 1241, Potential Core, $Re = 14.54$ ) . . . . .	119
XXVIII	Rotation in Pitch (Model 1241, Potential Core, $Re = 21.8$ ) . . . . .	120
XXIX	Variation in Fluid Temperature . . . . .	123
XXX	Calibration Curve Set Up Table, T1.5 Model 1214 .	126
XXXI	Calibration Curve Set Up Table, (T1.5 Model 1210, Overheat Ratio = 1.2) . . . . .	128
XXXII	Calibration Curve Set Up Table, (T1.5 Model 1210, Overheat Ratio = 1.5) . . . . .	130
XXXIII	Calibration Curve Set Up Table, (T1.5 Model 1210, Overheat Ratio = 1.8) . . . . .	132
XXXIV	Calibration Curve Set Up Table, (T1.5 Model 1240, Sensor No. 1, Normal) . . . . .	134
XXXV	Calibration Curve Set Up Table, (T1.5 Model 1240, Sensor No. 1, 45 Deg. Orientation) . . . . .	136
XXXVI	Calibration Curve Set Up Table (T1.5 Model 1240, No. 2, Normal) . . . . .	138
XXXVII	Calibration Curve Set Up Table (T1.5 Model 1240, No. 2, 45 Deg. Orientation) . . . . .	140
XXXVIII	Rotation in Yaw (Shear Layer, Model 1240, $Re = 7.2$ ) . . . . .	142
XXXIX	Rotation in Yaw (Shear Layer, Model 1240, $Re = 7.2$ ) . . . . .	143
XL	Rotation in Yaw (Shear Layer, Model 1240, $Re = 14.54$ ) . . . . .	144
XLI	Rotation in Yaw (Shear Layer, Model 1240, $Re = 14.54$ ) . . . . .	145

List of Tables

<u>Table</u>		<u>Page</u>
XLII	Rotation in Yaw (Shear Layer, Model 1240, Re = 21.8) . . . . .	146
XLIII	Rotation in Yaw (Shear Layer, Model 1240, Re = 21.8) . . . . .	147
XLIV	Rotation in Pitch (Shear Layer, Model 1240, Re = 7.2) . . . . .	148
XLV	Rotation in Pitch (Shear Layer, Model 1240, Re = 14.54) . . . . .	149
XLVI	Rotation in Pitch (Shear Layer, Model 1240, Re = 21.8) . . . . .	150
XLVII	Rotation in Yaw (Shear Layer, Model 1240, Ref. Orientation 135 Deg., Re = 7.2). . . . .	151
XLVIII	Rotation in Yaw (Shear Layer, Model 1240, Ref. Orientation 135 Deg., Re = 7.2). . . . .	152
XLIX	Rotation in Yaw (Shear Layer, Model 1240, Ref. Orientation 135 Deg., Re = 14.54) . . . . .	153
L	Rotation in Yaw (Shear Layer, Model 1240, Ref. Orientation 135 Deg., Re = 14.54) . . . . .	154
LI	Rotation in Yaw (Shear Layer, Model 1240, Ref. Orientation 135 Deg., Re = 21.8) . . . . .	155
LII	Rotation in Yaw (Shear Layer, Model 1240, Ref. Orientation 135 Deg., Re = 21.8) . . . . .	156

List of Symbols

<u>Symbol</u>	<u>Description</u>	<u>Units</u>
$A_e$	Nozzle exit area	cm <sup>2</sup>
$C_p$	Specific heat at constant pressure	BTU/ lbm°R
$C_1, C_2$	Constants in King's Law	--
$E$	Non-linear bridge voltage	volt
$E_L$	Linearized bridge voltage	volt
$E_{Corr}$	Corrected, non-linear, DC voltage	volt
$E_M$	Non-linear DC bridge voltage during measurements	volt
$E_{TC}$	Temperature corrected non-linear bridge voltage	volt
$E_{ZC}$	Zero corrected non-linear bridge voltage ( $E - E_0$ )	volt
$H_R$	Heat loss due to radiation	watt
$H_C$	Heat loss due to conduction	watt
$H_{FC}$	Heat loss due to forced convection	watt
$H_{NC}$	Heat loss due to natural convection	watt
$\Delta h$	Pressure difference	ins of water
$K$	1/slope of linearized curve	ft/sec/ volt
$k$	Ratio of specific heats	--
$M_e$	Mach number at nozzle exit	--

<u>Symbol</u>	<u>Description</u>	<u>Units</u>
n	King's Law exponent	--
$P_T$	Chamber stagnation pressure	$\text{lb}_f/\text{ft}^2$
$P_a$	Ambient pressure	$\text{lb}_f/\text{ft}^2$
$\bar{q}$	Resultant mean velocity	$\text{ft/sec}$
$R_W$	Sensor operating resistance	ohms
$R_e$	Reynold's number	--
$R_M$	Cold wire resistance during test	ohms
$R_C$	Cold wire resistance during calibration	ohms
R	Gas constant	$\text{ft lb}_f/\text{lbm}^\circ\text{R}$
$T_a$	Ambient temperature	$^\circ\text{R}$
$T_T$	Chamber stagnation temperature	$^\circ\text{R}$
$\bar{u}, \bar{U}$	Mean velocity component in S direction	$\text{ft/sec}$
$u', v', w'$	Fluctuating velocity components in X, Y and Z direction	$\text{ft/sec}$
$\bar{v}, \bar{V}$	Mean velocity component in Y direction	$\text{ft/sec}$
$\bar{w}, \bar{W}$	Mean velocity component in Z direction	$\text{ft/sec}$
$\Delta x, \Delta y, \Delta z$	Distances	inch or centimeter
$\alpha$	Mean flow direction angle	degree
$\beta$	Angle	degree
$\theta$	Pitch angle	degree
$\theta$	Overheat ratio $\frac{T_w}{T_{a1}}$	--
$\phi$	Yaw angle	degree

<u>Symbol</u>	<u>Description</u>	<u>Units</u>
$\epsilon$	$\frac{T_{a1} - T_{a2}}{T_{a1}}$	--
$\sigma$	$\theta - 1$	--
$\alpha_R$	Temperature coefficient of resistance	/°F

Abstract

This thesis reports the results of an experimental investigation of rotation tests conducted with two X wire sensor arrangements in the potential core of a free jet and the influence of small temperature variations on the linearized response of a hot wire sensor.

The tests were performed in the free jet issuing from a 10 cm x 1 cm nozzle having turbulence intensity of 0.3 per cent at the exit plane. The two X wire sensors used were TSI Model 1240 and TSI Model 1241. Each sensor arrangement consisted of two platinum coated, tungsten wires, having 3.81 micron diameter, active sensor length 1.25 millimeter and separated by 1 millimeter apart. The X sensor Model 1240 was yawed and pitched through  $\pm$  30 degrees and  $\pm$  10 degrees respectively. The size of the potential core, however, limited the movement in yaw and pitch of the Model 1241 to  $\pm$  10 degrees. The tests were conducted at three values of Reynolds Number 7.2, 14.54 and 21.8 based upon the wire diameter.

The investigation showed that both the X sensors had a strong preference for the direction of mean motion, and the error due to misalignment in yaw was largest at very small misalignment angles. The Model 1240 showed insensitivity to misalignment in pitch in the upper range of Reynolds Number but the Model 1241 was highly sensitive to the misalignment in pitch. In the second part of the

study, the air temperature was increased from 4°F to 20°F above the reference and its influence on the linearized response of the upstream sensor of Model 1240 was observed. The test results showed a strong influence of the variations in air temperature on the linearized sensor response at velocities below approximately 100 feet per second.

PERFORMANCE AND EVALUATION OF AN X  
HOT WIRE SENSOR IN A TWO DIMENSIONAL  
FREE JET IN THE PRESENCE OF  
CROSS FLOW COMPONENT

I. Introduction

Background

In many fluid flow problems of practical interest, for example, flow existing over the wing surface of an airplane, in the air intake of an air breathing engine, or in the test section of a subsonic wind tunnel, one is often required to measure the mean flow direction using an X hot wire sensor. Normally, the X hot wire sensor is aligned such that each sensor is at 45 degrees relative to the mean flow direction (Fig. 1). This particular orientation offers maximum sensitivity to the changes in the flow direction, interference caused by the prongs of one sensor over the sensitive part of the other sensor in a minimum and the sensor response equation is somewhat simplified. The X hot wire sensor, however, cannot be aligned as such when the mean flow direction is not known. It is, therefore, desirable to determine the magnitude of error incurred due to misalignment of the X hot wire sensor in a generalized fluid flow field.

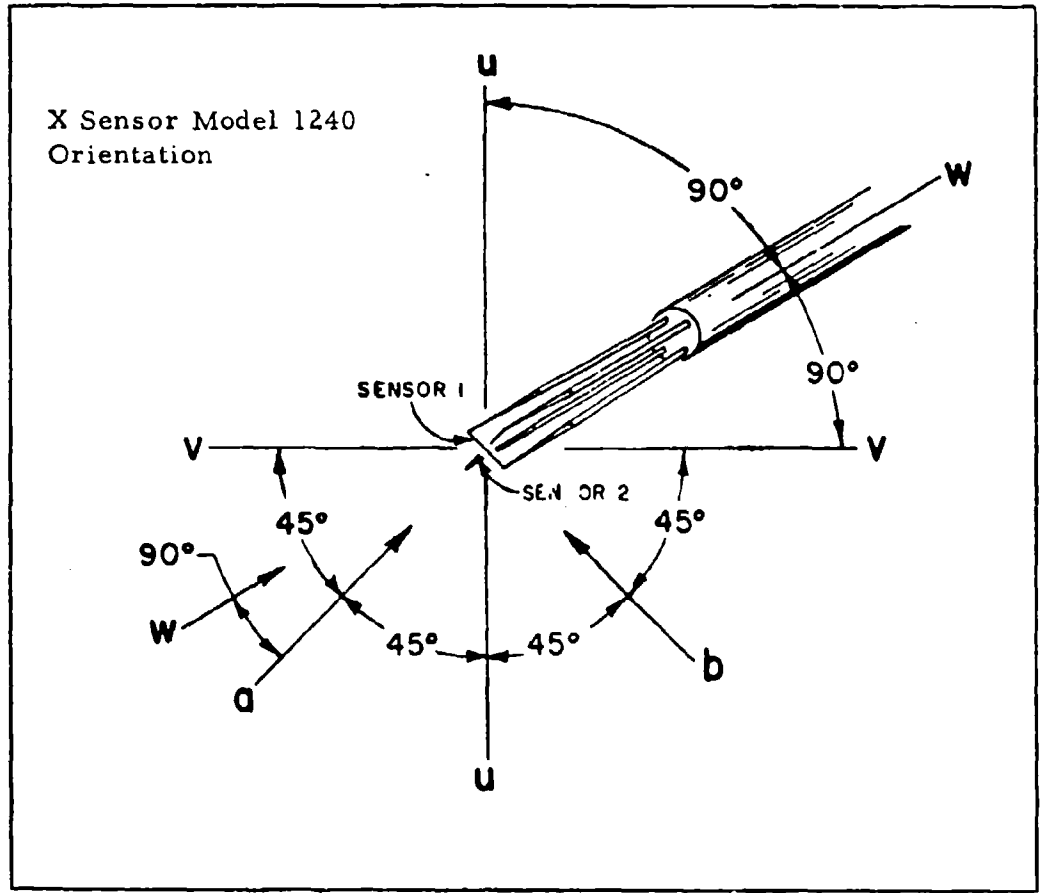


Fig. 1. Orientation of the X Sensor Model 1240 Relative to the Mean Flow Direction. Both Sensors Are Calibrated with the Flow from Either the "U" or "V" Direction (i.e.  $45^\circ$  to the Stream)

Another problem closely associated with the mean flow direction measurements using a constant temperature hot wire anemometer is directly related to the convective cooling effect of the flow passing over the wire and is dependent upon the temperature difference between the wire and the flow. The constant temperature anemometer, as its name implies, is designed to maintain the temperature of the sensing element constant under varying fluid temperature. Mere observation of the voltage output does not tell us whether the change in the output has been caused by a change in the flow velocity or change in the fluid temperature. A typical example of this problem is the changes in the air temperature of a closed circuit wind tunnel where the air temperature rises slowly due to viscous action.

Similarly, when one is dealing with the study of free flows such as jets, wakes and mixing zones, the fluid temperature may vary appreciably from the value at which calibration was performed or it may change during experiment due to drift in the ambient conditions. In any event, it is necessary to apply correction to the measured data particularly when the variations in the fluid temperature are appreciable.

This thesis is an experimental investigation of:

1. The error involved in the measurement of mean flow direction due to misalignment of the X hot wire sensor.
2. The error involved in the linearized response of a constant temperature hot wire anemometer system due to small variations in

fluid temperature.

The tests were conducted in the potential core of a two dimensional free jet resulting in a cross flow component.

### Objectives

The primary objectives were:

1. Using a two dimensional free jet of known direction, evaluate the error incurred in the mean flow direction as the X sensor was yawed and pitched inside the potential core of the free jet. Yawing is defined as the movement of the instantaneous velocity vector in the plane of X called the probe plane. Pitching, on the other hand, represents the movements of the instantaneous velocity vector out of the probe plane. The error was to be evaluated at three values of Reynolds numbers based upon the sensor diameter, namely 7.2, 14.54 and 21.7.

2. To evaluate the error involved in the linearized voltage output of the X sensor as the fluid temperature was changed by 20°F.

Secondary objectives were:

1. To evaluate the value of King's Law exponent n and compare with the published literature.

2. To repeat the primary objective item number 1 in the shear flow region downstream of the free jet.

The organization of this report is as follows: Section II covers the theoretical background including the sensor response equation,

measurements of the mean and fluctuating velocity components using X hot wire sensor, and a review of the existing methods available for applying correction to the sensor response to account for the variations in fluid temperature. Section III describes the test apparatus, instrumentation and types of the sensors employed for the present research. Section IV deals with the data reduction techniques adopted. Section V contains an explanation of the techniques adopted for calibrating the sensors, optimization of the anemometer system for maximum frequency response, linearizing the voltage velocity relationship of the sensor and the measurement techniques. Section VI includes the discussion of the results. Conclusions and recommendations are contained in Section VII.

## II. Theoretical Considerations

Measurements of the mean flow direction using an X hot wire sensor is complicated by many factors. Some of these are deviation of the sensor response from a simple cosine law (Ref 4, 8, 11, 12), thermal wake interference (Ref 13), probe interference effects (Ref 9), the presence of a velocity component in the direction perpendicular to the plane of X and mean flow direction, spatial resolution limitations and slip flow effects (Ref 12, 24). The problem would not lend itself to simple experimental investigation unless certain simplifying assumptions are made. In the present study, following fundamental assumptions were made:

1. The flow was assumed to be incompressible. This assumption gives a maximum error of less than 2% in the dynamic pressure under sea level standard conditions for the range of velocity under consideration (0-300 ft/sec).
2. During the measurements, the air pressure and temperature were assumed to remain constant. This assumption is quite valid in the case of measurements in a free jet exiting to atmosphere.
3. Simple cosine law cooling was assumed to be valid. According to this law, the sensor is sensitive only to the velocity component normal to the sensor and is independent of the tangential velocity components. This would indeed be true up to quite large yaw angles if

the wire was infinite in extent and maintained at a constant temperature throughout its length. Unfortunately, real hot wires must be finite in length, and possess non-uniform temperature distribution due to heat conduction to the supports.

4. The turbulent fluctuations of the flow velocity component acting on the hot wire are small compared to its time average. This requirement is satisfied inside the potential core of a free jet but the results are subject to increasing error with high turbulence intensities (Ref 11).

5. The flow is assumed to be continuum and the slip flow effects are negligible. A condition for the flow to be continuum is that the Knudsen Number should be less than 0.01 (Ref 10). The 3.8 micron diameter hot wire sensor while operating at 70°F and standard atmospheric pressure has Knudsen Number equal to 0.0173 and therefore may operate in slip flow regime. This implies a decrease in the value of heat transfer coefficient  $h$  between the hot wire and the cooling stream of air. The decrease in the value of  $h$  is caused by the "temperature jump" effect arising in consequence of the failure of the molecule to "accommodate" to the surface temperature (Ref 10). The slip flow effects may be observed in the range of Reynolds Number  $7 \leq Re \leq 22$  and give an error in Nusselt Number varying between 6% to 12%, approximately for 3.8 micron diameter, platinum coated tungsten wire (Ref 7) which is quite substantial.

### Sensor Response Equation

The constant temperature hot wire anemometer works on the principle that the rate of heat loss by the sensor is equal to the amount of electrical energy needed to maintain the sensor temperature at constant. In general, heat transfer takes place by all three modes namely conduction, convection and radiation. Writing down the heat balance equation, one has

$$\text{Heat Input} = \frac{E^2}{R_W} = H_R + H_C + H_{FC} + H_{NC} \quad (1)$$

Where E is Bridge voltage output,  $R_W$  is operating resistance of the sensor.  $H_R$  is the heat loss due to radiation. This is generally very small for tungsten or platinum wire operated below 300°C.  $H_C$  is the heat loss by conduction to the wire support needles and usually constitutes about 10% of the total energy loss.  $H_{FC}$  is the heat lost due to forced convection. It is a function of Reynolds Number, Mach Number, Prandtl Number, Knudsen Number, wire temperature, wire geometry, and its orientation relative to the flow. For a hot wire sensor operating in a continuum, low subsonic flow,  $H_{FC}$  can be represented by:

$$H_{FC} = C_1 + C_2 (U_{eff})^n \quad (2)$$

Where  $U_{eff}$  is the effective cooling velocity,  $C_1$ ,  $C_2$ , and  $n$  are constants which are determined experimentally. Noting that equation (2) is similar to well known King's Law for which  $n = \frac{1}{2}$ .

$H_{NC}$  is the heat loss due to natural convection. This heat loss is quite small and negligible for Reynolds Number greater than 0.5 (Ref 11). The heat loss due to conduction to the supports is taken into account in the calibration process. Therefore, overall response equation can be expressed as:

$$E^2 = C_1 + C_2 (U_{eff})^n$$

or

$$E^2 - E_0^2 = C_2 (U_{eff})^n \quad (3)$$

Where  $E_0$  is the bridge voltage output at zero flow.

In order to evaluate the value of exponent  $n$  from the calibration data, assume cosine law to be valid and take natural logarithm of both sides of equation (3),

$$\ln (E^2 - E_0^2) = \ln C_2 + n \ln \bar{V}_p$$

where  $\bar{V}_p$  is the mean velocity component normal to the sensor. The first term on the right hand side can be replaced by another constant  $D$ .

$$\therefore \ln (E^2 - E_0^2) = D + n \ln \bar{V}_p \quad (4)$$

A plot of  $\ln (E^2 - E_0^2)$  versus  $\ln \bar{V}_p$  enables one to calculate the value of exponent  $n$ . Collis and Williams investigations of the heat transfer from heated wires of very large aspect ratio gave values of  $n$  equal to 0.45 for  $0.02 < Re < 44$  and equal to 0.51 for  $44 < Re < 144$  (Ref 3).

More recently, Klatt (Ref 15) carried out calibration of a large number

of commercially available hot wire probes and found value of  $n$  varying between 0.25 and 0.42 corresponding to maximum Reynolds Number of 13. The values of  $n$  determined in the present investigation are tabulated on page 53.

Determining Mean Velocity Components with X-Sensor. The X-hot wire sensor offers a convenient way of determining mean velocity components  $\bar{u}$  and  $\bar{v}$  due to the fact that both of the components can be obtained in a single operation. A further simplification to the analysis is afforded by operating each sensor at 45 degree relative to the mean flow direction which has the added advantage of offering maximum directional sensitivity (Ref 6). For a linearized system, the output is proportional to velocity. Assuming simple cosine law cooling,  $u$  and  $v$  can be expressed in terms of  $V_{P_1}$  and  $V_{P_2}$ .

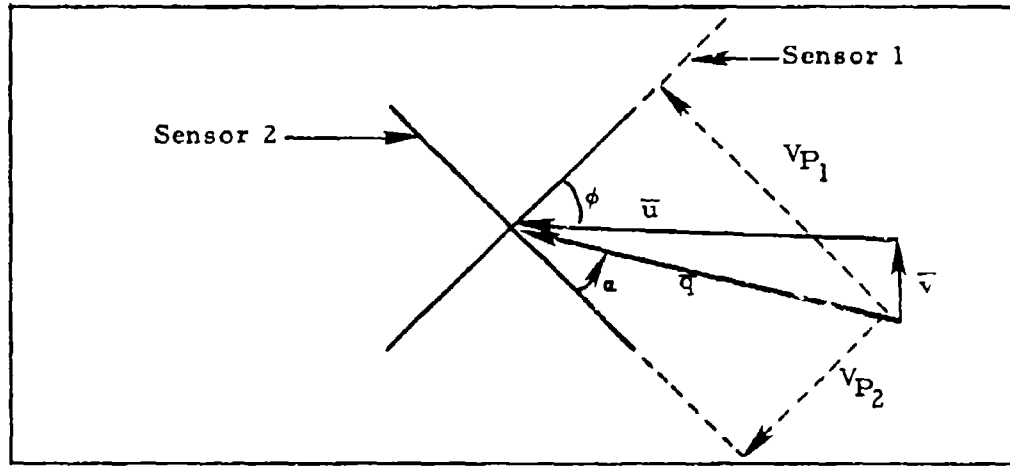


Fig. 2. Determination of Velocity Components

For the case of the flow only within the probe plane,

$$\bar{u} = \bar{q} \cos(\phi - \alpha) = \bar{q} (\cos \phi \cos \alpha + \sin \phi \sin \alpha) \quad (5)$$

$$\bar{v} = \bar{q} \sin(\phi - \alpha) = \bar{q} (\sin \phi \cos \alpha - \cos \phi \sin \alpha) \quad (6)$$

If the sensor is oriented such that yaw angle  $\phi = 45^\circ$ , then  $\cos \phi = \sin \phi = 0.707$ . Also

$$v_{P_1} = \bar{q} \sin(90 - \alpha) = \bar{q} \cos \alpha$$

$$v_{P_2} = \bar{q} \sin \alpha$$

$$\therefore \bar{u} = 0.707 (v_{P_1} + v_{P_2}) \quad (7)$$

$$\bar{v} = 0.707 (v_{P_1} - v_{P_2}) \quad (8)$$

For a linearized system,  $v_{P_1}$  and  $v_{P_2}$  are directly proportional to the voltage output of the two anemometers.

$$\therefore \bar{u} = 0.707 K(E_{L_1} + E_{L_2}) \quad (9)$$

$$\bar{v} = 0.707 K(E_{L_1} - E_{L_2}) \quad (10)$$

Where  $E_{L_1}, E_{L_2}$  are voltage signals from the sensors 1 and 2 respectively, and  $K$  is the constant of proportionality between the voltage and velocity for the linearized anemometer.

Determination of Fluctuating Velocity Components. For the measurements of velocity fluctuation, the wire must exchange heat at the frequency of the velocity fluctuations. A finite time is, however, required for the wire to come in to thermal equilibrium with its surroundings, and hence its resistance to reach a value corresponding to the conditions in the fluid medium. This is due to the thermal inertia of the sensor which, at high frequencies, decreases its sensitivity and

shifts the signal out of phase. A constant temperature hot wire system minimizes the effect of thermal inertia by keeping the sensitive element at a constant temperature and hence resistance and using the heating current as the measure of heat transfer, and, therefore, of the velocity. The linear frequency range of the constant temperature anemometer increases with the mean velocity and within the velocity range  $10 \leq \bar{q} \leq 100$  meter per second, the upper frequency limit  $f_o$  (-3 db) is approximately given by:

$$f_o = (10 + 0.5 \bar{q}) \text{ K C/S} \quad (11)$$

Where  $\bar{q}$  is the mean velocity in meter per second (Ref 19).

Assuming the system possesses satisfactory arrangement for optimizing its frequency response, if the turbulence intensity is less than 10%, equations (9) and (10) would give the fluctuating velocity components provided AC values of the voltages are used instead of DC voltages. For highly turbulent flows, Hinze (Ref 11) has suggested the following correction applicable to isotropic turbulence with velocity components being normally correlated:

$$f(u'_1, u'_2) = -\frac{7}{128} \frac{\bar{u}^2}{\bar{q}^2} \quad (12)$$

This implies the linearized theory would predict too high a value for the turbulence intensity. The errors arise primarily from non-linear character of the instrumentation response to fluctuations in magnitude and direction of the fluid velocity and in the fluid temperature (Ref 20).

If a linearizer is incorporated in the electronic circuit, the curvature of the basic calibration curve can be handled conveniently. However, linearization does not always improve the accuracy of measurements (Ref 21). In fact, for small fluctuations, accuracy can be improved by not linearizing since the elimination of analogue electronics equipment normally removes a source of possible uncertainty in the data.

Effect of Fluid Temperature Variations. In almost all the experiments on velocity measurements using a constant temperature hot wire anemometer, it is very difficult to maintain the fluid temperature constant and equal to the temperature at which the calibration was performed. In some cases, appreciable changes in the fluid temperature may take place even during the experiment as for example, in a closed circuit wind tunnel where slow increase in temperature takes place before reaching an equilibrium state. Bearman (Ref 2) suggested the following corrections.

For the non-linear system,

$$E_{\text{Corr}} = E_M / (1 + \epsilon / 2\sigma)^{1/2} \quad (11)$$

Where  $E_{\text{Corr}}$  and  $E_M$  stand for corrected and measures values of DC voltage output respectively.  $\epsilon$  and  $\sigma$  are functions of overheat ratio ( $\theta$ ) defined as:

$$\epsilon = \frac{T_{a1} - T_{a2}}{T_{a1}}$$

$$\sigma = \theta - 1$$

For the linearized constant temperature system,

$$E_{L_{corr}} \cong E_{L_M} \left(1 - \frac{6T}{T_{a1}} F\right) \quad (12)$$

where  $E_{L_{corr}}$  and  $E_{L_M}$  are corrected and measured values of the linearized DC voltage output respectively.  $F$  is the correction function dependent upon  $n$ ,  $\sigma$  and voltage ratios.  $T_{a1}$ ,  $T_{a2}$  are the original and new values of fluid temperature respectively. Bearman concluded that for a linearized hot wire system, his correction formulae give an accuracy of 1% up to a temperature rise of  $10^{\circ}\text{C}$ . He assumed that the properties of the fluid adjacent to the wire are related to the wire surface temperature. Kanevce and Oka (Ref 14) dealt with the low velocity range (0.1 to 11 m/sec) and recommended the following correction for the non-linear constant temperature hot wire system:

$$E_C^2 = E_M^2 \frac{(R_W - R_C)}{(R_W - R_M)} \quad (13)$$

Where  $R_W$ ,  $R_C$  and  $R_M$  are the hot wire resistances at wire operating temperature, cold wire resistance during calibration and cold wire resistance during measurement respectively.

In the present investigation, only the influence of fluid temperature variation on a linearized hot wire system was determined experimentally. The formulae used as well as the example calculations are given in Appendix B.

### III. Test Apparatus

#### Free Jet Facility

The free jet facility used for conducting experiments consisted of a 10 cm by 1 cm nozzle having a turbulence intensity of approximately 0.3% in the nozzle exit plane. A schematic of the flow field is shown in Fig. 3. The calming chamber had a diameter of 27 cm and was 2.13 meter in length. Flow was first directed over two 7,000 watts electric resistance type heaters which could raise the air temperature by 90°F at exit Mach Number equal to 0.8 (Ref 23). An orifice 10 cm in diameter was placed just downstream of the heaters to induce turbulent mixing. A replaceable paper filter prior to the nozzle entrance was used to prevent foreign particles striking against the sensor and resulting in sensor breakage. The nozzle had an area contraction ratio of 50:1 which was partially responsible for the low turbulence flow in the nozzle exit plane.

#### Cathodometer

A Gaertner Scientific Company three dimensional traversing mechanism (Fig. 4) was used to position the sensor within  $\pm 0.001$  inch of desired position in X, Z directions and within  $\pm 0.001$  centimeter in the Y direction.

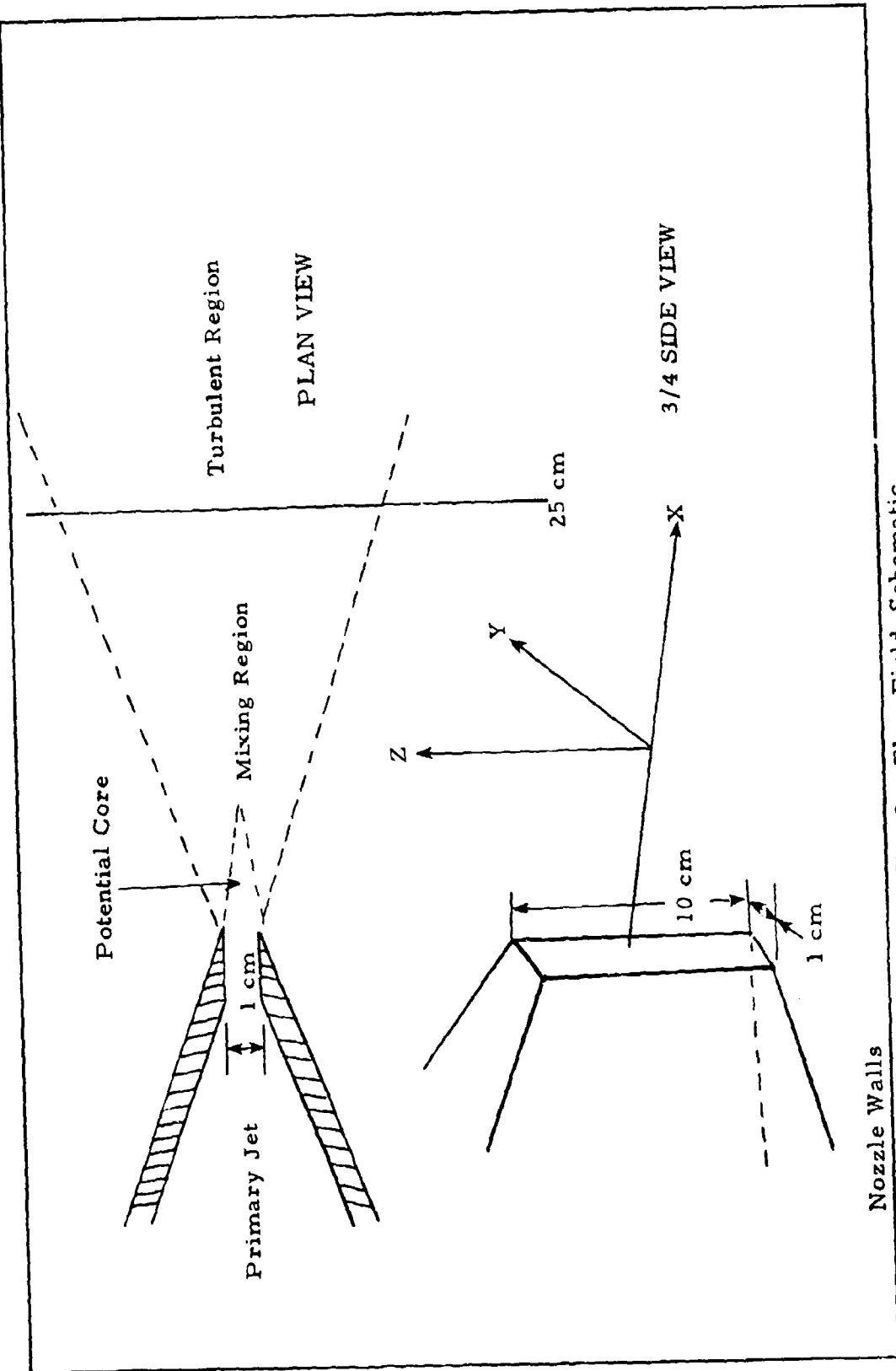


Fig. 3. Flow Field Schematic

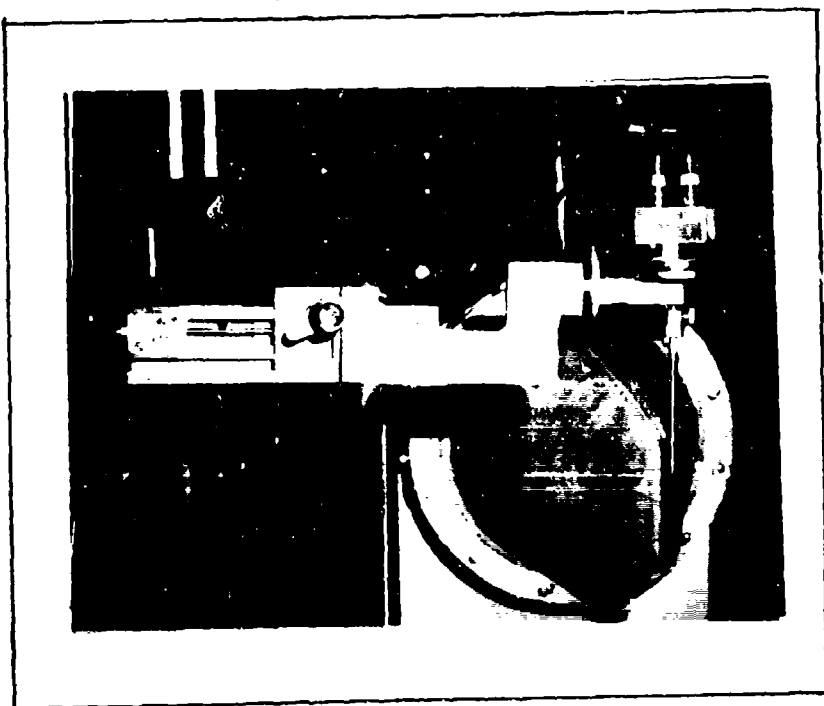


Fig. 4. Sensor Attachment on Cathodometer

## Sensors

Figure 5 shows the types of sensors used in the present investigation. All the sensors used were cylindrical, platinum coated tungsten wire type having diameter of 3.8 micron and 1.25 millimeter active sensor length, separated by a distance of 1 millimeter. The nomenclature used by Thermo-Systems for different types of sensors is as follows:

The number code identifies the diameter of the cylindrical sensor. For example, T1.5 implies tungsten wire sensors having 0.00015 inch diameter. Similarly -20 refers to a hot film type sensor having diameter of 0.002 inch. The Model number identifies the probe configuration. For example, Fig. 5(a) shows the Model 1210 standard straight probe whereas Fig. 5(b) shows Model 1214 probe which is streamlined wedge shape suitable for supersonic flow.

T1.5 Models 1210 and 1214 were used for gaining experience in the calibration technique as well as for performing a number of secondary experiments. The T1.5 Model 1240, which has two wires mounted at right angle to each other, was used for measurements of velocity components in the XY plane. For velocity measurements in the XZ plane, T1.5 Model 1241 X wire sensor was used. This sensor has two wires arranged such that they are orthogonal to each other but the "X" lies parallel to probe axis. The spacing between the wires of both X type sensors was one millimeter.

Owing to engineering tolerances, the angular arrangement of the two wires of X type sensors is not normally exact. Careful

observations under microscope may reveal an error of about  $\pm$  5 degrees in the arrangement.

### Instrumentation

The primary instrumentation used consisted of Thermo-Systems, Inc. Model 1125 calibrator (Fig. 6), Model 1050 dual, constant temperature hot wire system (Fig. 7) equipped with TSI Model 1052 Linearizer and TSI Model 1057 signal conditioner. Thermo-Systems Model 1015C correlator (Fig. 8) was available separately.

### Calibrator

The flow diagram illustrates the sequence of operation of the TSI Model 1125 calibrator. A low turbulence level (less than 0.17 percent) free jet was provided by the 0.15 inch diameter nozzle having speed range varying between 3 feet per second to Mach No. 1. The Uni Slide three dimensional sliding mechanism provided means of supporting the probe in the exit plane of the nozzle. The pressure regulator and needle valve provided good control of the velocity through the calibrator. The pressure port on the calming chamber provided a means of recording stagnation temperature.

### Signal Processing by Anemometer

Figure 9 shows a block diagram of how the X hot wire signals are processed in the TSI Model 1050 constant temperature anemometer

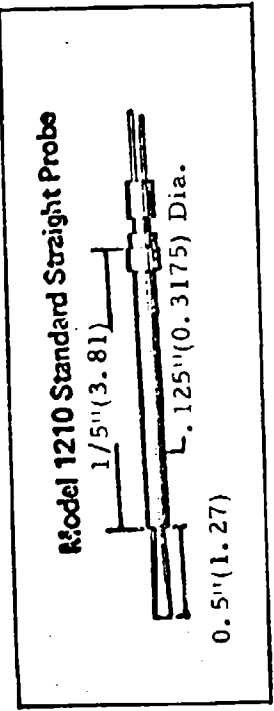


Fig. 5a. Sensor Configuration

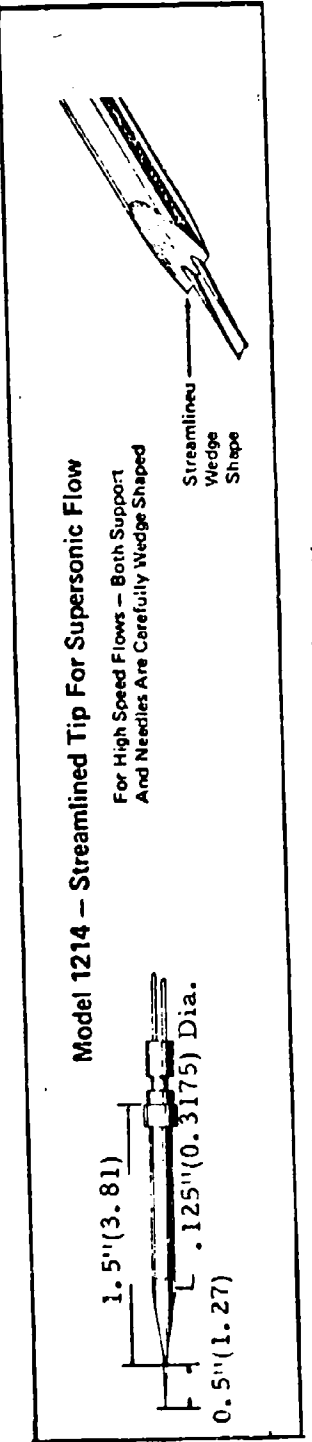
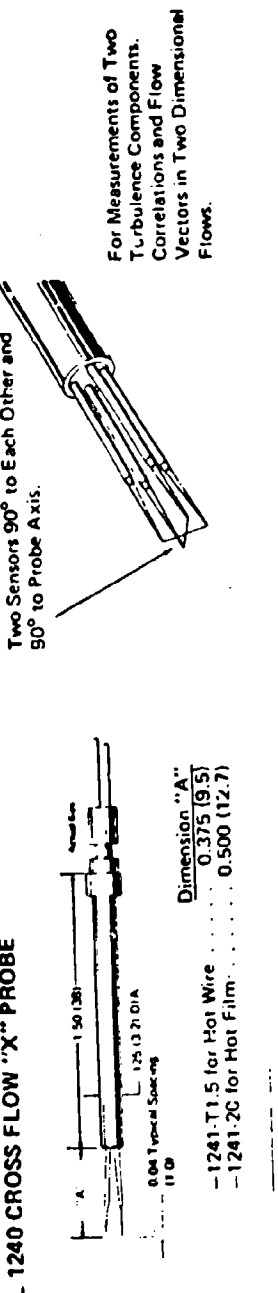


Fig. 5b. Sensor Configuration

### MODEL 1240 CROSS FLOW "X" PROBE

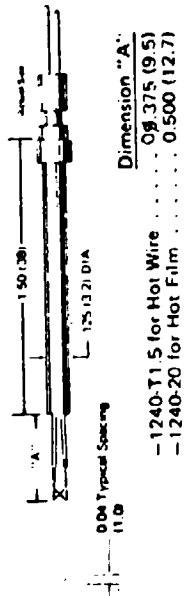


Two Sensors 90° to Each Other and  
90° to Probe Axis.

For Measurements of Two  
Turbulence Components.  
Correlations and Flow  
Vectors in Two Dimensional  
Flows.

Fig. 5c. Sensor Configuration

### MODEL 1241 END FLOW "X" PROBE



Two Sensors 90° to each Other and 45° to  
Probe Axis, in Closely Spaced Planes  
Parallel to Probe

Similar to 1240 Above but  
with Sensor "X" in Plane of  
Probe

Fig. 5d. Sensor Configuration

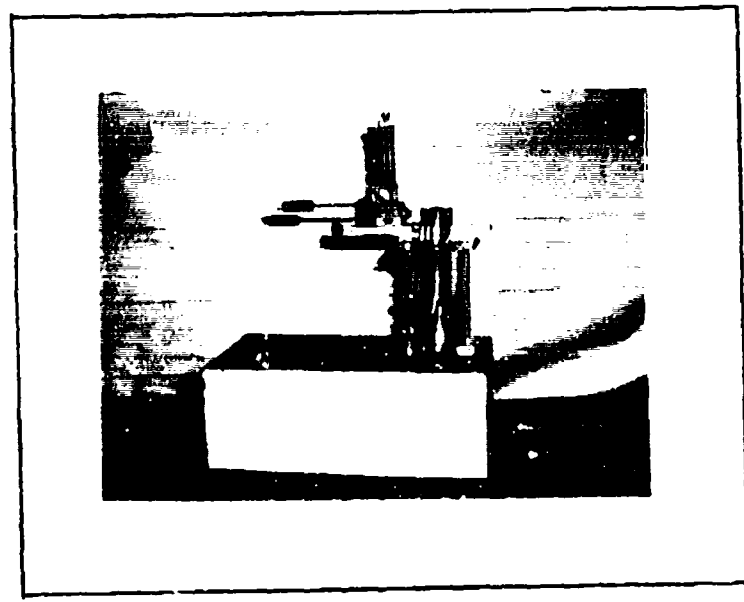


Fig. 6(a). TSI Model 1125 Calibrator

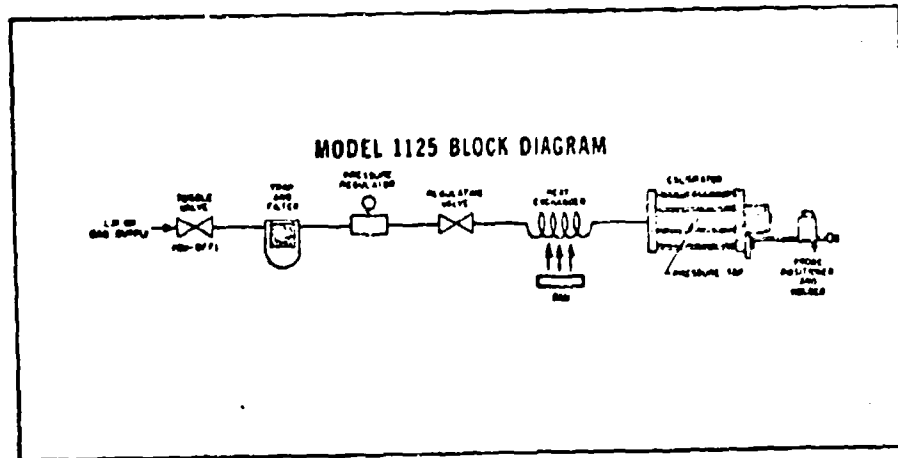


Fig. 6(b). TSI Model 1125 Calibrator  
Flow Diagram

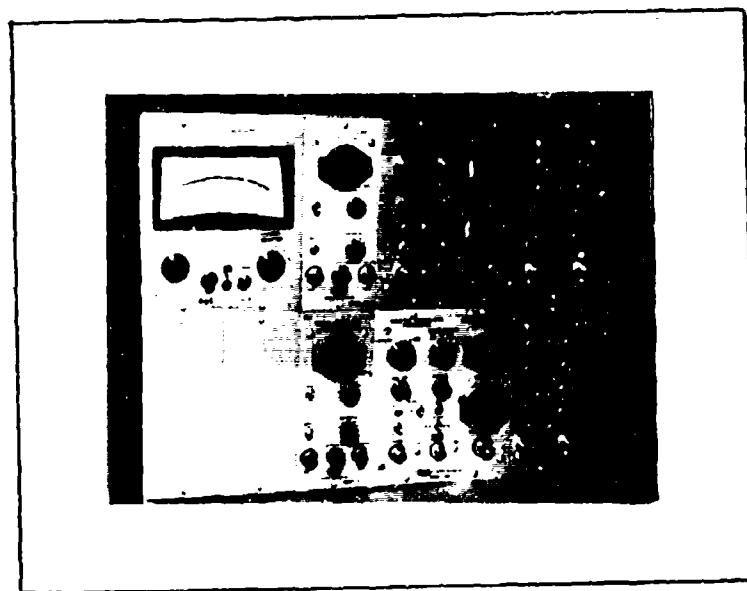


Fig. 7. TSI Model 1050 Dual Constant Temperature  
Hot Wire Anemometer with Linearizer

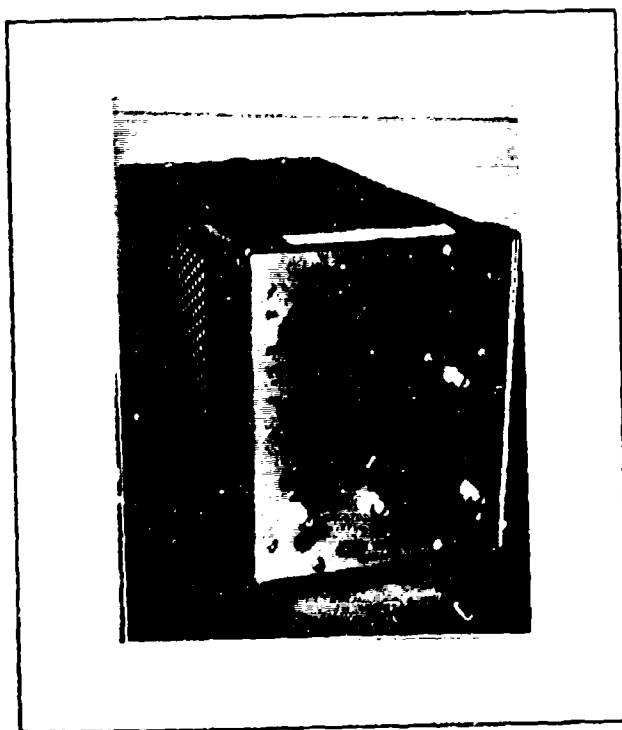


Fig. 8. TSI Model 1015C Correlator

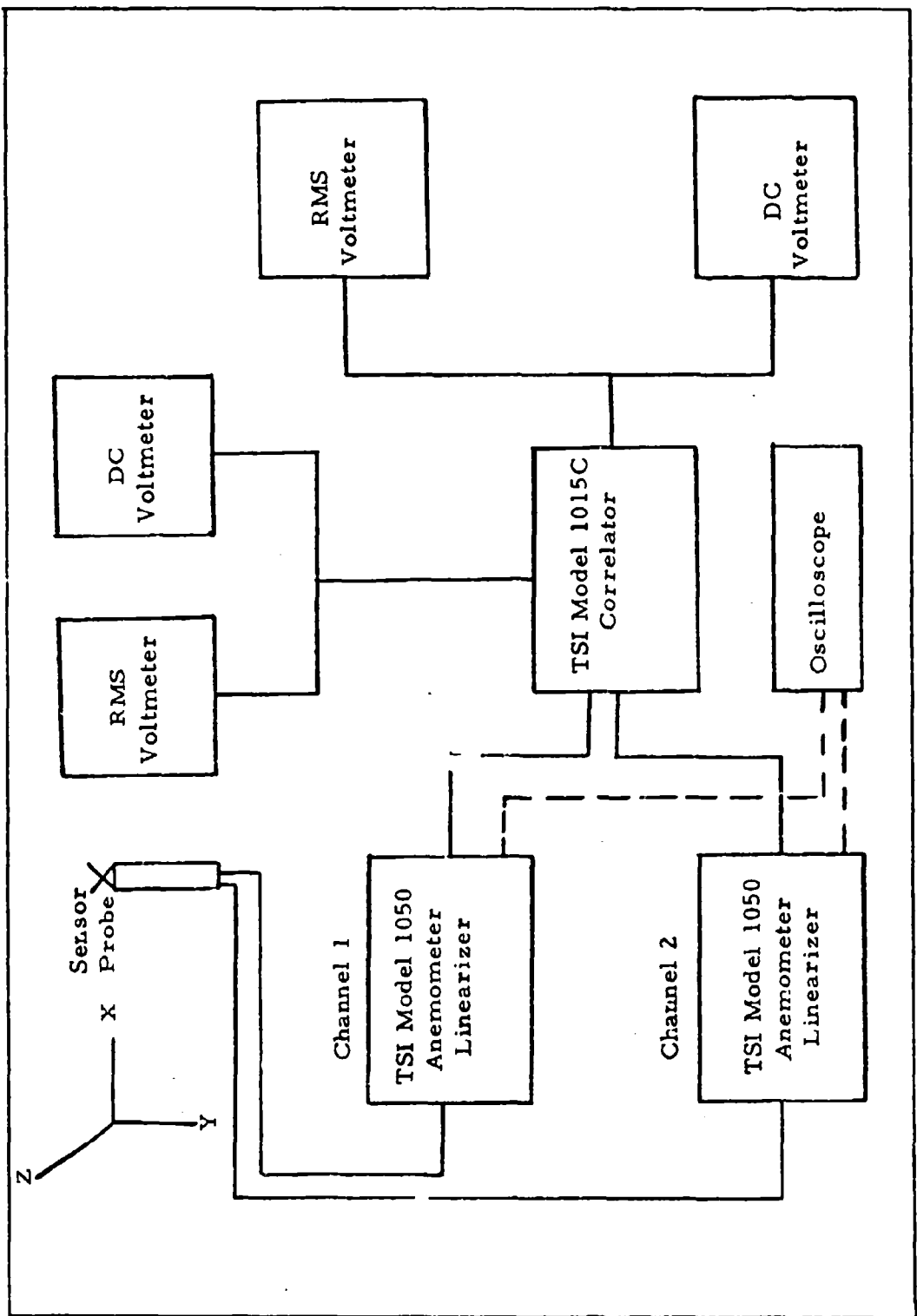


Fig. 9. Block Diagram Showing Signal Processing

system. The non-linear bridge voltage output of the two sensors from their respective channels are each fed into a linearizer. The linearized output signals are then fed to TSI Model 1015C correlator. The mean velocity components were read on DC voltmeter and fluctuating velocity components on RMS voltmeter after selecting the power switch to AC position.

#### Correlator

The TSI Model 1015C correlator which is capable of performing a number of analogue computations was used to separate the two velocity components of the X hot wire sensor. For a linearized system, sum of the voltages was proportional to the velocity component parallel to mean flow direction whereas the difference was equal to the velocity component normal to the mean flow direction (Ref 26).

#### Oscilloscope

A Tektronix Inc. Type 531 oscilloscope was used to test the anemometer system for maximum frequency response.

#### Voltmeters

Two Digitec Model 268 DC Millivoltmeters and two Hewlett Packard Model 3400A RMS voltmeters were used for measuring DC linearized output and AC linearized output respectively. The DC output was proportional to mean velocity and AC output proportional to fluctuating velocity.

### Manometer

A Mariam 20 inch water micro manometer was used to measure the total pressure in the settling chamber during calibration and experimentation.

### Thermocouple

A Honeywell Model 2732 potentiometer and copper-constantan thermocouple was used to measure the stagnation temperature in the calming chamber of the test nozzle assembly based on the assumption that velocity in the calming chamber was negligible.

### DC Power Supply

It was determined that an external power source provided a more stable voltage when compared to the internal voltage source of the linearizer. An HP Model 6205B dual DC power supply was, therefore, used to provide the necessary external voltage input of 10.000 volts to the linearizer.

### Variac

In order to control the heating of the flow, a General Electric Radio Co. Type 50-B variac was used. This variac provided adequate control to vary the voltage across the two 7,000 watt electric resistance type heaters between 0-200 volts.

#### IV. Data Reduction

##### CDC 6600 Computer

The potentiometer coefficients for the TSI Model 1052 Linearizer supplied by Thermo-Systems, Inc. for the desired velocity range (0-300 feet per second) for T1.5 hot wire sensors (Ref 25) were found to be unsatisfactory due to the fact that they did not yield an acceptable linear voltage velocity relationship. A computer programme was developed to provide a fourth order least square polynomial curve fit to the data points obtained from the calibrator. This programme is given in Appendix D. Standard procedure as recommended by Thermo-Systems (Ref 25) was employed for the determination of the polynomial coefficients. The programme gave non-normalized polynomial coefficients which were normalized manually prior to feeding into the potentiometers of the linearizer of the constant temperature anemometer system. During the normalization process, 10 volts of the linearized system were taken to correspond to full scale flow of 300 feet per second. These coefficients are tabulated in Appendix C. The Air Force Institute of Technology data link system was used to tie into Air Force Aeronautical Systems Division control Data Corporation 6600 computer for data plotting.

## V. Experimental Procedures

### Control of Test Conditions

A hot wire sensor, strictly speaking, is sensitive to the mass flow rate rather than velocity. As the range of speeds of interest (0-300 feet per second) was almost in the incompressible flow regime, the sensor was assumed to be sensitive to velocity instead of mass flow rate. The calculation of velocities was also based upon incompressible Bernoulli's Equation.

The variations in the ambient air temperature on day to day basis were taken into account by adjusting the fine "span control" on the linearizer. Constant pressure in the calming chamber of the free jet facility was maintained by adjusting the compressed air bypass valve which was vented to the atmosphere until a steady flow at the desired pressure was obtained, with the compressor running continuously under constant load conditions.

### Calibration

Single Sensor. The main purpose of calibration is to reproduce the test environment as accurately as possible. In the present investigation, calibration of the sensors constituted the most important phase of the research due to many reasons. Firstly, by calibrating the sensor, the heat conduction losses to the sensor supports become part

of the calibration. Secondly, small variations in the sensor temperature, imperfect sensor geometry, dirt accumulation and aging effects etc. are all taken into account. The single sensors TSI T1.5 Model 1210 and Model 1214 were calibrated normal to the mean flow direction using TSI Model 1125 calibrator. An overheat ratio of 1.5 was used which gave good sensor sensitivity to velocity variations and signal to noise ratio of the anemometer system.

The normal orientation of the sensor was first attained visually and then fine adjustments were made at some low constant airspeed, until the non linear bridge output was a maximum. This technique was considered essential because the sensor response was highly dependent upon its orientation relative to the mean flow direction; necessitating that the same orientation should be used during actual tests as that employed during calibration.

As a secondary test, the single sensor model 1210 was calibrated at two additional overheat ratios, namely 1.2 and 1.8 with the intention of determining the influence the overheat ratio on the linear and non linear bridge outputs and the error involved in case the overheat ratio is inadvertently set to an incorrect value during actual test. The calibration curves are shown in Fig.50 and results are tabulated in Appendix C.

#### X Wire Sensor.

(1) Model 1240. Each wire of the Model 1240 sensor was calibrated independently; first, normal to the mean flow direction and then

each wire aligned 45 degrees to the mean flow direction. The 45 degrees orientation was achieved by rotating the sensor from its normal orientation until the linearized voltage output was 7.07 volts with 10.00 volts corresponding to full scale flow conditions of 300 feet per second. The same procedure when repeated using the cathodometer before conducting actual tests corresponded to sensor orientation of 48 degrees with the sensor operating in the potential core of the free jet. In order to maintain consistency, the X hot wire sensor was oriented 48 degrees relative to the mean flow direction for all subsequent tests. A further check was made on the Model 1240 sensor orientation relative to the mean flow direction using TSI Model 1015C correlator. Using the fact that X hot wire sensor would be at 45 degrees relative to the mean flow direction when the difference between the voltage outputs of the linearized system were zero (see Equation 10), the X sensor was again rotated in the potential core of the free jet. This test gave the same result, that is, the difference ( $E_{L_1} - E_{L_2}$ ) corresponded to the sensor orientation of 48 degrees instead of 45 degrees. The X probe calibration technique used by Thermo-Systems (Ref 25) was tried but it did not yield satisfactory results.

(2) Model 1241. The calibration of Model 1241 was relatively simple. The orientation of this sensor offered no difficulties since the

two sensors were arranged such that each sensor was at 45 degrees relative to the mean flow direction with the "X" lying parallel to the probe axis as opposed to Model 1240 in which case "X" lies normal to the probe axis (see Fig. 5(c) and (d)).

#### Optimizing Frequency Response

The frequency response of the anemometer system was optimized according to the procedure recommended by the manufacturer (Ref 25). In order to observe the output test signal shape, a Tektronix Inc. Type 531 oscilloscope was connected to the Bridge Output jack. With the probe exposed to the flow at maximum speed (300 feet per second), trim control on (5:1) Bridge and stability control of the anemometer were adjusted initially with 1 KHZ square wave signal across the bridge circuit and then 20 KHZ signal. Ref Set control was not normally used for optimization purposes. However, very slight movements of the Ref Set control was found to be helpful in improving upon the output signal shape. The output signal for a hot wire sensor should appear as shown in Fig. 10 if the system has been optimized properly. With sufficient practice, it was possible to attain the desired output signal shape.

#### Linearization

Once an accurate calibration curve had been obtained, the next step was to determine the four polynomial coefficients to be set into the linearizer potentiometers. For this purpose, a fourth order least

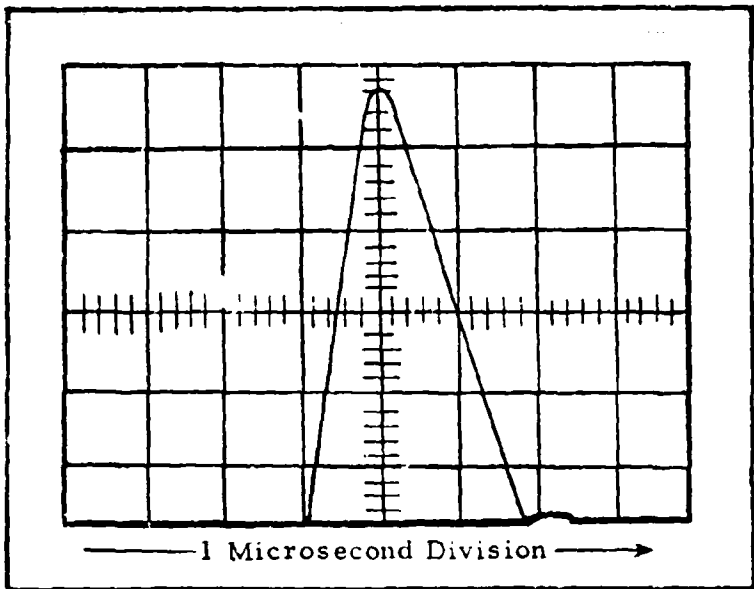


Fig.10. Square Wave Test Signal on a 3.8 Micron Tungsten Hot Wire (From Ref 30)

square polynomial curve fit was applied to the data points. Only 20 data points at approximately equal interval were selected from the calibration curve. These values were fed in as data to the programme listed in Appendix D. The first and the last data points were weighted heavily where second, third, fourth, fifth and sixth data points were given 80, 60, 40, 20 and 10 percent weighting respectively. All the remaining data points were allotted 1% weighting only.

Figure 11 shows a typical fourth order least square curve fit to the selected data points. The technique was repeated for every sensor calibrated for the present study. These polynomial coefficients were in disagreement with those provided by Thermo-Systems (Ref 28). In fact the polynomial coefficients supplied by Thermo-Systems did not

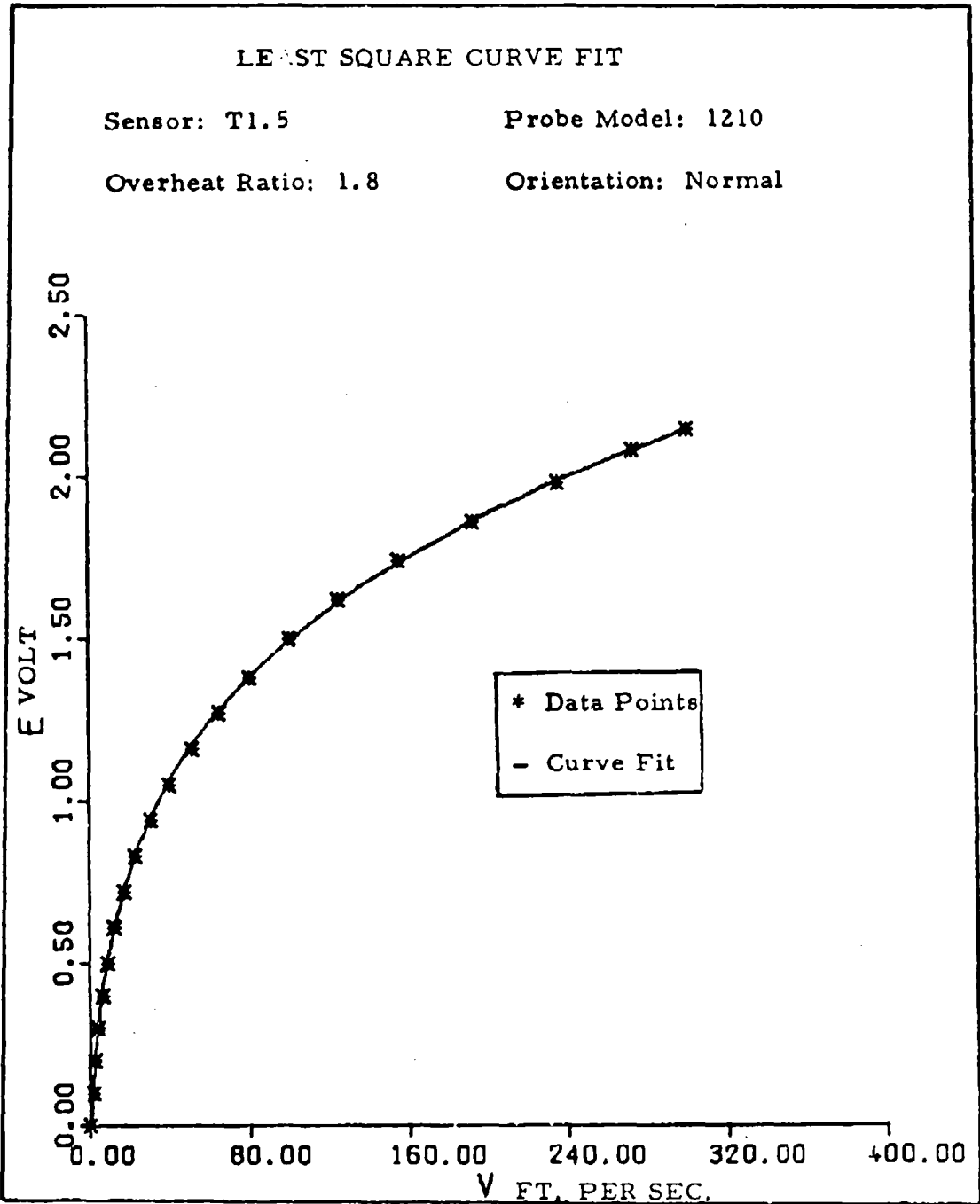


Fig. 11. Fourth Order Least Square Polynomial Curve Fit for Evaluation of Linearized Coefficients

yield linear bridge voltage output and were, therefore, discarded. Standard procedure for setting up the polynomial coefficients in the linearizer potentiometers was adopted (Ref 25). The accuracy of linearization was found to be highly dependent upon the linearizer coefficients and the precision with which these coefficients were set. The coefficients were found to drift and a check was made each time before collecting any data.

#### Experimental Measurements

Experimental Arrangement. Rotation in yaw, which was defined as the movement of the resultant velocity vector within the probe plane, was performed by rotating the sensor itself and noting the amount of angular displacement on the fixed table (see Fig. 12a). The fixed table located in XY plane was graduated in 1 degree interval and the pointer attached to the probe provided reasonably accurate control of the angular displacements of the probe and hence of the sensor.

Rotation in pitch, which was defined as the movement of the resultant velocity vector out of the probe plane, in the case of Model 1240 was achieved by the movements of the turn-table located in XZ plane. The figure 13 explains the technique adopted for conducting pitch movements with the X sensor Model 1240. The moment arm 1 was measured accurately in the School Shop and was equal to 7.068 inches. For clockwise rotation in pitch, the probe was moved by

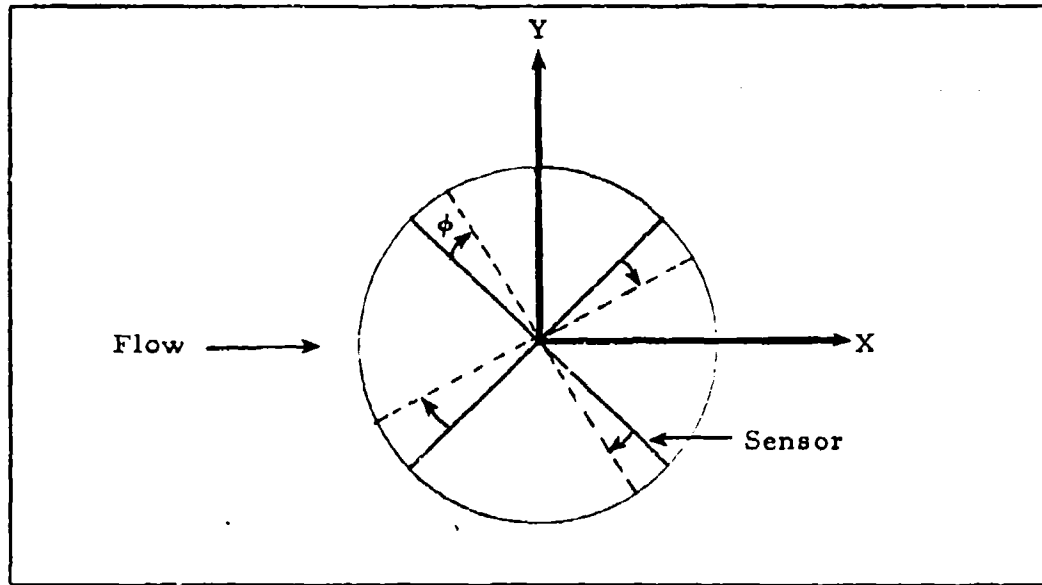


Fig. 12a. Definition of Yaw Angle

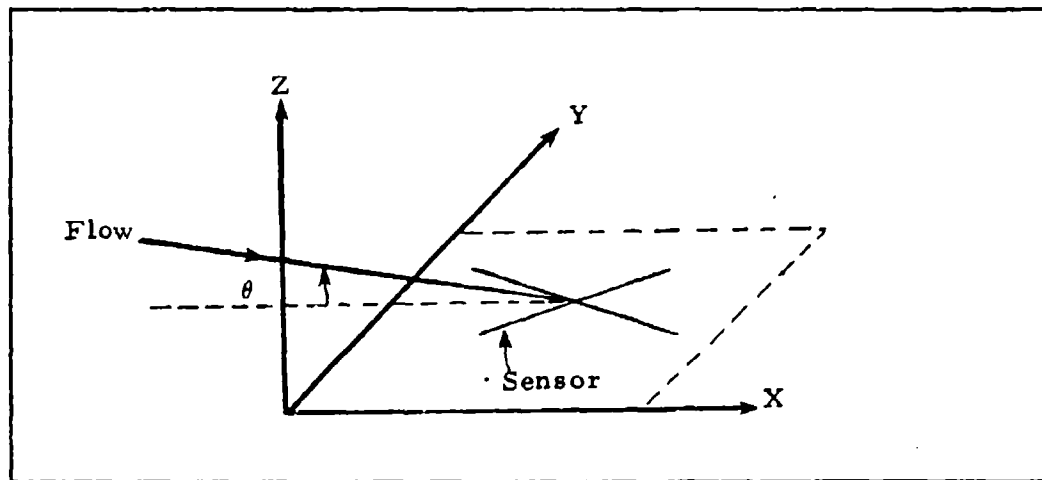


Fig. 12b. Definition of Pitch Angle

$\Delta x = l \sin \beta$  downstream and by  $\Delta z = l (1 - \cos \beta)$  downwards in order to coincide with the initial reference location. For counterclockwise rotation in pitch, the probe must be moved by  $\Delta x = l \sin \beta$  upstream and  $\Delta z = l (1 - \cos \beta)$  downwards in order to coincide with reference location. Similar technique was adopted for the rotations in yaw and pitch with the sensor Model 1241.

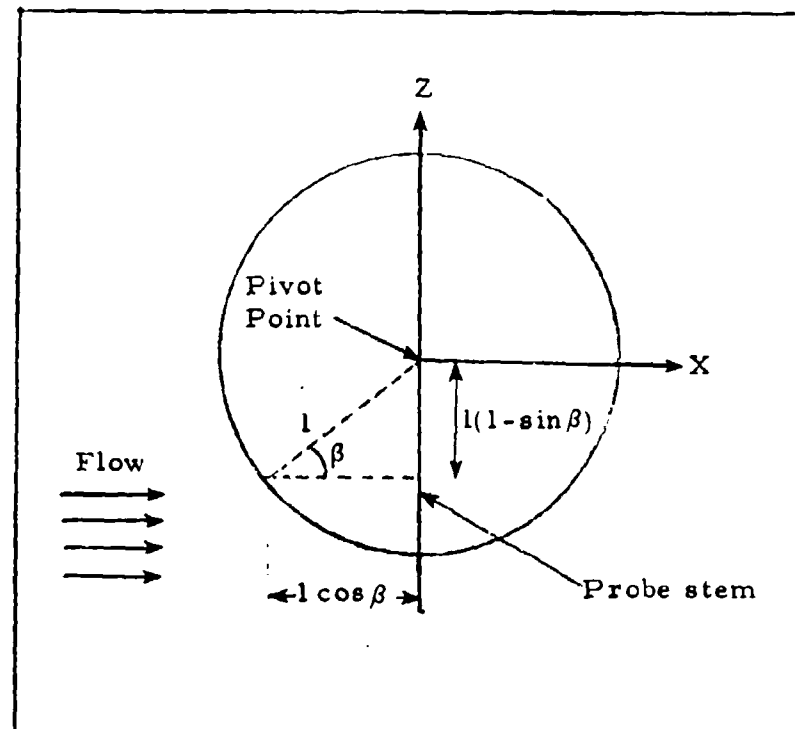


Fig. 13. Pitch Movement of the Sensor

#### Flow Direction Measurements

Measurements in Potential Core. The X sensors Model 1240 and 1241 were located in the potential core at 1 centimeter downstream of the nozzle exit plane and at the center line. The turbulence intensity

at this location was 0.32 percent. The X sensor Model 1240 was employed to measure the mean velocity components  $\bar{u}$ ,  $\bar{v}$  and hence the flow direction in XY plane, whereas Model 1241 was used to determine  $\bar{u}$ ,  $\bar{w}$  and, therefore, the flow direction in XZ plane. The sensor orientation relative to the mean flow direction during calibration corresponded to 48 degrees instead of 45 degrees. This orientation was, therefore, used as reference for all the measurements in the potential core. The sensors were yawed and pitched inside the potential core through  $\pm$  30 degrees and  $\pm$  10 degrees respectively. The clockwise rotation in a plane was defined to be positive and the counterclockwise rotation negative. The size of the potential core limited the rotation in pitch to  $\pm$  10 degrees because the probe support was almost touching the nozzle edges at pitch angles of  $\pm$  10 degrees. The rotations in yaw and pitch were made at three values of Reynolds Numbers, namely 7.2, 14.54 and 21.8. These Reynolds Numbers corresponded to nozzle exit velocities of 100 feet per second (30.48 meters per second), 200 feet per second (60.96 meters per second), and 300 feet per second (91.44 meters per second) respectively under standard sea level conditions. While performing rotation experiments in yaw with Model 1240 in the potential core, the turbulence intensity was observed to vary from 0.32 percent to a maximum of 0.81 percent as the sensor was yawed through +30 degrees but the turbulence intensity nearly remained constant at 0.3 percent when the sensor was rotated in the counterclockwise direction. This indicated strong sensor

prongs and supporting structure interference effect on the sensitive portions of the two sensors and led to the idea of repeating all the above rotations in yaw starting with a new reference orientation of 135 degrees instead of 48 degrees. These rotation tests inside the potential core at the three Reynolds Numbers of interest are shown in Figures 15 thru 28. The calibration of each sensor at 135 degrees reference orientation was checked and found to be satisfactory. The same was repeated for the other reference orientation prior to and after conducting each rotation experiment. Slight shift in the calibration curve was observed due to aging of the wire but the deviations in the sensor sensitivity was found to be less than 0.1 percent. The rotation of the sensor was performed manually by rotating the probe itself in steps of 2 degrees interval. For measurements of  $\bar{u}$  and  $\bar{w}$  with the Model 1241, the sensor was mounted on a 90 degree elbow and oriented such that the sensor faced the flow direction and the sensor "X" was parallel to the probe plane. The rotations in yaw and pitch were repeated at the three values of the Reynolds Numbers mentioned earlier. As opposed to the sensor Model 1240, rotation in yaw in the potential core was restricted to  $\pm$  10 degrees due to limited size of the potential core (1 centimeter). In order to prolong the sensor life, the sensor was not exposed to the flow until the velocity in the nozzle exit plane had attained a steady value. Normally, the time taken for the flow to attain a steady state was more than 30 minutes.

Measurements in Shear Flow Region. One of the secondary objectives of the present investigation was to repeat the rotation tests in the shear flow region of the free jet. To achieve this goal, the X sensor Model 1240 was used. The sensor was located downstream of the nozzle exit plane at 25 centimeters from the center line. At Reynolds Number of 21.8 based upon the flow conditions at the nozzle exit plane, the mean velocity at this location was 200.7 feet per second (61.73 meters per second) and turbulence intensity 15.85 percent. The X sensor was yawed through  $\pm$  30 degrees and pitched through  $\pm$  10 degrees at the three values of Reynolds Numbers of interest for each value of the reference orientations, namely 48 degrees and 135 degrees. These rotation tests in shear flow regions are shown in Figures 41 thru 46.

Measurement of the Influence of Fluid Temperature Variations on the Linearized System

The second objective of this investigation was to determine the error involved in the linearized bridge output of the constant temperature anemometer system due to small variation in the fluid temperature. To achieve this goal, the sensor Model 1240 (No. 1) was oriented 48 degrees to the mean flow direction at 1 centimeter from the nozzle exit plane and at the center line. The two electric heaters installed inside the calming chamber of the free jet facility were used to provide the necessary heating. The heating was controlled by a variac and the fluid temperature was increased in steps of 4°F up to a

maximum value of 20°F. The amount of voltage drop across the two heaters to yield a given temperature rise of the fluid was precalculated. The calculations are given in Appendix B. The stagnation temperature was measured by a copper-constantan thermocouple as well as by an ordinary mercury bulb thermometer. As the flow in the calming chamber was stationary for all practical purposes, and since the temperature was measured under steady state only, the temperature measured by the thermocouple was assumed to represent the stagnation temperature of the fluid. The tests were conducted in the velocity range from 25 feet per second (7.62 meters per second) to 300 feet per second (91.44 meters per second).

In order to prolong the sensor life, the sensor was not exposed to the flow until it had attained a steady value of temperature at a given velocity. Normally, the time taken by the flow to attain a steady value of temperature was more than 45 minutes.

## VI. Discussion of Results

In this section, discussion of the rotation tests performed with the X sensors Model 1240 and Model 1241 in the potential core of the free jet is covered first. The second part covers the discussion on the influence of the air temperature variations on the linearized response of the hot wire. Lastly, a number of secondary tests performed during the study are considered.

### Measurements in the Potential Core with the X Sensor Model 1240

The X sensor Model 1240 consisting of two platinum coated, tungsten wires, having 0.00015 inch (3.8 micron) diameter, 0.05 inch (1.25 millimeter) active length, separated by 1 millimeter was yawed through  $\pm$  30 degrees and pitched through  $\pm$  10 degrees in the potential core (turbulence intensity 0.3 per cent) of the free jet. The free jet facility existing in the Aero Mechanical Engineering Department of Air Force Institute of Technology (AFIT) was used mainly because it provided potential core of sufficient size.

#### Rotation in Yaw

For rotation tests in yaw with the X sensor Model 1240, the sensor was located on the center line and at 1 centimeter downstream of the nozzle exit plane. The results of these tests are tabulated in Appendix A.

Figures 14 through 19 show the variations of the mean velocity components  $\bar{u}$  and  $\bar{v}$  with the yaw angle  $\phi$ . The "actual velocity components" are also plotted in these figures in order to illustrate the error in  $\bar{u}$  and  $\bar{v}$  for a given angle  $\phi$ . The actual mean velocity component in X direction was defined as  $\bar{q} \cos \phi$  and in the Y direction as  $\bar{q} \sin \phi$  where  $\bar{q}$  denotes the resultant mean velocity vector and  $\phi$  the yaw angle. A summary of the error analysis in  $\bar{u}$  and  $\bar{v}$  due to misalignment in yaw is given in Table I.

Table I  
Rotation in Yaw (Potential Core)  
(Reference Orientation 48 deg)

Re. No.	Misalign- ment Angle (deg)	Percent Error in			
		$\bar{u}$		$\bar{v}$	
		Clockwise Rotation	Counter Clockwise Rotation	Clockwise Rotation	Counter Clockwise Rotation
7.2 (100 ft/ sec)	+ 10.0	+1.33%	+6.9%	+2.0%	-10%
	+ 20.0	+4.7%	+1.78%	+17.49%	-1.7%
	+ 30.0	+10.33%	+1.02%	+28.7%	-6.46%
14.54 (200 ft/ sec)	+ 10.0	+1.18%	+1.0%	+21.0%	+20.4%
	+ 20.0	+4.49%	+8.3%	+21.9%	+16.19%
	+ 30.0	+9.7%	+9.7%	+29.98%	+14.93%
21.8 (300 ft/ sec)	+ 10.0	+2.8%	-2.58%	+24.24%	+ 7.33%
	+ 20.0	+8.25%	-3.1%	+32.17%	+15.83%
	+ 30.0	+15.48%	-4.1%	+35.64%	+19.66%

The angle through which the sensor is yawed can be regarded as the misalignment angle relative to the reference orientation and the percent error in mean velocity being defined as:

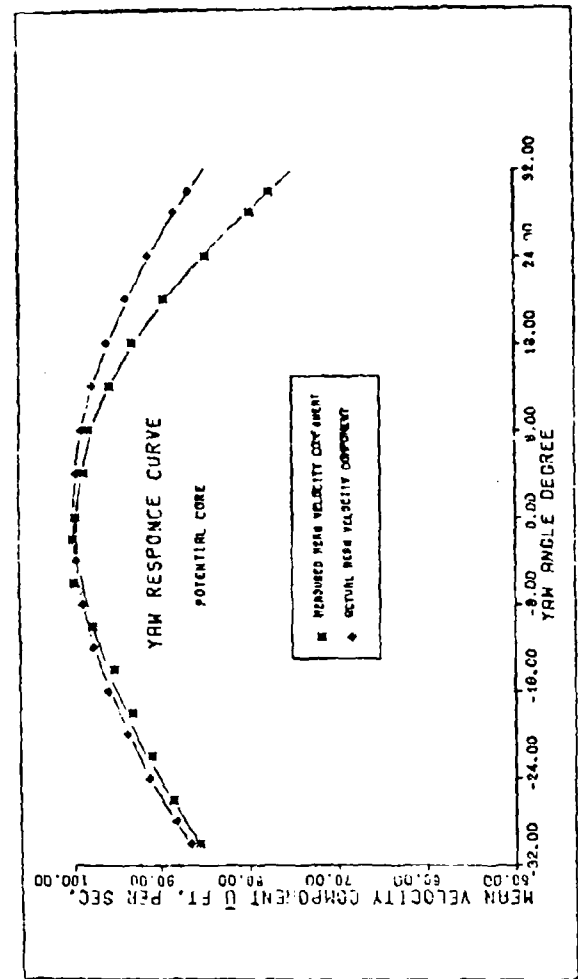


Fig. 14. Error in  $\bar{u}$  Due to Misalignment in Yaw (Re. No. = 7.2)

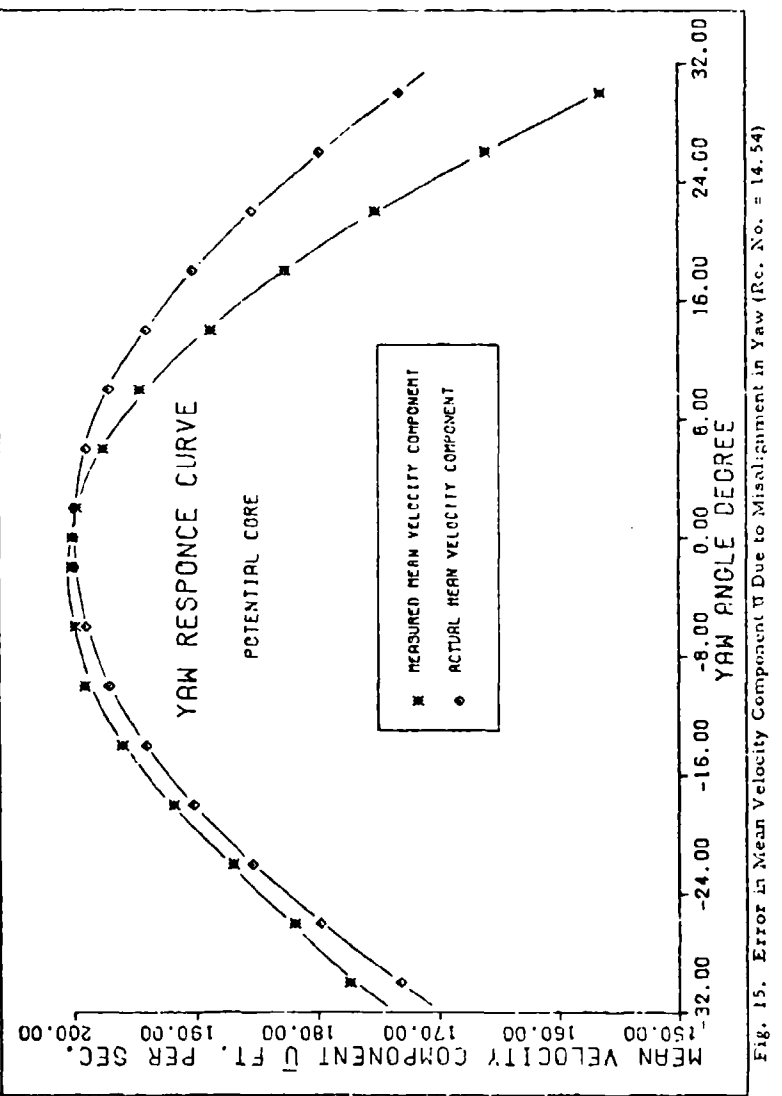


Fig. 15. Error in Mean Velocity Component Due to Misalignment in Yaw (Rec. No. = 14. 54)

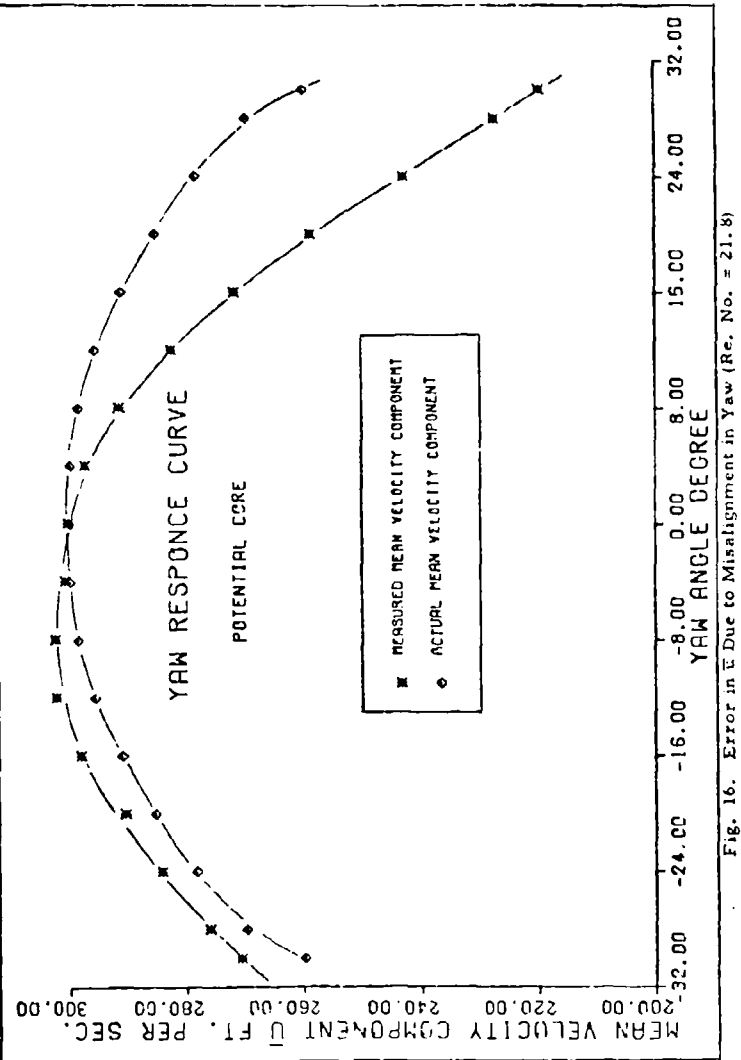


Fig. 16. Error in  $\bar{U}$  Due to Misalignment in Yaw (Re. No. = 21.8)

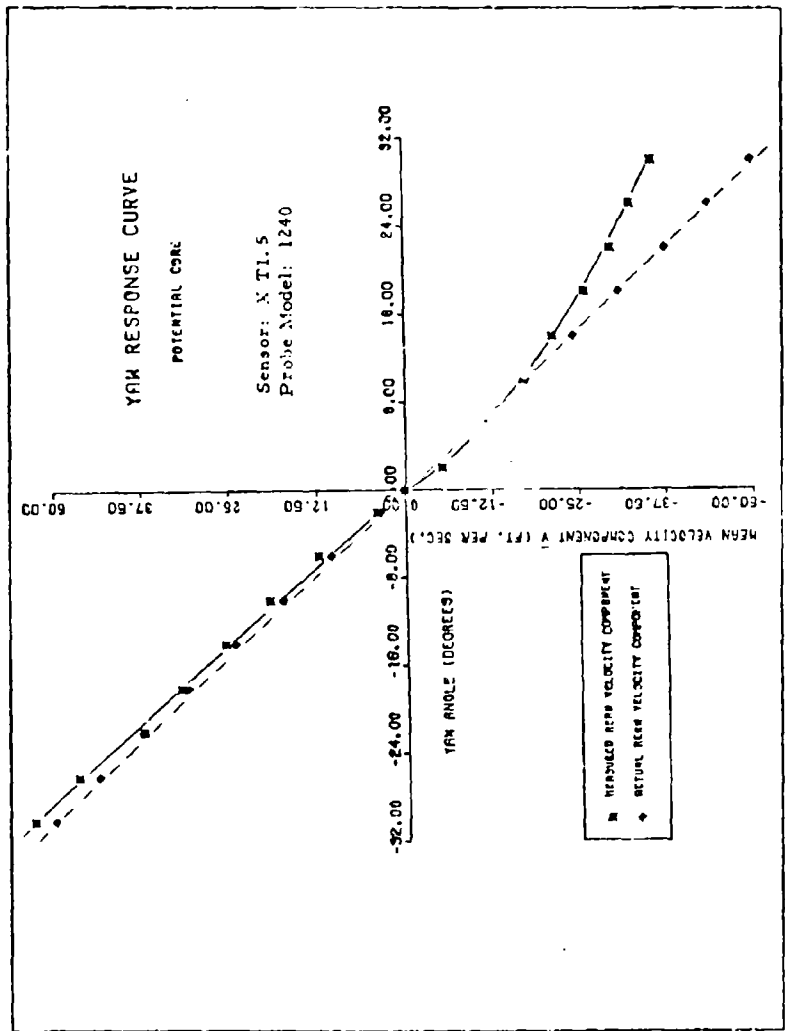


Fig. 17. Error in  $\dot{V}$  Due to Misalignment in Yaw (Re. No. = 7.2);

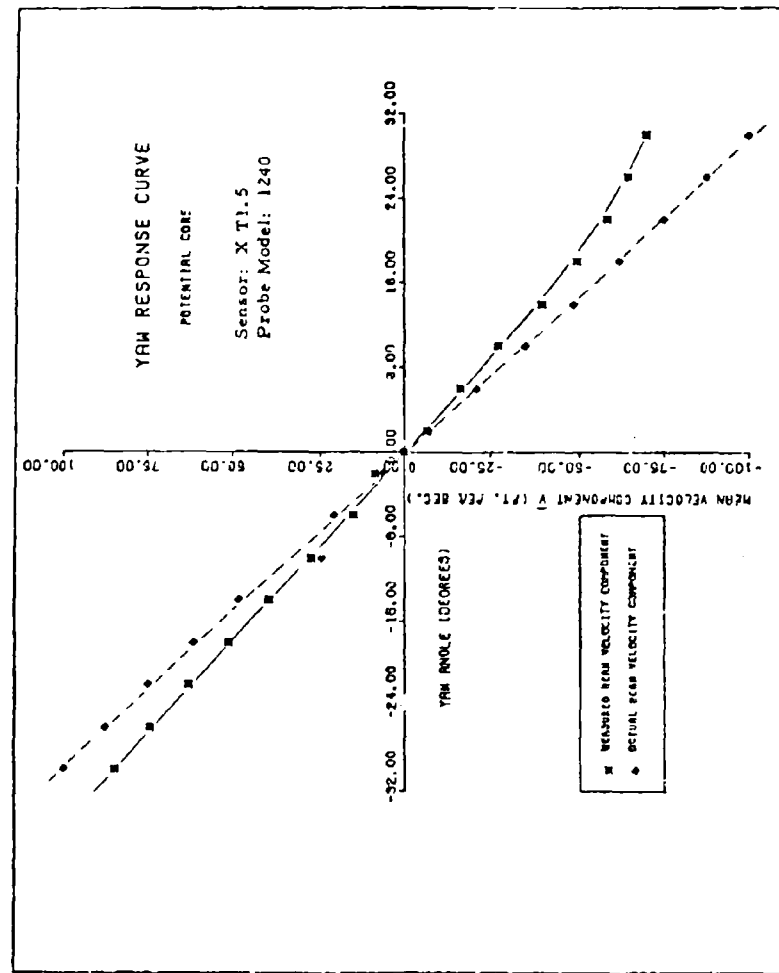


Fig. 18. Error in  $\vec{V}$  Due to Misalignment in Yaw (Re. No. = 14,54)

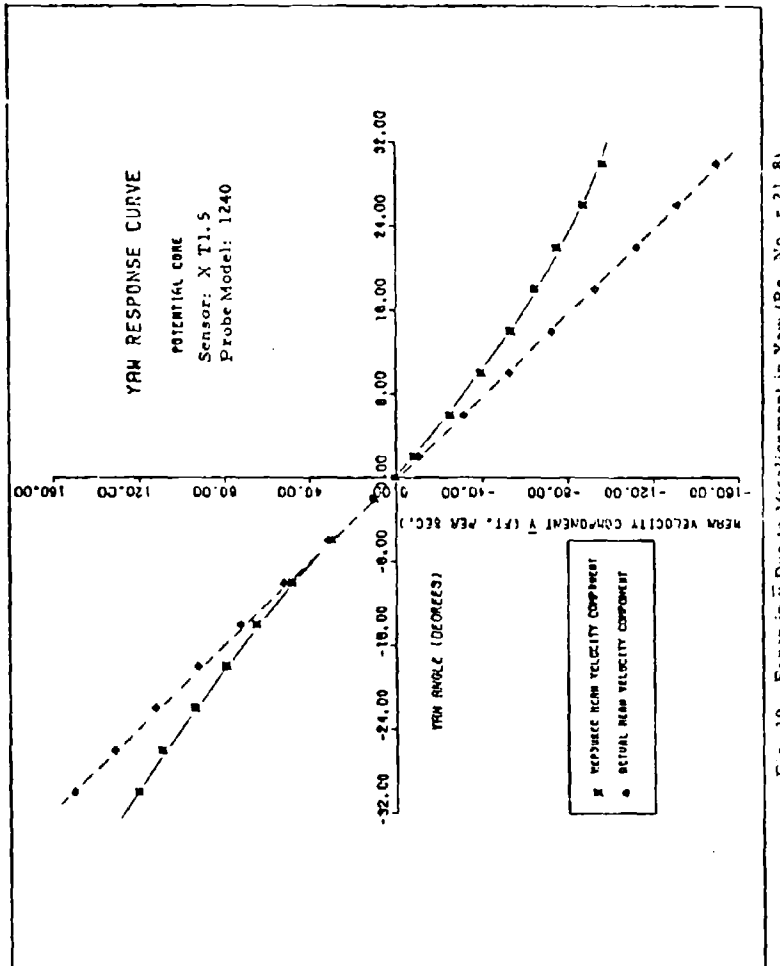


Fig. 19. Error in  $\bar{v}$  Due to Misalignment in Yaw (Re. No. = 21.8)

$$\left[ 1 - \frac{\text{measured mean velocity component}}{\text{actual mean velocity component}} \right] \times 100$$

The positive yaw (misalignment) angle is associated with clockwise rotation of the sensor in XY plane and negative yaw (misalignment) angle corresponds to counterclockwise rotation. From Table I, the following observations are made:

In the range of Reynolds Numbers  $7.2 \leq Re \leq 21.8$ :

1. The per cent error in the measurement of  $\bar{u}$  and  $\bar{v}$  is not the same and vary with the sense of rotation.
2.  $\bar{u}$  is relatively insensitive to misalignment in yaw.
3. Relatively large errors due to misalignment of the X sensor occur in  $\bar{v}$ .

As regard observation 1, it can be remarked that the asymmetry in the sensor response curves is mainly responsible for the unequal per cent error incurred with one rotation or the other. There are many factors which might contribute to the skewness in the X sensor response curves. The two wires of the X sensor may not be aligned accurately at right angle to each other. In fact, a discrepancy of approximately 3 degrees was observed in the sensor arrangement.

Comte-Bellot, Strohl and Alcaraz (Ref 5) observed similar asymmetry in the sensor response curves. They discovered that the wires had the tendency to slide to the one side of the prongs or the other each time new wires were soldered. A similar problem was observed by

Gilmore (Ref 9). Other possible causes of skewness in the sensor response curves are unequal lengths of the active part of the sensor, poor plating at the tips or poor joints. In order to further investigate the asymmetry in the X sensor Model 1240 response curve, the reference orientation was changed to 135 degrees and the rotation tests were repeated. The results of these rotation tests are tabulated in Appendix A. Figures 20 thru 22 show a comparison of the sensor response curves for the two reference orientations. The asymmetry is seen to persist even with this new reference orientation. The crosswire arrangement was also observed under a microscope (Fig. 73) having magnification of 50. It was found that the two sensors were indeed not aligned accurately relative to each other. Another factor which might have contributed to the asymmetry is the fact that the two wires of the X sensor do not operate in a single plane (perpendicular to the probe axis). This leads to the influence of the support of one sensor on the other occurring sooner with one direction of rotation than the other. Figures 23 thru 25 show the error incurred in the mean flow direction due to misalignment in yaw in the range of Reynolds Number  $7.2 \leq Re \leq 21.8$ . The results are tabulated in Appendix A. The mean flow direction is given by  $\tan^{-1} \frac{\bar{v}}{\bar{u}}$  where  $\bar{u}$  and  $\bar{v}$  are the mean velocity components in the X and Y direction, respectively. Table II gives a summary of the errors in the flow direction associated with misalignment in yaw. It can be seen that in the Reynolds Number range  $7.2 \leq Re \leq 21.8$ .

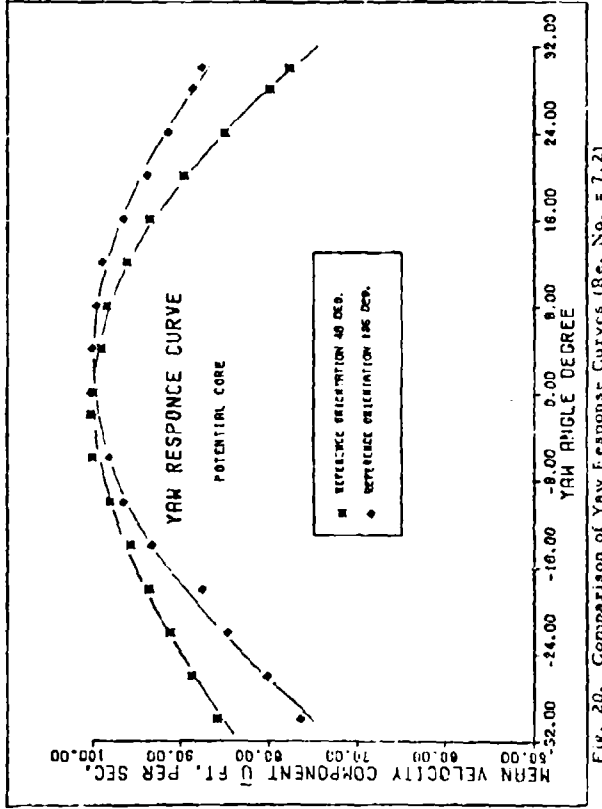


FIG. 20. Comparison of Yaw Response Curves (Re. No. = 7.2)

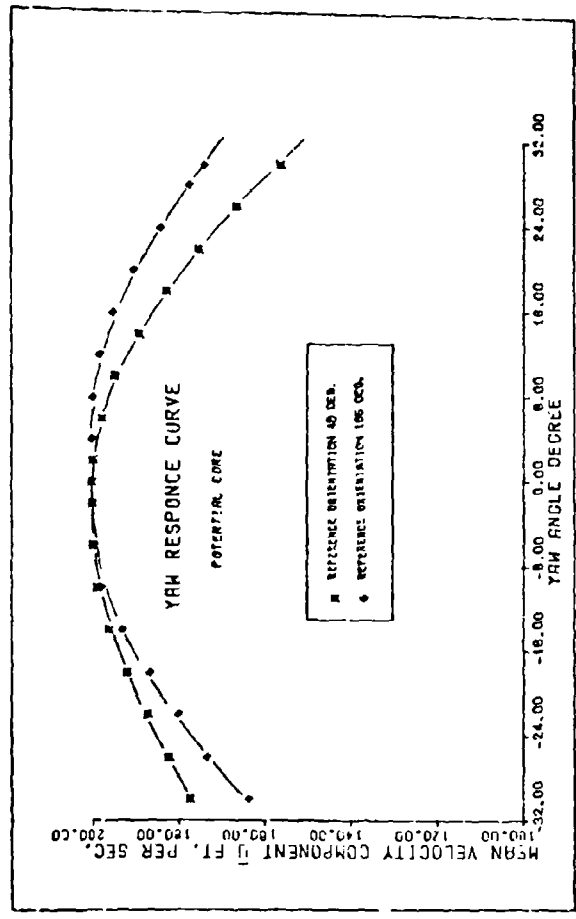


Fig. 21. Comparison of Yaw Response Curves (Re. No. = 14.54)

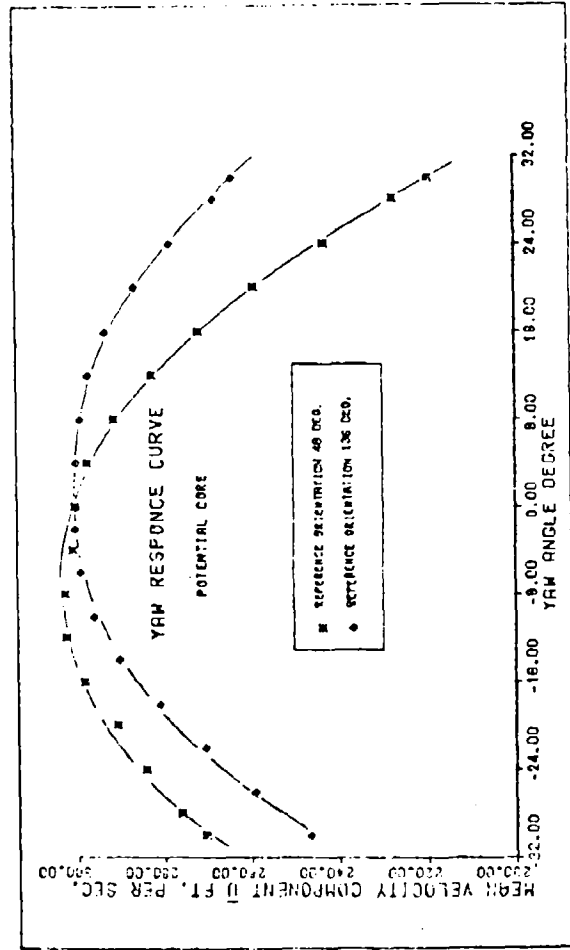


Fig. 22. Comparison of Yaw Response Curves (Ref. No. - 21.8)

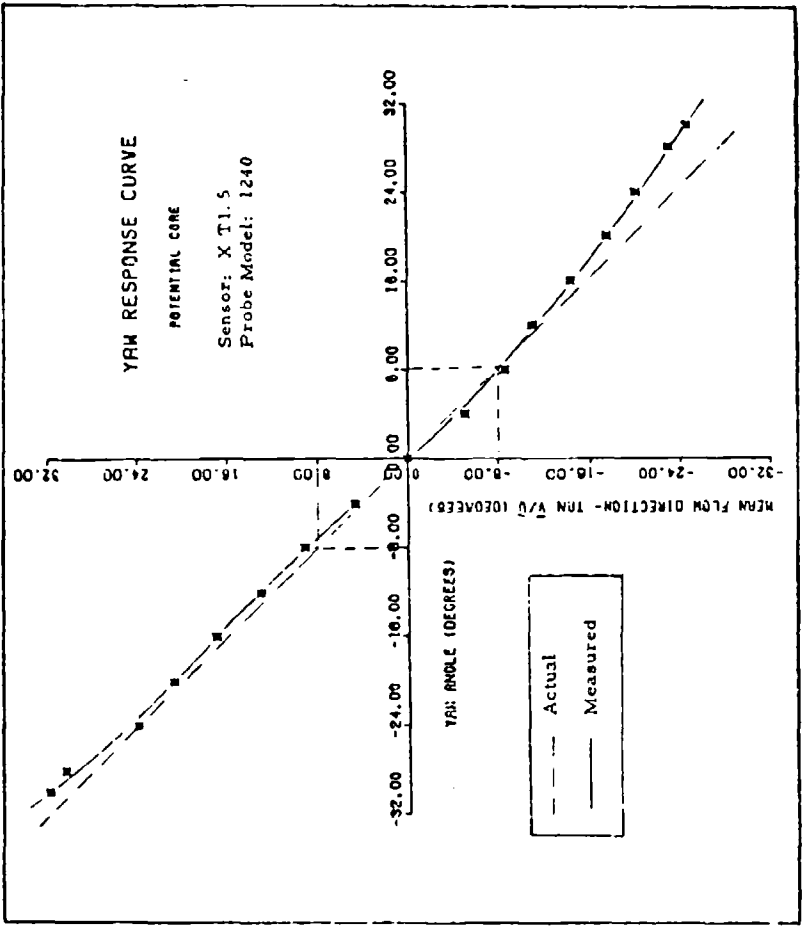


Fig. 23. Error in Mean Flow Direction Due to Misalignment in Yaw (Re. No. = 7.2)

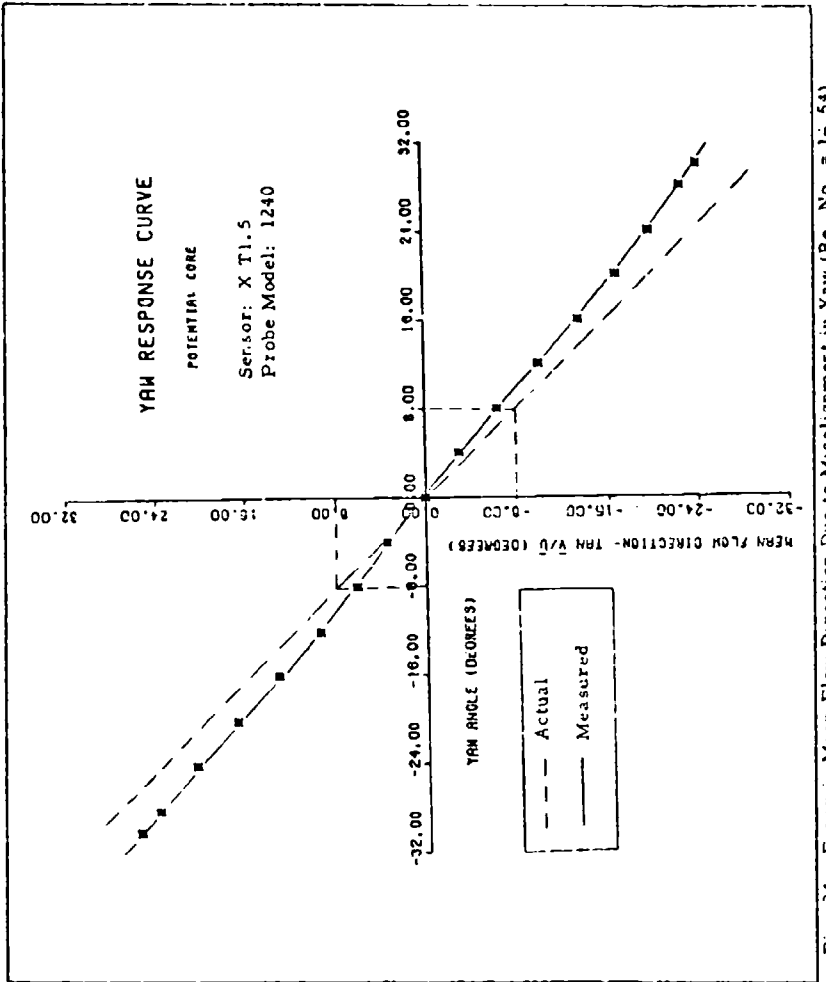


Fig. 24. Error in Mean Flow Direction Due to Misalignment in Yaw (Rev. No. = 1; 54)

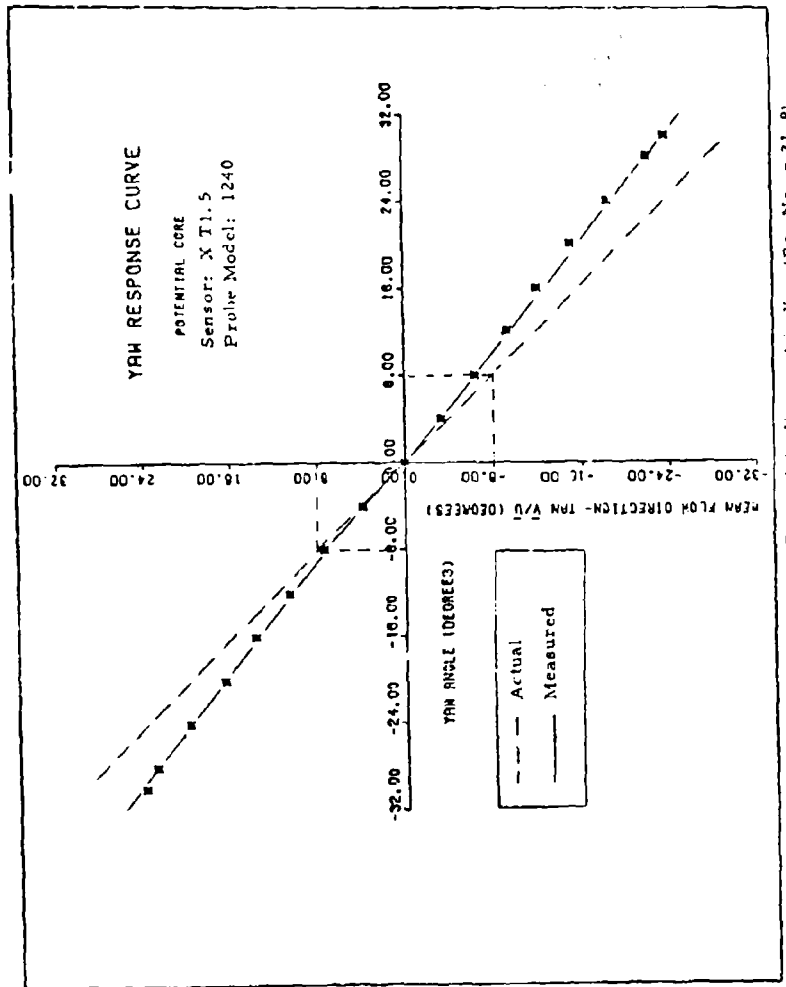


Fig. 25. Error in Mean Flow Direction Due to Misalignment in Yaw (Re. No. = 21.8)

1. Large error in the flow direction occurs at very small misalignment angles (1 to 4 degrees).
2. The per cent error is not constant and depends upon the direction of rotation.
3. For a given misalignment angle greater than 4 degrees, the per cent error increases with Reynolds Number.

The conclusion drawn from these tests is that the X sensor should not be misaligned in yaw at very small angle. If the misalignment is unavoidable, it would be better to misalign the sensor by say 8 to 10 degrees! This remark is applicable particularly in the range  $7.2 \leq Re \leq 14.54$ .

Table II  
Rotation in Yaw (Potential Core)  
(Reference Orientation 48 deg)

Re. No.	Misalignment Angle (Deg)	Per Cent Error in Mean Flow Direction	
		Clockwise Rotation	Counterclockwise Rotation
7.2 (100 ft/sec)	<u>+ 4</u>	-27.75%	-14.7%
	<u>+ 10</u>	+0.71%	-10.59%
	<u>+ 20</u>	+12.55%	-3.28%
	<u>+ 30</u>	+17.83%	+7.5%
15.54 (200 ft/sec)	<u>+ 4</u>	+28.7%	+11.25%
	<u>+ 10</u>	+19.78%	+20.98%
	<u>+ 20</u>	+16.13%	+15.84%
	<u>+ 30</u>	+19.59%	+14.54%
21.8 (300 ft/sec)	<u>+ 4</u>	+16.77%	+4.0%
	<u>+ 10</u>	+21.73%	+9.5%
	<u>+ 20</u>	+24.7%	+17.27%
	<u>+ 30</u>	+20.99%	+19.96%

### Rotation Tests in Pitch

In order to investigate the error involved due to misalignment of the X sensor in pitch, the X sensor Model 1240 was pitched through  $\pm 10$  degrees in the potential core of the free jet at the three values of the Reynolds Numbers of interest. The results of these tests are given in Appendix A and plotted in Figures 26 thru 28. A summary of the test results is given in Table III. Following comments are applicable to these test results:

1. The error due to misalignment in pitch depends upon the sense of rotation.
2. The error is a function of Reynolds Number. At small Reynolds Numbers, the error is relatively large. The relatively large error at small Reynolds Number is probably caused by the fact that the frequency of the vortices being shed by the sensor prongs is small at low speed but the fluctuations possess the tendency to spread laterally to a larger extent. This causes a relatively greater reduction in the sensor sensitivity at low speed than when the sensor is operated at high speed. From the error analysis shown in Table III, it can be concluded that the X sensor Model 1240 is relatively insensitive to misalignment in pitch in the range of Reynold Number  $14.54 \leq Re \leq 21.8$ . For  $\pm 10$  degrees sensor misalignment in pitch, the error may vary between 0.4 per cent to as high as 13 per cent depending upon the sense of rotation.

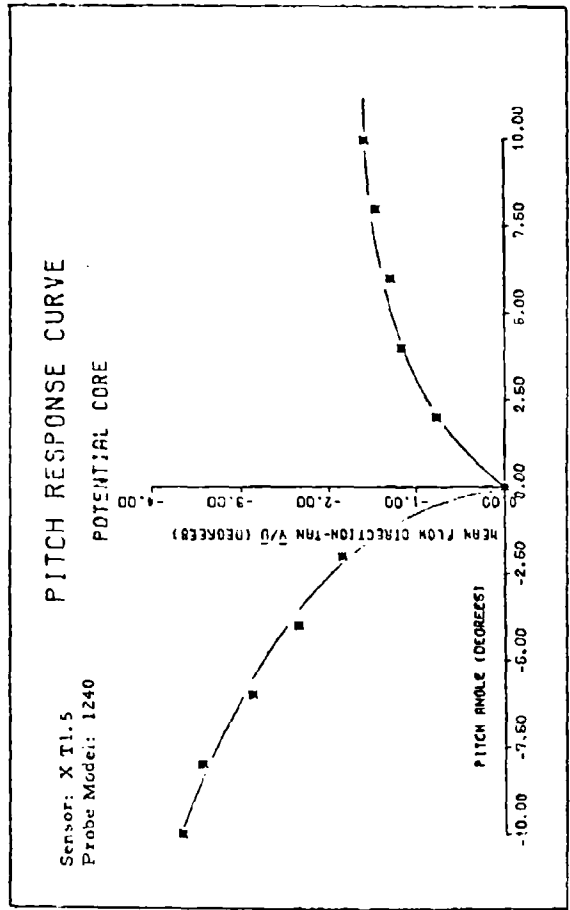


Fig. 26. Error in Mean Flow Direction Due to Misalignment in Pitch (Re. No. = 7.2)

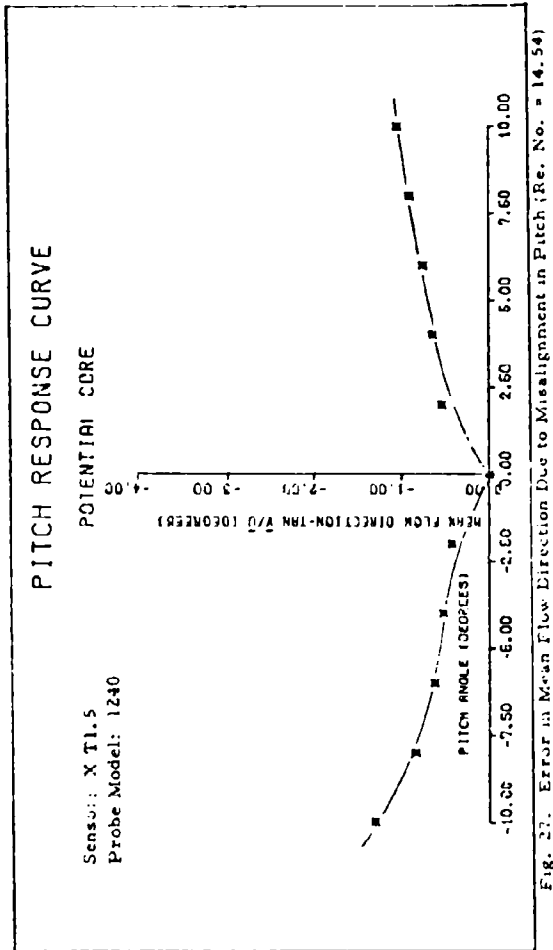


Fig. 27. Error in Mean Flow Direction Due to Misalignment in Pitch (Re. No. = 14.54)

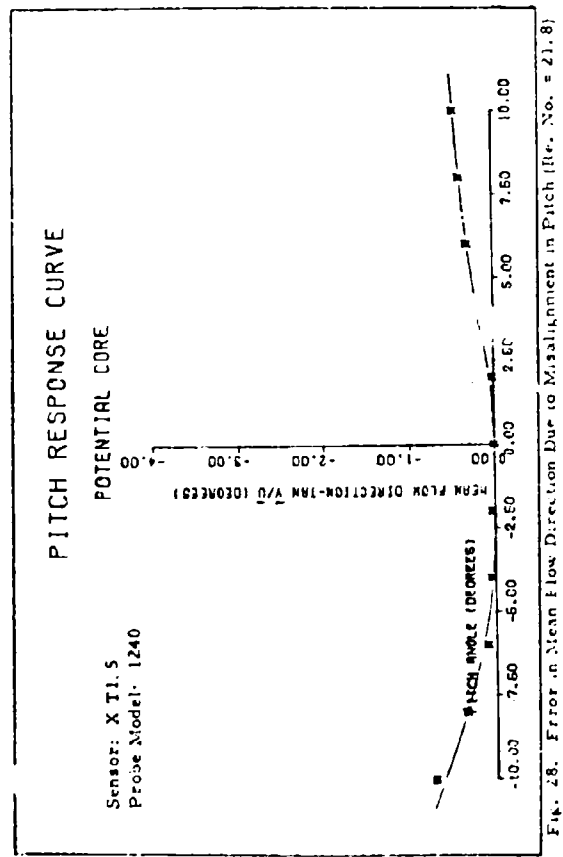


Fig. 28. Error in Mean Flow Direction Due to Misalignment in Pitch (Ref. No. = 21.8)

**Table III**  
**Rotation in Pitch (Potential Core)**  
**(Reference Orientation 48 deg)**

Re. No.	Misalignment Angle (Deg)	Mean Flow Direction (Measured) Deg.	
		Clockwise Rotation	Counterclockwise Rotation
7.2 (100 ft/sec)	$\pm 4$ $\pm 10$	-1.18 -1.57	-2.34 -3.64
14.54 (200 ft/sec)	$\pm 4$ $\pm 10$	-.656 -1.035	-.537 -1.30
21.8 (300 ft/sec)	$\pm 4$ $\pm 10$	-.210 -0.434	-.034 -.343

Rotation Tests With the X Sensor Model 1241

X sensor Model 1241 having two sensors arranged at right angles to each other with the sensor "X" lying in a plane normal to the probe axis was yawed and pitched through  $\pm 10$  degrees in the potential core. The sensor dimensions were identical to those of Model 1240 described earlier. The results of the rotation tests in X are tabulated in Appendix A. Figures 29 thru 34 show the variations of  $\bar{u}$  and  $\bar{w}$  with the yaw angle  $\phi$ . A summary of these tests is given in Table IVa. From Table IVa, it can be observed that in the range of Reynolds Number  $7.2 \leq Re \leq 21.8$ :

1. The error due to misalignment in yaw is not constant and changes with the direction of rotation.

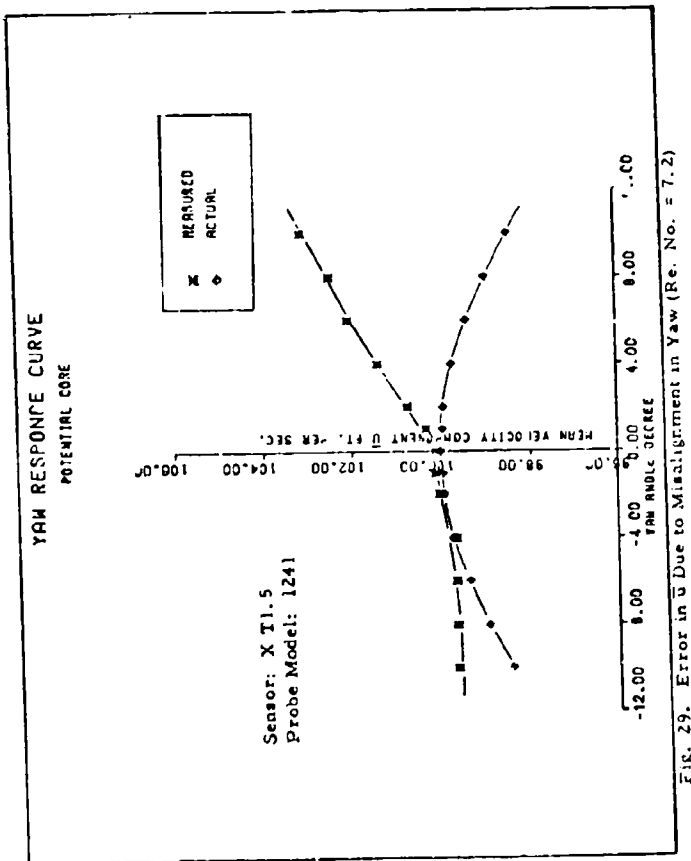


FIG. 29. Error in  $\bar{U}$  Due to Misalignment in Yaw (Re. No. = 7.2)

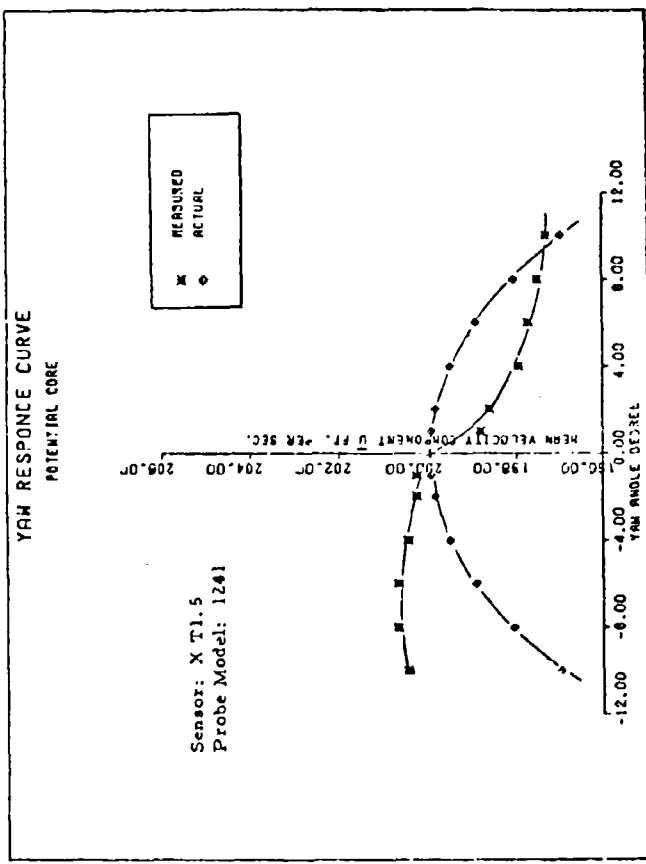


Fig. 30. Error in  $\bar{U}$  Due to Misalignment in Yaw (Re. No. = 14.54)

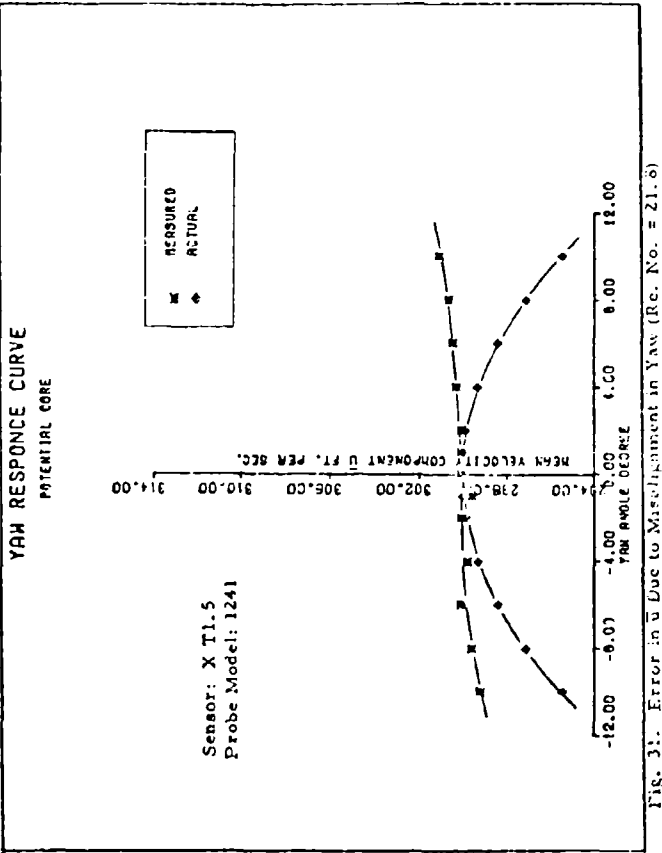


FIG. 31. Error in  $\bar{u}$  Due to Misalignment in Yaw (Re. No. = 21.6)

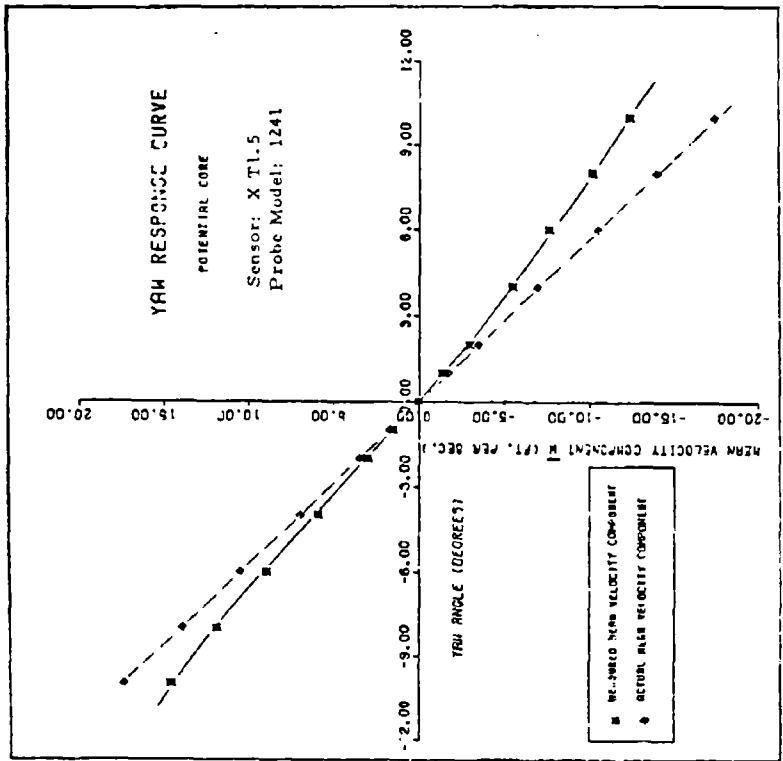


Fig. 32. Error in  $\dot{\gamma}$  Due to Misalignment in Yaw (Re. No. = 7.2)

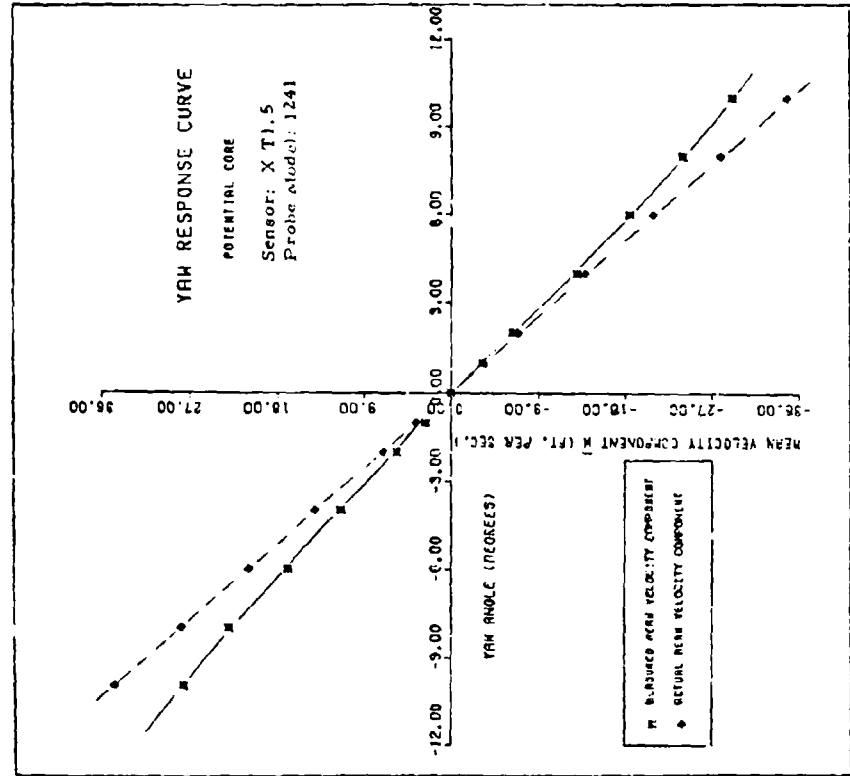


FIG. 33. Error in  $\bar{v}$  due to misalignment in Yaw (Re.No. = 14,53)

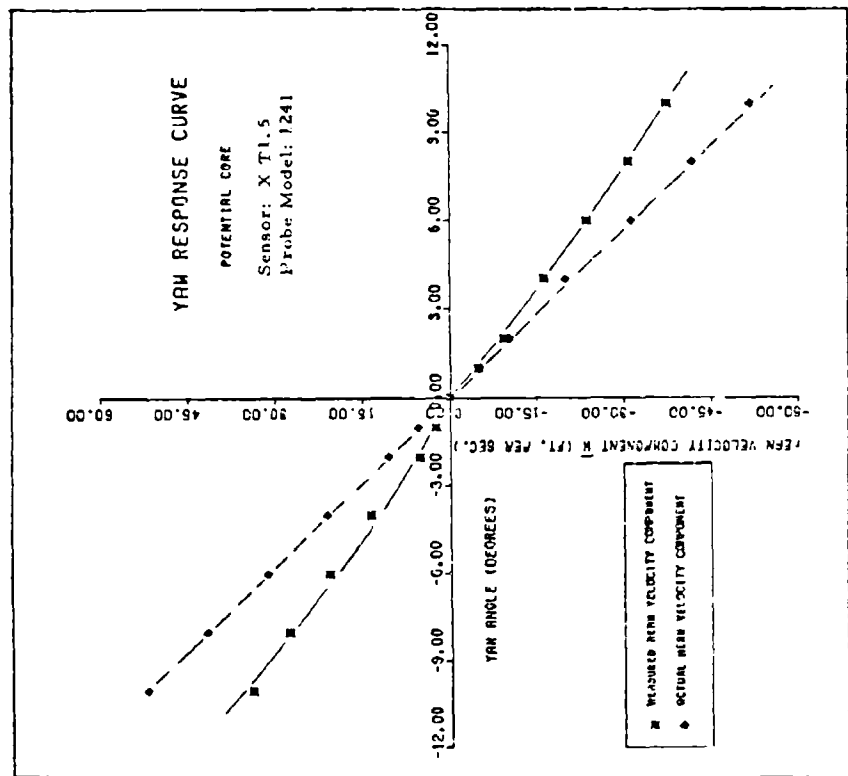


Fig. 34. Error in  $\bar{W}$  Due to Misalignment in Yaw (Re. No. = 21.8)

Table IVa  
Rotation in Yaw (Potential Core)  
(Reference Orientation 48 deg)

Re. No.	Misalign- ment Angle (deg)	Per Cent Error in			
		$\bar{u}$		$\bar{w}$	
		Clockwise Rotation	Counter Clockwise Rotation	Clockwise Rotation	Counter Clockwise Rotation
7.2 (100 ft/ sec)	$\pm 4$ $\pm 10$	-0.48% -1.47%	-1.2% -3.4%	+20.9% +28.5%	+14.55% +15.79%
14.54 (200 ft/ sec)	$\pm 4$ $\pm 10$	-0.78% +0.177%	-0.49% -1.79%	+6.3% +16.3%	+18.8% +20.4%
21.8 (300 ft/ sec)	$\pm 4$ $\pm 10$	-0.45% -1.8%	-0.157% -1.25%	+21.8% +27.9%	+35.0% +34.7%

2. The per cent error in  $\bar{u}$  due to  $\pm 10$  degrees misalignment in yaw is less than 3.5 per cent.

3. Large error occurs in  $\bar{w}$ , particularly at high Reynolds Number. Comparison with the X sensor Model 1240 (Table I) shows that for misalignment angle of 10 degrees in yaw, both the X sensors behave in somewhat similar manner. In general, it can be remarked that the mean velocity component  $\bar{u}$  can be determined quite accurately with both the X sensor arrangements in the range of Reynolds Number  $7.2 \leq Re \leq 21.8$ . However, very large error (up to 35 per cent) may occur in the measurements of  $\bar{v}$  or  $\bar{w}$  for the same misalignment angle in the same range of Reynolds Number. Figures 35 through 37 show the curves of the variations in the mean flow direction with the rotation in

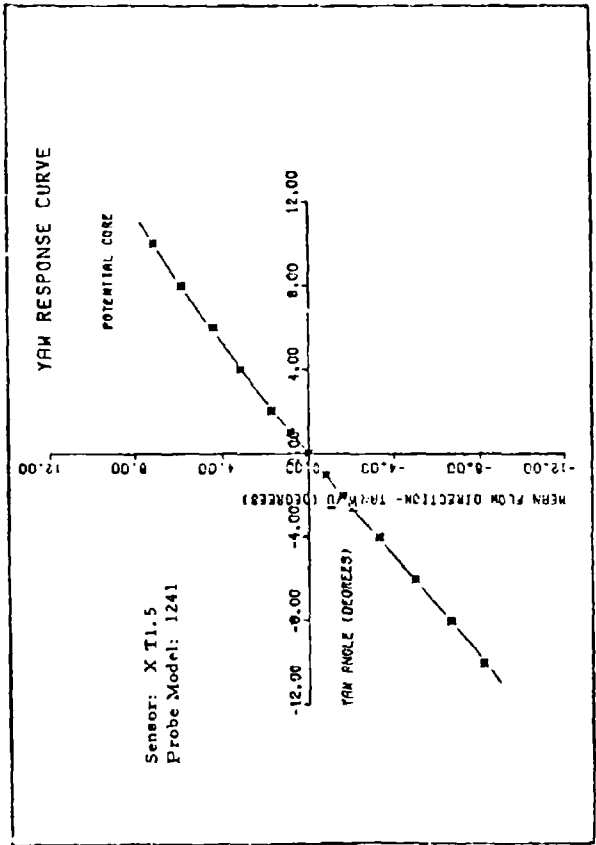


FIG. 35. Error in Mean Flow Direction Due to Misalignment in Yaw (Re. No. = 7.2)

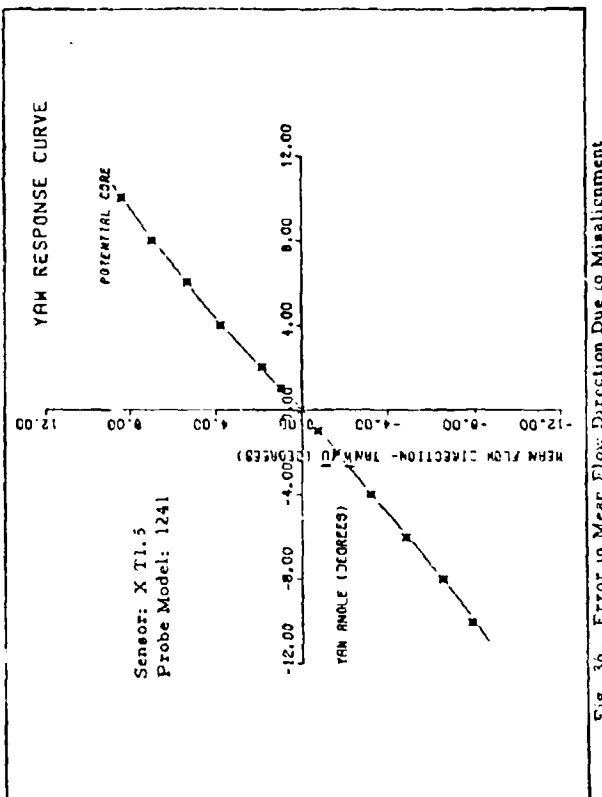


Fig. 36. Error in Mean Flow Direction Due to Misalignment  
in Yaw (Re. No. = 14,54)

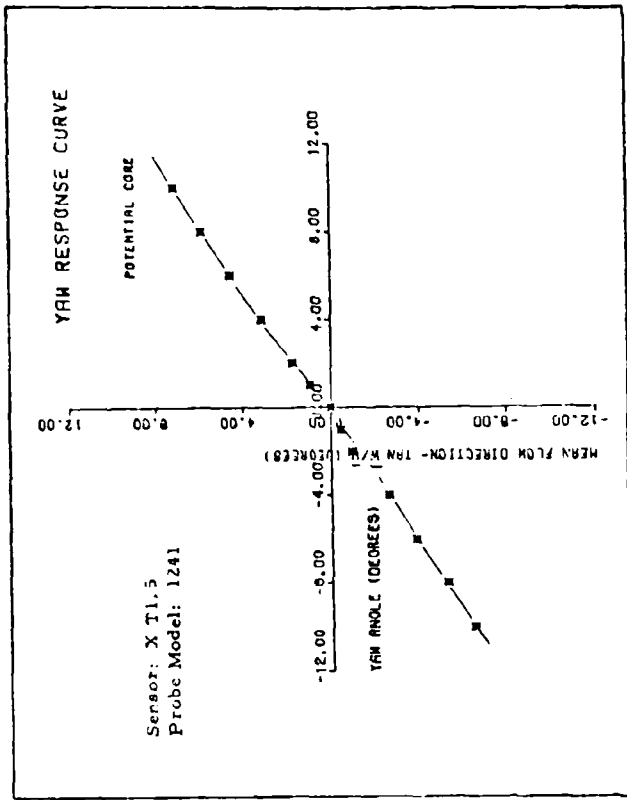


Fig. 37. Error in Mean Flow Direction Due to Misalignment in Yaw (Re. No. = 21.8)

yaw for three values of the Reynolds Numbers of interest. A summary of the error analysis is presented in Table IVb.

Table IVb  
Rotation in Yaw (Potential Core)  
(Reference Orientation 48 deg)

Re. No.	Misalignment Angle (Deg)	Per Cent Error in Mean Flow Direction	
		Clockwise Rotation	Counterclockwise Rotation
7.2 (100 ft/sec)	$\pm 4$ $\pm 10$	+15.55% +18.31%	+21.42% +29.2%
14.54 (200 ft/sec)	$\pm 4$ $\pm 10$	+19.25% +21.6%	+5.6% +16.2%
21.8 (300 ft/sec)	$\pm 4$ $\pm 10$	+35.17% +35.16%	+22.15% +28.9%

From these figures, it can be inferred that the performance of the X sensor Model 1241 is again somewhat similar to that of the Model 1240. Comparison of Tables II and IV indicates that the Model 1240 resulted in an error of 5-20 per cent due to misalignment angle of  $\pm 10$  degrees in the range of  $7.2 \leq Re \leq 21.8$ , whereas the Model 1241 yields an error which varies from 16-32 per cent approximately in the same range of Reynolds Numbers. Thus it can be remarked that it is advantageous to place the two wires out of the plane of the prongs. In other words, the X sensor Model 1240 is relatively superior for mean flow direction measurements. This conclusion is further supported by the rotation tests in pitch carried out with the Model 1241 in the potential core. The results of these tests are tabulated in Appendix A. These tests

revealed that the sensor Model 1241 was sensitive to the misalignments angles in pitch at all the three values of Reynolds Numbers of interest. From practical point of view, this represents another objectionable feature of the X sensor Model 1241.

Influence of the Air Temperature Variations  
on the Linearized Response

The second objective of the present research was to investigate experimentally the per cent error involved in the linearized bridge voltage output of the constant temperature anemometer system due to small variations in the air temperature. The results of these tests are tabulated in Appendix B and presented graphically in Figure 38. The tests were conducted in the speed range 25 feet per second (7.62 meter per second) to 300 feet per second (91.44 meter per second) in the potential core of the free jet. The air temperature was increased from 4°F to 20°F above the reference temperature (77°F). Table V shows the error analysis. For a given temperature rise  $\Delta T$ , the per cent error in the linearized bridge output is observed to remain approximately constant at airspeeds above 100 feet per second (30.48 meter per second). Below 100 feet per second, however, the per cent error in the linearized bridge output is relatively high. This is probably due to greater sensitivity of the sensor caused by rapid variations in the thickness of the thermal boundary layer in the lower range of Reynolds Number. The correction to the linearized bridge output obtained from these tests was applied to the test data and was found to yield good

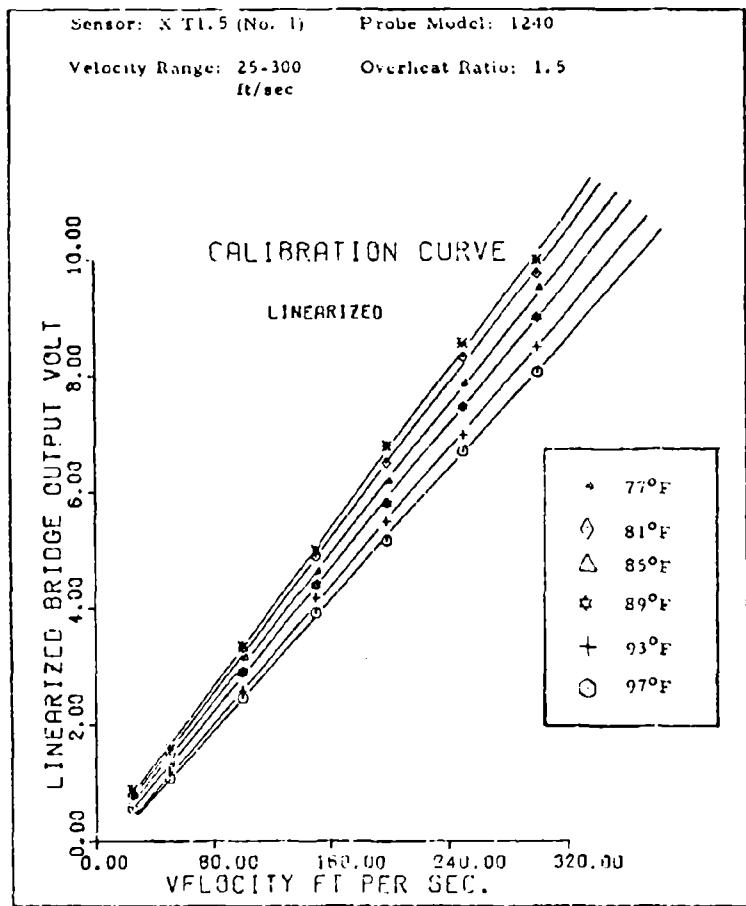


Fig. 38. Influence of Fluid Temperature Variations on Linearized Constant Temperature Anemometer System

**Table V**  
**Influence of Fluid Temperature Variations**  
**on Linearized Response**

$\Delta T$	Air Velocity (ft/sec)	25	50	100	150	200	250	300
4°F	Per Cent Error in the Linearized Bridge Voltage Output	-12.5	-8.1	-3.3	-2.4	-4.97	-2.8	-2.5
8°F	Per Cent Error in the Linearized Bridge Voltage Output	-22.98	-15.0	-6.96	-8.4	-10.1	-8.6	-5.4
12°F	Per Cent Error in the Linearized Bridge Voltage Output	-33.4	-19.37	-12.91	-12.0	-15.37	-12.85	-10.0
16°F	Per Cent Error in the Linearized Bridge Voltage Output	-41.79	-25.0	-22.5	-16.4	-19.47	-18.45	-15.0
20°F	Per Cent Error in the Linearized Bridge Voltage Output	-47.76	-33.12	-26.12	-21.8	-24.59	-21.72	-19.5

results. In addition, a comparison of these test results was made with similar tests performed by Bearman (Ref 2), and relatively large disagreement was observed at higher values of  $4T$ . Bearman, however, used an overheat ratio of 1.8 and assumed the value of King's Law exponent  $n$  equal to 0.465. Nevertheless, these tests have indicated a very strong influence of the variations in the air temperature on the linearized response of the constant temperature anemometer system particularly when the temperature changes are higher than  $4^{\circ}\text{F}$ . At low speeds (below 100 feet per second), error as high as 48 per cent in the linearized bridge output might occur, and correction to the experimental data assumes paramount importance.

#### Secondary Tests

The use of a constant temperature hot wire anemometer system for measuring the mean (and fluctuating) components of any flow requires high degree of precision and accuracy in the calibration technique. The importance of accurate calibration cannot be overemphasized and is well recognized by many experimenters. In order to gain experience and achieve perfection, a number of hot wire sensors were calibrated in the early stages of this research. During these calibrations, a number of secondary tests were conducted. These tests had significant bearing on the actual research and contributed immensely in arriving at meaningful results. The first of these tests is depicted in Fig. 39 which shows a comparison of the linearized bridge voltage output of

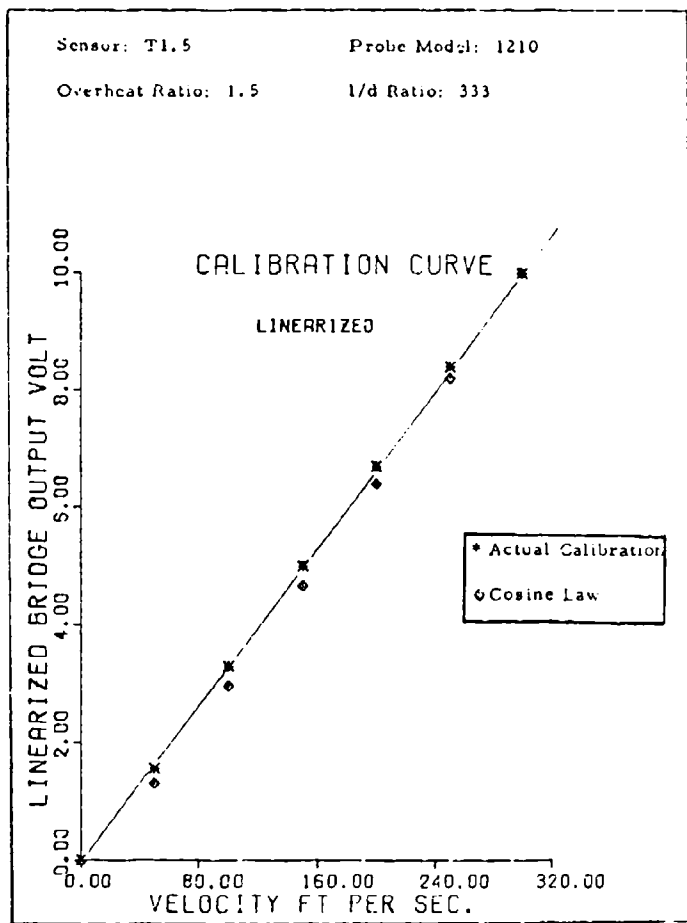


Fig. 39. Comparison of Linearized Bridge Output  
With and Without Cosine Law Cooling Assumption

the X sensor No. 1 (outer) Model 1240 with and without the assumption of "cosine law." According to this law, the sensor responds to the velocity component normal to the sensor only and is independent of the tangential velocity component. As shown by Champagne (Ref 4) and many other investigators, this assumption is valid only for wire having infinite aspect ratio. From a practical point of view, l/d ratio of 600 and above can be regarded to behave like a wire having infinite aspect ratio. In the present investigation, all the sensors had l/d ratio of approximately 333 and consequently tangential cooling effect can no longer be ignored. The calibration test, however, indicated an error of less than 1 per cent in the sensitivity of the sensor. Therefore, use of cosine law is well founded unless a high degree of accuracy is desired and one is willing to pay for it. In the second test, the single sensor Model 1210 was calibrated at three overheat ratios 1.2, 1.5 and 1.8 and its linear and non-linear calibration curves were compared. Figure 40 shows that provided relevant linearizer coefficients are used for each overheat ratio, all the data points fall on a single curve and no correction to the slope of the linearized curve is needed. On the other hand, if appropriate linearizer coefficients are not used, large error in the sensor sensitivity and hence in the velocity (both mean and fluctuating) measurement should be expected. The conclusion drawn from these tests is that it is essential to maintain the same overheat ratio during calibration and actual tests as it has significant influence on the sensor sensitivity. As the calibration data on a number of sensors was

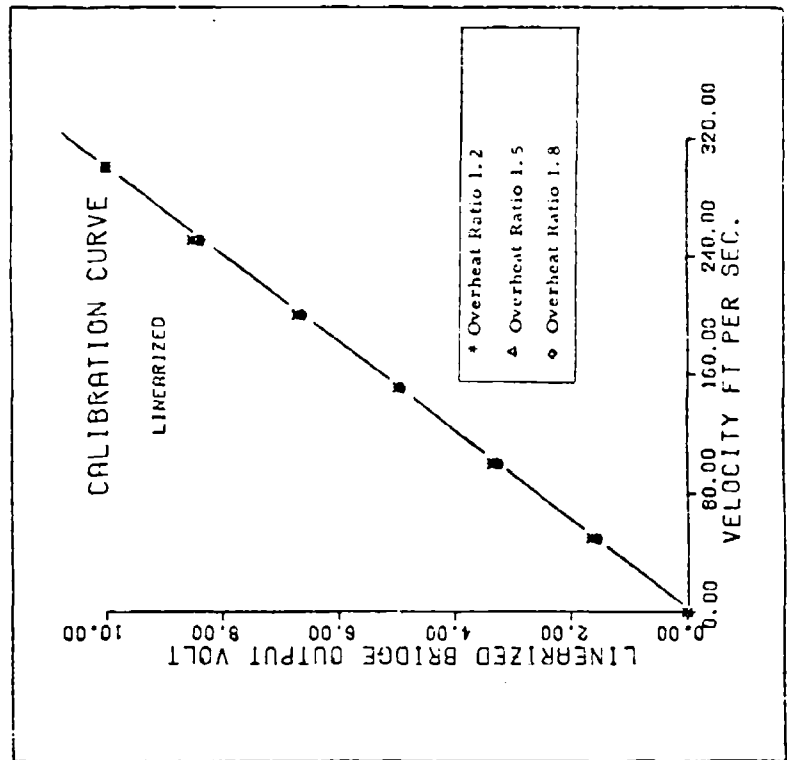


Fig. 40. Linearized Response Curve at Different Overheat Ratios

available, it was considered worthwhile to calculate the value of King's Law exponent n and compare it with the published literature. Calibration of the different sensors at overheat ratio of 1.5 gave the following results over the range of  $7.2 \leq Re \leq 2.18$ .

Table VI  
Value of King's Law Exponent n

Sensor	Orientation	Overheat Ratio	n
T1.5 Model 1214	Normal	1.5	0.245
T1.5 Model 1210	Normal	1.5	0.25
T1.5 Model 1240 (No. 1)	Normal	1.5	0.254
T1.5 Model 1210	Normal	1.2	0.404
T1.5 Model 1210	Normal	1.8	0.210
T1.5 Model 1240 (No. 1)	45 Deg	1.5	0.288
T1.5 Model 1240 (No. 2)	45 Deg	1.5	0.285

This value of n differs considerably from that quoted by Collis and Williams (Ref 3). In the range  $0 \leq Re \leq 44$  Collis and Williams obtained value of the King's Law exponent n equal to 0.45 for wires having very large aspect ratios. More recently, Klatt (Ref 15) carried out calibration of a large number of commercially available hot wire sensor in the speed range 1-40 meter per second and suggested that the value of n lies in the range 0.26-0.42. The value of n obtained from the present investigation is seen to be in excellent agreement with the results of similar tests conducted by Klatt. Table VI clearly indicates that the King's Law exponent n is dependent upon the sensor orientation and overheat ratio, in addition to the sensor aspect ratio and the range of Reynolds Number. The dirt accumulation and aging effects may also

change the value of  $n$ . Thus it is always advisable to determine the value of  $n$  from the actual calibration data rather than relying on empirical data if better accuracy of the test results is desired.

#### Rotation Tests in Shear Flow Region

One of the secondary objectives of the present investigation was to repeat the rotation tests in the shear flow region of the free jet. To achieve this goal, the X sensor Model 1240 was located at the center line and 25 centimeter away from the nozzle exit plane. The maximum turbulence intensity at this location was measured to be 15.8 per cent. Like the tests conducted in the potential core, the X sensor was yawed through  $\pm 30$  degrees and pitched through  $\pm 10$  degrees at three values of Reynolds Numbers, namely 7.2, 14.54 and 21.8 respectively. The results of these rotations are tabulated in Appendix C and represented graphically in Figures 41 thru 46. A summary of the error incurred in the mean flow direction measurement due to sensor misalignment in yaw is presented in Table VII.

As before, the per cent error is not constant for a given misalignment angle and strongly depends upon the direction of rotation. In other words, the X sensor has a strong preference for the direction of rotation in the shear flow region as well. The second feature which is common with the test results obtained in the potential core is that relatively large error occurs at very small misalignment angles. The fundamental difference between the results of the rotation tests

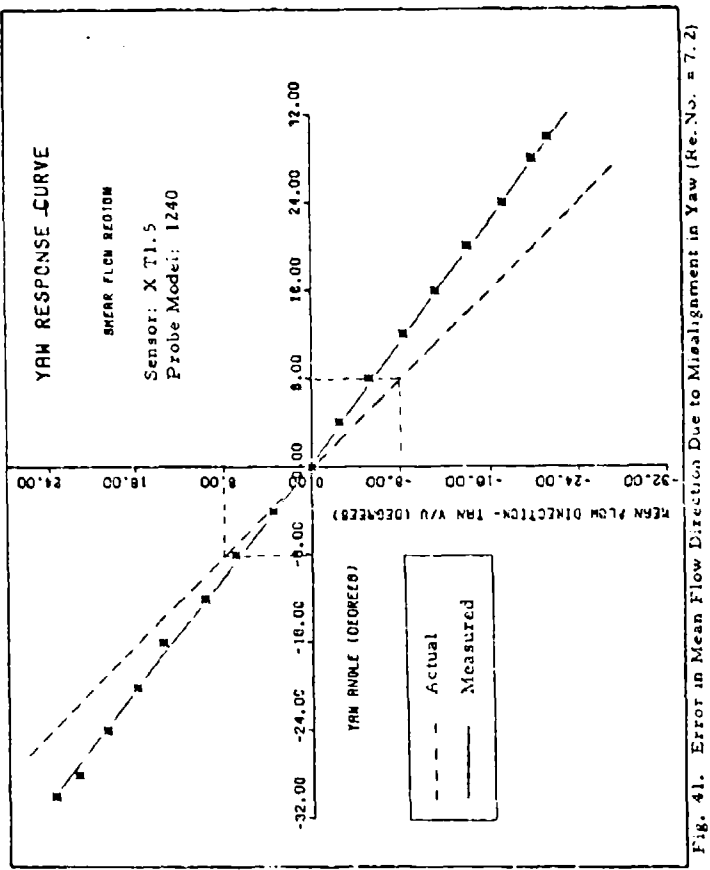


Fig. 41. Error in Mean Flow Direction Due to Misalignment in Yaw (Ref. No. = 7.2)

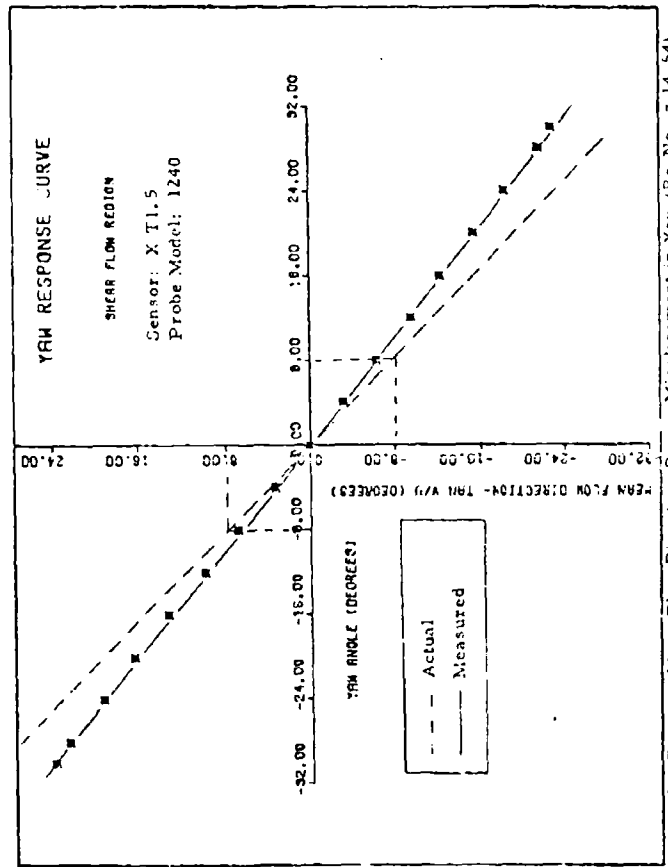


Fig. 42. Error in Mean Flow Direction Due to Misalignment in Yaw ( $Re, Nc = 14,54$ )

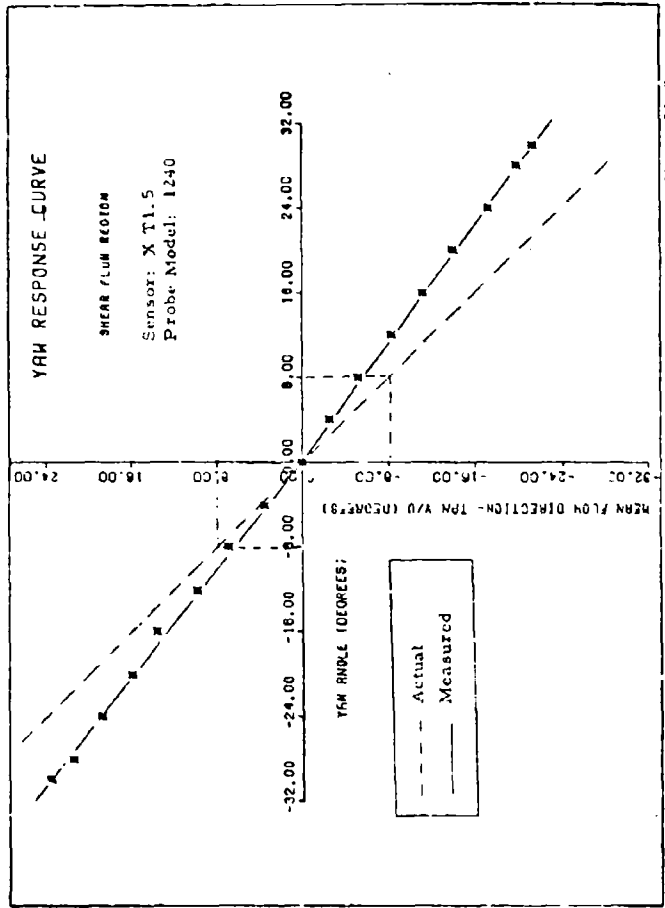
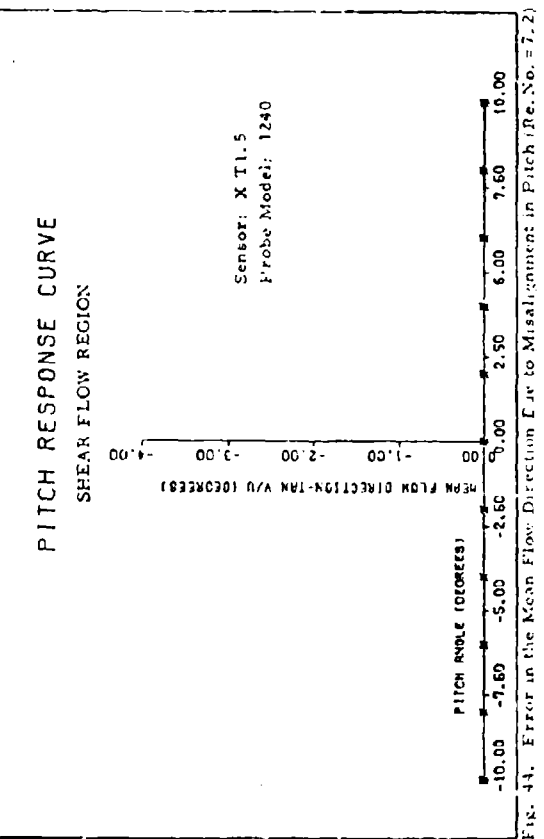


Fig. 43. Error in Mean Flow Direction Due to Misalignment in Yaw (Re. No. = 21.8)



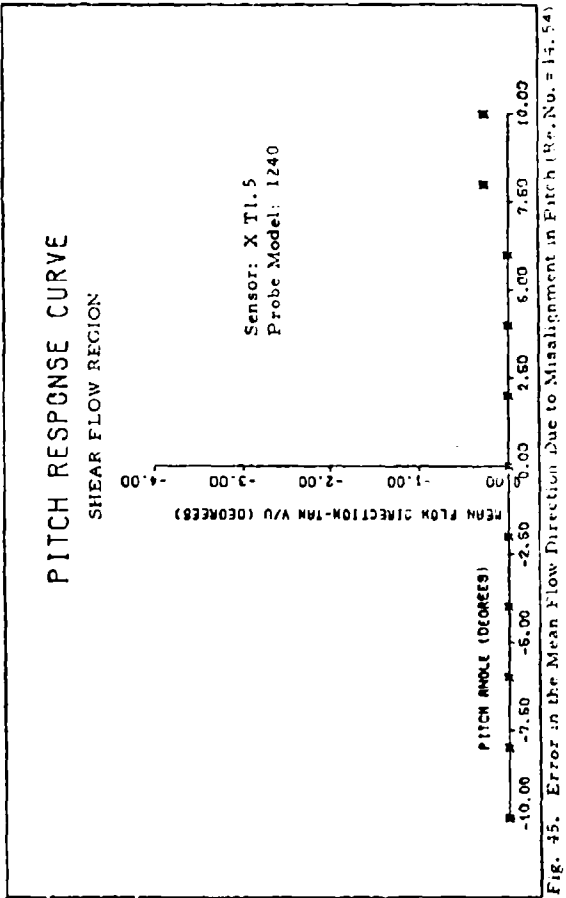


FIG. 45. Error in the Mean Flow Direction Due to Misalignment in Pitch Rn. No. = 14.54.

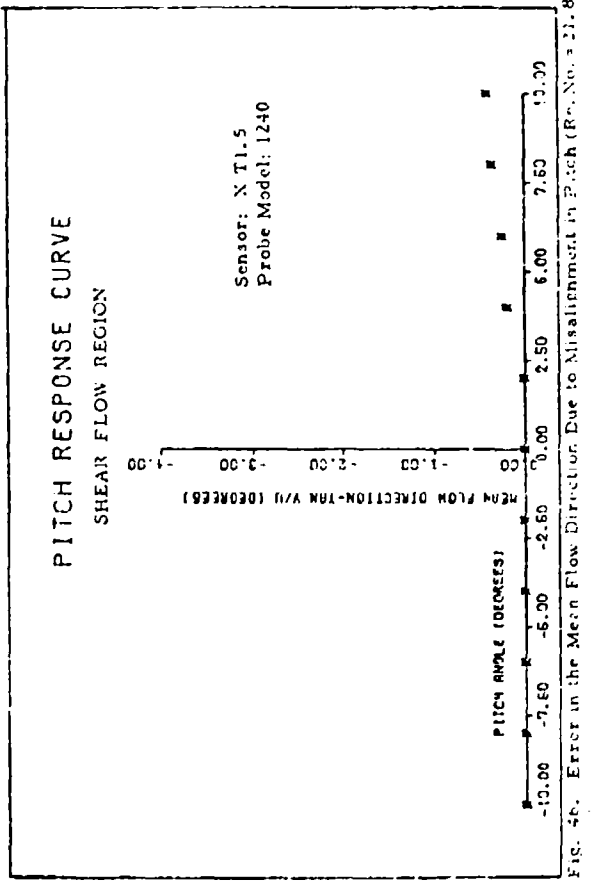


FIG. 4c. Error in the Mean Flow Direction Due to Misalignment in Pitch (Ref. No. 21.8)

Table VII  
Rotation in Yaw (Shear Flow Region)  
(Reference Orientation 48 Deg)

Re. No.	Misalignment Angle (Deg)	Per Cent Error in the Mean Flow Direction	
		Clockwise Rotation	Counterclockwise Rotation
7.2	4.0	-37.5%	-12.7%
	10.0	-29.8%	-16.23%
	20.0	-29.36%	-20.29%
	30.0	-28.9%	-21.25%
14.54	4.0	-33.75%	-28.1%
	10.0	-14.08%	-26.02%
	20.0	-17.93%	-25.59%
	30.0	-18.73%	-26.15%
21.8	4.0	-13.35%	-23.4%
	10.0	-16.6%	-21.89%
	20.0	-17.77%	-22.70%
	30.0	-20.29%	-23.76%

performed in the potential core and the shear flow regions is that the per cent error practically remains constant at approximately 22 per cent (on the average) in the range  $14.54 \leq Re \leq 21.8$  and at 25 per cent at  $Re$  equal to 7.2. In other words, the interference effects of the sensor prongs on the active portion of the downstream sensor are not as severe. The large error encountered in the mean flow direction measurements leads to the conclusion that the assumption of fluctuating velocity components being negligible as compared to their respective mean values is no longer valid.

### Rotation Tests in Pitch

The X sensor Model 1240 was pitched through  $\pm 10$  degrees in the shear flow region at the location mentioned earlier. The results of these rotation tests are tabulated in Appendix C and represented graphically in Figures 44 thru 46. These tests revealed that the Model 1240 sensor was insensitive to the misalignment in pitch up to angles as high as 30 degrees in the range  $7.2 \leq Re \leq 21.8$ .

## VII. Conclusions and Recommendations

### Conclusions

The sensor rotation tests carried out with the two X wire arrangements (TSI Model 1240 and TSI Model 1241) in the potential core of the free jet have led to the following conclusions:

1. Both the X sensor arrangements possess a strong preferred direction of mean motion resulting in errors which vary considerably with rotation in one direction than the other. This trend existed throughout the Reynolds Number range  $7.2 \leq Re \leq 21.8$ . This asymmetry in the sensor response makes it difficult to quote a single value for the per cent error due to misalignment in yaw or pitch and that only the range of errors due to a certain misalignment can be specified.

2. The mean velocity component  $\bar{u}$  can be measured within 4 per cent error approximately with both the sensor arrangements for misalignment in yaw up to 10 degrees in the range of Reynolds Number  $7.2 \leq Re \leq 21.8$ . However, for the same misalignment angle in yaw, errors in v and w are quite large and vary between 2-35 percent depending upon the sense of rotation and Reynolds Number.

3. The X sensor Model 1240 resulted in 5-20 percent error approximately in the mean flow direction due to 10 degrees misalignment in yaw in the range of Reynolds Number  $7.2 \leq Re \leq 21.8$ . The X

sensor Model 1241, on the other hand, resulted in 19-32 per cent error for the same misalignment angle in yaw in the same Reynolds Number range. From these figures, it appears that the X wire arrangement having sensors out of the probe plane is relatively superior.

4. At very small misalignment angles (1-4 degrees) in yaw, both the sensors displayed large error (up to 28 per cent approximately). This leads to the conclusion that the very small misalignments in yaw should be avoided.

5. The X sensor Model 1240 is less sensitive to misalignment in pitch as compared to Model 1241. With the Model 1240, misalignment in pitch of  $\pm 10$  degrees resulted in 0.3-10 per cent error in the range  $14.54 \leq Re \leq 21.8$ . This proves another useful characteristic of the X wire arrangement of Model 1240 as compared to Model 1241.

Conclusions from the second part of the research are:

1. Large errors in the linearized response of the hot wire sensor occur due to variations in the air temperature particularly if the changes in the fluid temperature are in excess of  $4^{\circ}\text{F}$ .
2. At low speeds (below 100 feet per second), the error in the linearized sensor response is considerably higher even at low values of  $\Delta T$ .

From the secondary tests conducted during this research, the following conclusions are drawn:

1. The linearized response of a hot wire sensor is highly dependent upon the precision and accuracy of calibration.

2. For normal laboratory investigation, simple cosine cooling law gives adequate accuracy.

3. The value of King's Law exponent  $n$  is not only a function of Reynolds Number, sensor aspect ratio, dirt accumulation, aging effects but it also depends upon the overheat ratio and the sensor orientation relative to the mean flow direction.

4. Overheat ratio has significant effect on the sensor response, both linear and non-linear. Care must, therefore, be exercised to maintain the same overheat ratio during calibration and actual tests.

5. The tendency of the X sensor to have preference for the direction of mean motion exists in the shear flow region to a larger extent.

6. The per cent error in the mean flow direction due to sensor misalignment in yaw is much greater than that in the potential core for the same yaw angle. However, spread in the data is considerably less as compared to potential core.

7. At very small misalignment angles, the performance of the X sensor is identical to that in the potential core.

8. The X sensor Model 1240 is insensitive to the misalignment in pitch up to pitch angle of 10 degrees in the shear flow region.

9. The assumption of negligible fluctuating velocity components relative to their respective mean values is no longer valid in the shear flow region.

### Recommendations

After investigating the performance of the X sensors in the potential core and the shear flow regions of the free jet, the following recommendations are made for further research:

1. A number of X sensors can be tested in the potential core of the free jet and "active" lengths of the two wires varied appropriately in order to investigate if it results in improved sensor response as far as asymmetry of the sensor response curves is concerned.
2. The sensor was assumed to operate in continuum flow and slip flow effects were neglected. It would be illuminating to investigate the X sensor performance in the potential core and in the shear flow regions of the free jet when slip flow effects are taken into account.
3. The variac Model 50-B had the capacity of raising the air temperature up to 50°F. It would be interesting to extend the range of correction to the linearized bridge voltage output of the constant temperature anemometer system to variations in the air temperature of 50°F and above, both in the potential core and shear flow regions of the free jet.
4. It would be desirable to improve upon free jet facility settling chamber pressure control system. A pressure regulating valve and a needle valve if incorporated in the system would offer considerable time saving and improve the accuracy.

5. The cathodometer and the sensor attachment system may be improved upon so that the sensor can be aligned relative to the mean flow direction with a high degree of precision.

### Bibliography

1. Bruun, H. H. "Interpretation of X Hot Wire Signals," Disa Information No. 18 (September 1975).
2. Bearman, P. W. "Correction for the Effect of Ambient Temperature Drift on Hot Wire Measurements in Incompressible Flow," Disa Information No. 11 (May 1971).
3. Collis, D. C., and Williams M. J. "Two Dimensional Convection from Heated Wires at Low Reynolds Numbers," Journal of Fluid Mechanics, Vol. 6, pp. 357-384 (1959).
4. Champagne, F. H. "Turbulence Measurements with Inclined Hot Wires," Boeing Scientific Research Laboratories, Flight Science Lab Report No. 103 (December 1965).
5. Comte-Bellot G., Strohl, A. and Alcaraz E. "On Aerodynamic Disturbances Caused by Single Hot Wire Probe," Journal of Applied Mechanics, pp. 767-773 (December 1971).
6. Dean, R. C., Jr. "Aerodynamic Measurements," Gas Turbine Laboratory, M.I.T. (1953).
7. Eckert, E. R. G., and Drake, R. M. "Analysis of Heat and Mass Transfer," McGraw Hill Book Company (1972).
8. Frieche, C. A., and Schwartz, W. H. "Deviation from Cosine Law for Yawed Cylindrical Anemometer Sensors," A.S.M.E. Series E, J. Appl. Mech., Vol. 35, p. 665 (1968).
9. Gilmore, D. C. "The Probe Interference Effect of Hot Wire Anemometer," TN 67-3, Mechanical Engineering Research Laboratories, McGill University, Montreal (July 1967).
10. Holman, J. P. "Heat Transfer," Second Edition, McGraw Hill Book Company (1968).
11. Hinze, J. O. "Turbulence," Second Edition, McGraw Hill Book Company (1975).

12. Jorgensen, F. E. "Directional Sensitivity of Wires and Fibre Film Probes." Disa Information No. 11, pp. 31-37 (May 1971).
13. Jerome, F. E., Guilton, D. E. and Patel, R. P. "Experimental Study of the Thermal Wake Interference Between Closely Spaced Wires of a X Type Hot Wire Probe," The Aeronautical Quarterly (May 1971).
14. Kanevce, G., and Oka, S. "Correcting Hot Wire Readings for Influence of Fluid Temperature Variations," Disa Information No. 15 (October 1973).
15. Klatt, F. "The X Hot Wire Probe in a Plane Flow Field," Disa Information No. 8 (July 1969).
16. Ko, N. W. M., and Davies, P. O. A. L. "Interference Effect of Hot Wires," IEEE Transactions on Instrumentation and Measurements IM 20 pp. 76-78 (1970).
17. Norman, B. O. "Hot Wire Anemometer Calibration at High Subsonic Speeds," Disa Information No. 5
18. Perkins, H. J. "The Measurement of Reynolds Stresses in Low Intensity Turbulent Flow," Department of Engineering, University of Cambridge Report and Memoranda No. 3668 (January 1970).
19. Rasmussen, C. G. "Measurement of Turbulent Characteristics," Disa Information No. 3
20. Rose, W. G. "Some Corrections to the Linearized Response of a Constant Temperature Hot Wire Anemometer Operated in a Low Speed Flow," Transactions of ASME, pp. 554-558 (September 1962).
21. Parthasarathy, S. P., and Tritton, D. J. "Impossibility of Linearizing a Hot Wire Anemometer for Turbulent Flows," AIAA Journal, Vol. 1, No. 5 (May 1963).
22. Saastrup, Kristensen, H. "Hot Wire Measurements in Turbulent Flows," Fluid Mechanics Department Technical University of Denmark, Disa Information Department (November 1973).
23. Shepard, W. K. "Turbulence Measurements in a Plane Free Jet at High Subsonic Speeds," AFIT MS Thesis GAE/AE/74D-24, Air Force Institute of Technology, WPAFB, Ohio.

24. Sandborn, V. A. "Resistance Temperature Transducers," Metrology Press, Fort Collins, Colorado (1972).
25. Thermo-Systems, Inc. "Operating and Service Manual for 1050 Series Constant Temperature Anenometers and Related Accessories," Thermo-Systems, Inc., St. Paul, Minnesota.
26. Thermo-Systems, Inc. "Instruction Manual for Model 1015C Correlator," Thermo-Systems, Inc., St. Paul, Minnesota.
27. Thermo-Systems, Inc. "Calibrator Model 1125 Instruction Manual," St. Paul, Minnesota, Thermo-Systems, Inc.
28. Thermo-Systems, Inc., "X Probe Calibration Set Up Procedure," Technical Bulletin TB12, St. Paul, Minnesota. Thermo-Systems, Inc.
29. Tennekes, H., and Lumley, J. L. "A First Course in Turbulence," The MIT Press (1972).
30. Thermo-Systems, Inc. "Hot Wire-Hot Film-Ion Anenometer Systems Catalogue," St. Paul, Minnesota, Thermo-Systems, Inc.
31. Webster, C. A. G. "A Note on the Sensitivity to Yaw of a Hot Wire Anenometer," J. Fluid Mechanics, Vol. 13, p. 307 (1962).

Appendix A  
Experimental Data of Rotation Tests

Table VIII  
Rotation in Yaw

Run No.	Yaw Angle $\phi$ Deg.	Rotation Deg.	DC Voltmeter-Volt (A+B) (A-B)	ft/sec $\bar{u}$	ft/sec $\bar{v}$	Deg. $\tan^{-1} \frac{\bar{v}}{\bar{u}}$
1	48	0	4.71	-0.003	99.93	0.00
2	49	+1	4.67	-0.115	99.08	-2.433
3	50	+2	4.66	-0.253	98.868	-5.367
4	51	+3	4.65	-0.328	98.65	-6.958
5	52	+4	4.66	-0.417	98.868	-8.847
6	54	+6	4.63	-0.556	98.23	-12.00
7	56	+8	4.63	-0.701	98.23	-14.87
8	58	+10	4.58	-0.802	97.17	-17.01
9	60	+12	4.52	-0.890	95.898	-18.88
10	62	+14	4.44	-1.00	94.20	-21.21
11	64	+16	4.39	-1.12	93.14	-23.76
12	66	+18	4.30	-1.22	91.23	-25.88
13	68	+20	4.22	-1.33	89.53	-28.218
14	70	+22	4.12	-1.40	87.41	-29.70
15	72	+24	4.00	-1.46	84.86	-30.97
16	74	+26	3.88	-1.53	82.31	-32.46
17	76	+28	3.77	-1.60	79.78	-33.94
18	78	+30	3.66	-1.68	77.65	-35.64

Table IX  
Rotation in Yaw

				Sensor Location: 1 cm			
				Probe Model: 1240			
				Slopes: $K_1 = K_2 = 30 \text{ ft/sec/volt}$			
				Cathodometer: $X_0 = 3.136 \text{ ins}$			
				$Y_0 = 8.871 \text{ cm}$			
				$Z_0 = 7.716 \text{ ins}$			
Run No.	Yaw Angle	Rotation Deg	DC Voltmeter-Volt (A+B)	$\bar{u}$ ft/sec	$\bar{v}$ ft/sec	$\tan^{-1} \frac{\bar{v}}{\bar{u}}$ Deg	
1	48	0	4.71	-0.003	99.93	0.00	0.00
2	49	-1	4.71	+0.102	99.93	2.164	+1.24
3	50	-2	4.72	+0.190	100.14	4.031	+2.30
4	51	-3	4.73	+0.318	100.35	5.746	+3.27
5	52	-4	4.71	+0.378	99.93	8.0198	+4.588
6	54	-6	4.75	+0.580	100.77	12.30	+6.962
7	56	-8	4.66	+0.748	98.86	15.87	+9.120
8	58	-10	4.61	+0.901	97.80	19.11	+11.059
9	60	-12	4.56	+1.05	96.74	22.27	+12.968
10	62	-14	4.50	+1.20	95.50	25.459	+15.092
11	64	-16	4.45	+1.36	94.41	28.85	+16.99
12	66	-18	4.40	+1.50	93.36	31.82	+18.823
13	68	-20	4.35	+1.64	92.29	34.79	+20.657
14	70	-22	4.29	+1.76	91.01	37.34	+22.30
15	72	-24	4.24	+1.89	89.95	40.03	24.026
16	74	-26	4.18	+2.20	88.68	46.67	27.75
17	76	-28	4.12	+2.418	87.40	51.30	
18	78	-30	4.04	+2.509	85.71	53.23	

Table X  
Rotation in Yaw

Region: Potential Core  
 Sensor: X T1.5  
 Re. No.: 14.54 (200 ft/sec)  
 Ref. Orientation: 48 deg.  
 Fluid Temperature: 78°F

Run No.	Yaw Angle ϕ Deg.	Rotation Deg.	DC Voltmeter-Volt (A+B)	ft/sec $\bar{u}$	ft/sec $\bar{v}$	Deg. $\tan^{-1} \frac{\bar{v}}{\bar{u}}$
1	48	0	9.430	0.00	200.07	0.0
2	49	+1	9.42	-0.155	199.86	-3.288
3	50	+2	9.412	-0.315	199.70	-6.68
4	52	+4	9.355	-0.463	198.50	-9.82
5	54	+6	9.30	-0.773	197.50	-16.40
6	56	+8	9.25	-1.044	196.25	-22.15
7	58	+10	9.174	-1.293	194.64	-27.43
8	60	+12	9.044	-1.585	191.88	-33.628
9	62	+14	8.90	-1.855	188.82	-39.35
10	64	+16	8.77	-2.09	186.06	-44.34
11	66	+18	8.61	-2.33	182.67	-49.43
12	68	+20	8.46	-2.55	179.49	-54.10
13	70	+22	8.26	-2.74	175.24	-58.13
14	72	+24	8.07	-2.90	171.21	-61.52
15	74	+26	7.83	-3.04	166.12	-64.49
16	76	+28	7.58	-3.16	160.82	-67.04
17	78	+30	7.37	-3.30	156.36	-70.014

Table XI  
Rotation in Yaw

Region: Potential Core					Sensor Location: 1 cm		
Run No.	Yaw Angle ϕ Deg.	Rotation Deg.	DC Voltmeter-Volt (A+B)	ft/sec $\bar{v}$	ft/sec $\bar{v}$	Deg⁻¹ $\frac{\bar{v}}{\bar{u}}$	
1	48	0	9.430	0.00	200.07	0.0	
2	47	-1	9.420	+0.281	199.85	5.9618	
3	46	-2	9.430	+0.427	200.07	9.059	
4	44	-4	9.430	+0.586	200.07	12.43	
5	42	-6	9.418	+0.725	199.816	15.38	
6	40	-8	9.406	+1.016	199.56	21.55	
7	38	-10	9.380	+1.302	199.0	27.62	
8	36	-12	9.328	+1.568	197.9	33.26	
9	3.	-14	9.236	+1.864	195.95	39.54	
10	32	-16	9.129	+2.149	193.68	45.59	
11	30	-18	9.040	+2.423	191.79	51.407	
12	28	-20	8.932	+2.702	189.50	57.326	
13	26	-22	8.812	+2.976	186.96	63.140	
14	24	-24	8.702	+3.244	184.62	68.82	
15	22	-26	8.579	+3.497	182.01	74.19	
16	20	-28	8.459	+3.752	179.47	79.60	
17	18	-30	8.355	+4.010	177.26	85.07	

Table XII  
Rotation in Yaw

Region: Potential Core  
 Sensor Type: X Tr. 5  
 Re. No.: 21.8 (300 ft/sec)  
 Slopes:  $K_1 = K_2 = 30$  ft/sec/volt

Fluid Temperature: 80°F

Sensor Location: 1 cm  
 Probe Model: 1240  
 Reference Orientation: 48 deg  
 Cathodometer:  $X_0 = 3.136$  ins  
 $Y_0 = 8.871$  cm  
 $Z_0 = 7.716$  ins

Run No.	Yaw Angle $\phi$ Deg.	Rotation Deg.	DC Voltmeter-Volt (A+B)	ft/sec $\bar{u}$	ft/sec $\bar{v}$	$\frac{\bar{v}}{\bar{u}}$	$\tan^{-1} \frac{\bar{v}}{\bar{u}}$
1	48	0	14.154	-0.002	300.29	-0.042	0.00
2	49	+1	14.13	-0.205	299.787	-4.349	-0.0145
3	50	+2	14.10	-0.405	299.15	-8.592	-0.287
4	51	+3	14.065	-0.614	298.408	-13.027	-0.4365
5	52	+4	14.01	-0.815	297.24	-17.291	-0.5817
6	54	+6	13.89	-1.18	294.69	-25.035	-0.8495
7	56	+8	13.73	-1.52	291.36	-32.248	-1.107
8	58	+10	13.53	-1.86	287.057	-39.46	-1.37464
9	60	+12	13.31	-2.18	282.39	-46.25	-1.63780
10	62	+14	13.07	-2.48	277.298	-52.6	-1.89687
11	64	+16	12.80	-2.72	271.57	-57.708	-2.12497
12	66	+18	12.49	-3.03	264.99	-64.285	-2.1792
13	68	+20	12.19	-3.28	258.628	-69.589	-2.6907
14	70	+22	11.85	-3.54	251.41	-75.10	-2.98715
15	72	+24	11.45	-3.84	242.92	-81.47	-3.35378
16	74	+26	11.05	-4.12	234.4	-87.411	-3.729138
17	76	+28	10.72	-4.35	227.4	-92.29	-4.058487
18	78	+30	10.35	-4.55	219.58	-96.53	-4.39612

Table XIII  
Rotation in Yaw

Run No.	Yaw Angle $\phi$ Deg.	Rotation Deg.	DC Voltmeter-Volt (A+B)		ft/sec $\bar{v}$	ft/sec $\bar{v}$	$\tan^{-1} \frac{\bar{v}}{\bar{u}}$ Deg.
			(A-E)				
1	47	-1	14.16	+0.265	300.4	5.622	1.07
2	46	-2	14.16	+0.480	300.4	10.1833	1.941
3	45	-3	14.17	+0.710	300.6	15.0636	2.868
4	44	-4	14.18	+0.951	300.8	20.176	3.8373
5	42	-6	14.23	+1.405	301.90	29.809	5.6389
6	40	-8	14.265	+1.855	302.55	39.356	7.41147
7	38	-10	14.286	+2.275	303.07	48.267	9.0489
8	36	-12	14.25	+2.692	302.33	57.1145	10.697
9	34	-14	14.18	+3.06	300.848	64.92	12.177
10	32	-16	14.05	+3.43	298.09	72.77	13.719
11	30	-18	13.88	+3.75	294.48	79.56	15.1187
12	28	-20	13.70	+4.07	290.66	86.35	16.545
13	26	-22	13.55	+4.45	287.48	94.41	18.180
14	24	-24	13.40	+4.84	284.29	102.68	19.858
15	22	-26	13.19	+5.15	279.84	109.26	21.327
16	20	-28	13.01	+5.48	276.02	116.659	22.911
17	18	-30	12.75	+5.68	270.5	120.5	24.011

Table XIV  
Rotation in Yaw

Region: Potential Core		Sensor Location: 1 cm	
Sensor Type: X T1.5	Probe Model: 1240	Slopes: $K_1 = K_2 = 30$ ft/sec/volt	
R. No.: 7.2 (100 ft/sec)		Cathodometer: $X_0 = 3.136$ ins	
Reference Orientation: 135 deg.		$Y_0 = 8.871$ cm	
Fluid Temperature: 75°F		$Z_0 = 7.716$ ins	
			Deg. $\frac{\bar{v}}{\tan^{-1} \frac{\bar{v}}{u}}$
1	135	0	0.00
2	136	+1	+0.043
3	137	+2	+0.09
4	138	+3	+0.147
5	140	+5	+0.250
6	142	+7	+0.352
7	144	+9	+0.467
8	146	+11	+0.590
9	148	+13	+0.747
10	150	+15	+0.900
11	152	+17	+1.065
12	154	+19	+1.208
13	156	+21	+1.350
14	158	+23	+1.50
15	160	+25	+1.629
16	162	+27	+1.75
17	164	+29	+1.86
18	166	+31	+1.965

**Table XV**  
Rotation in Yaw

Region: Potential Core		Sensor Type: X T1.5		Sensor Location: 1 cm		Probe Model: 1240	
Re. No.: 7.2 (100 ft/sec)		Reference Orientation: 135 deg		Cathodometer: $X_0 = 3.136$ ins			
Fluid Temperature: 75°F				$Z_0 = 7.716$ ins			
Run No.	Yaw Angle $\phi$ Deg.	Rotation Deg.	DC Voltmeter-Volt (A+B)	DC Voltmeter-Volt (A-B)	ft/sec $\underline{u}$	ft/sec $\bar{v}$	Deg. $\tan^{-1} \frac{\bar{v}}{\underline{u}}$
1	135	0	4.71	0.00	99.93	0.00	0.00
2	134	-1	4.71	-0.048	99.93	-1.018	-0.584
3	133	-2	4.685	-0.111	99.39	-2.35	-1.357
4	132	-3	4.668	-0.160	99.03	-3.39	-1.963
5	130	-5	4.640	-0.280	98.44	-5.94	-3.45
6	128	-7	4.62	-0.402	98.01	-8.528	-4.97
7	126	-9	4.58	-0.51	97.17	-10.82	-6.35
8	124	-11	4.51	-0.598	95.68	-12.68	-7.55
9	122	-13	4.40	-0.640	93.35	-13.58	-8.276
10	120	-15	4.28	-0.690	90.08	-14.633	-9.23
11	118	-17	4.16	-0.748	88.26	-15.86	-10.193
12	116	-19	4.08	-0.830	86.56	-17.60	-11.499
13	114	-21	4.00	-0.910	84.86	-19.30	-12.817
14	112	-23	3.93	-1.040	83.38	-22.06	-14.82
15	110	-25	3.84	-1.120	81.47	-23.76	-16.26
16	108	-27	3.75	-1.170	79.56	-24.82	-17.328
17	106	-29	3.64	-1.240	77.22	-25.308	-18.813
18	104	-31	3.53	-1.30	74.89	-27.58	-20.218

**Table XVI**  
**Rotation in Yaw**

Run No.	Potential Core Sensor: X T1.5	Yaw Angle φ Deg.	Rotation Deg.	DC Voltmeter-Volt (A+B)	DC Voltmeter-Volt (A-B)	ft/sec $\bar{u}$	ft/sec $\bar{v}$	Deg. $\tan^{-1} \frac{\bar{v}}{\bar{u}}$
1	Region: 135	0	9.43	0.0	200.07	0.00	0.00	0.00
2	Sensor: 136	+1	9.43	+0.128	200.07	2.7157	0.7776	
3	Re. No.: 137	+2	9.44	+0.260	200.28	5.516	1.5776	
4	Ref. Orientation: 138	+3	9.44	+0.404	200.28	8.571	2.450	
5	Fluid Temperature: 140	+5	9.43	+0.657	200.07	13.939	3.985	
6	75°F	+7	9.43	+0.948	200.07	20.113	5.740	
7	142	+9	9.41	+1.220	199.64	25.88	7.386	
8	144	+11	9.38	+1.475	199.0	31.29	8.9358	
9	146	+13	9.31	+1.741	197.52	36.937	10.592	
10	148	+15	9.23	+2.02	195.827	42.857	12.378	
11	150	+17	9.145	+2.27	194.024	48.161	13.940	
12	152	+19	9.04	+2.53	191.79	53.677	15.635	
13	154	+21	8.90	+2.83	188.82	60.04	17.639	
14	156	+23	8.75	+3.11	186.64	65.98	19.469	
15	158	+25	8.60	+3.40	182.46	72.1357	21.571	
16	160	+27	8.44	+3.68	179.06	78.076	23.558	
17	162	+29	8.30	+3.93	176.035	83.38	25.3447	
18	164	+31	8.18	+4.15	173.55	88.04	26.898	

Table XVII  
Rotation in Yaw

Run No.	Yaw Angle $\phi$ Deg.	Rotation Deg.	DC Voltmeter-Volt		ft/sec $\bar{u}$	ft/sec $\bar{v}$	$\tan^{-1} \frac{\bar{v}}{\bar{u}}$	Deg. $\tan^{-1} \frac{\bar{v}}{\bar{u}}$
			(A+B)	(A-B)				
1	135	0	9.43	0.00	200.07	0.00	0.00	0.00
2	134	-1	9.43	-0.134	200.07	-2.842	-0.8138	
3	133	-2	9.43	-0.276	200.07	-5.855	-1.676	
4	132	-3	9.428	-0.428	200.028	-9.08	-2.599	
5	130	-5	9.41	-0.702	199.64	-14.89	-4.265	
6	128	-7	9.38	-0.978	199.0	-20.749	-5.952	
7	126	-9	9.36	-1.25	198.58	-26.52	-7.6067	
8	124	-11	9.30	-1.47	197.31	-31.188	-8.98	
9	122	-13	9.17	-1.66	194.55	-35.219	-10.26	
10	120	-15	9.02	-1.84	191.37	-39.038	-11.5297	
11	118	-17	8.85	-2.02	187.76	-42.857	-12.857	
12	116	-19	8.70	-2.27	184.58	-48.16	-14.623	
13	114	-21	8.58	-2.52	182.036	-53.465	-16.367	
14	112	-23	8.43	-2.72	178.85	-57.70	-17.880	
15	110	-25	8.23	-2.92	174.61	-61.95	-19.534	
16	108	-27	8.00	-3.06	169.73	-64.92	-20.93	
17	106	-29	7.82	-3.20	165.91	-67.89	-22.54	
18	104	-31	7.62	-3.34	161.669	-70.86	-23.667	

Table XVIII  
Rotation in Yaw

Run No.	Yaw Angle $\phi$	Angle Deg.	Rotation (A+B)	DC Voltmeter-Volt (A-B) $\sqrt{(A+B)^2}$	RMS Voltmeter-Volt $\sqrt{(A+B)^2}$	$\frac{\text{ft/sec}}{\sqrt{(A-B)^2}}$	Sensor Location: 1 cm				
							$\bar{u}$	$\bar{v}$	$\bar{u}'$	$\bar{v}'$	$\tan^{-1} \frac{\bar{v}}{\bar{u}}$ Deg.
1	135	0	14.14	0.00	.04	.04	300	0.0	0.848	0.848	0.0
2	136	1	14.135	+0.218	0.04	0.04	299	.89	4.625	0.848	0.883
3	137	2	14.132	+0.448	0.038	0.038	299	.83	9.505	0.806	1.8157
4	138	3	14.130	+0.684	.038	.038	299	.78	14.512	0.806	2.771
5	140	5	14.128	+1.077	.038	.038	299	.74	22.85	0.806	4.359
6	142	7	14.11	+1.506	0.04	0.04	299	.36	31.95	0.848	6.092
7	144	9	14.08	+1.938	0.04	0.04	298	.72	41.117	0.848	7.837
8	146	11	14.02	+2.32	0.038	0.038	297	.45	49.22	0.806	9.395
9	148	13	13.95	+2.70	0.04	0.04	295	.97	47.28	0.848	10.953
10	150	15	13.87	+3.05	0.047	0.047	294	.27	64.71	0.997	0.997
11	152	17	13.75	+3.44	0.048	0.048	291	.72	72.98	1.018	12.4019
12	154	19	13.62	+3.85	0.075	0.075	288	.96	81.68	1.591	15.783
13	156	21	13.42	+4.26	0.09	0.09	284	.72	90.38	1.909	17.611
14	158	23	13.23	+4.64	0.10	0.10	280	.69	98.44	2.12	19.326
15	160	25	12.98	+5.02	0.115	0.115	275	.38	106.50	2.439	21.4339
16	162	27	12.76	+5.41	0.08	0.08	270	.72	114.78	1.697	22.976
17	165	30	12.43	+6.00	0.07	0.07	263	.72	127.298	1.485	25.765

Table XIX  
Rotation in Yaw

Region: Potential Core  
 Sensor Type: X T1.5  
 Re. No.: 21.8 (300 ft/sec)  
 Slopes:  $K_1=K_2=30$  ft/sec/volt  
 Fluid Temperature: 75°F

Run No.	Yaw Angle $\phi$	Rotation Deg.	DC Voltmeter-Volt	RMS Voltmeter-Volt	$\sqrt{(A+B)Z}$	$\sqrt{(A-B)Z}$	ft/sec	ft/sec	ft/sec	ft/sec	$v'$	$\tan^{-1} \frac{v}{U}$ Deg.
1	135	0	14.14	0.00	0.040	0.040	300	0.0	0.848	0.848	0	0
2	134	-1	14.14	-0.219	0.04	0.04	300	-4.646	0.848	0.848	-0.887	
3	133	-2	14.16	-0.468	0.032	0.032	300	4.224	-9.292	0.678	0.678	-1.771
4	132	-3	14.16	-0.658	0.03	0.03	300	4.224	-13.96	0.636	0.636	-2.660
5	130	-5	14.128	-1.08	0.03	0.03	299.74	-22.913	0.636	0.636	0.636	-4.371
6	128	-7	14.08	-1.50	0.03	0.03	298.72	-31.82	0.636	0.636	0.636	-6.080
7	126	-9	14.00	-1.87	0.02	0.02	297.029	-39.67	0.424	0.424	0.424	-7.607
8	124	-11	13.91	-2.22	0.023	0.023	295.12	-47.10	0.488	0.488	0.488	-9.067
9	122	-13	13.75	-2.56	0.028	0.028	291.72	-54.31	0.594	0.594	0.594	-10.546
10	120	-15	13.55	-2.85	0.025	0.025	287.48	-60.46	0.530	0.530	0.530	-11.876
11	118	-17	13.35	-3.11	0.043	0.043	283.24	-65.98	0.912	0.912	0.912	-13.113
12	116	-19	13.11	-3.40	0.04	0.04	278.14	-72.13	0.848	0.848	0.848	-14.538
13	114	-21	12.88	-3.75	0.035	0.035	273.26	-79.56	0.742	0.742	0.742	-16.232
14	112	-23	12.63	-4.05	0.04	0.04	267.96	-85.92	0.848	0.848	0.848	-17.778
15	110	-25	12.36	-4.38	0.042	0.042	262.34	-92.92	0.891	0.891	0.891	-19.436
16	108	-27	12.07	-4.69	0.036	0.036	256.08	-99.50	0.763	0.763	0.763	-21.233
17	105	-30	11.62	-5.00	0.036	0.036	246.53	106.08	0.763	0.763	0.763	-23.281

Table XX  
Rotation in Pitch

Fluid Temperature: 75°F			Region: Potential Core					
Calibration Temperature: 70°F			Probe Model: 1240					
Sensor Location: 1 cm			Slopes: K <sub>1</sub> = 30 ft/sec/volt					
Sensor Type: X T1.5 M1240			K <sub>2</sub> = 30 ft/sec/volt					
Zero Reading of Cathodometer: X <sub>0</sub> = 3.136 ins								
Y <sub>0</sub> = 8.864 cm								
Z <sub>0</sub> = 7.716 ins								
Re. No.: 7.2 (based upon wire diameter) (100 ft per sec)								
Run No.	Rotation Deg.	DC Voltmeter-Volt (A+B) Volts	DC Voltmeter-Volt (A-B) Volts	$\bar{u}$ ft/sec	$\bar{v}$ ft/sec			
				X <sub>0</sub> + ΔX	Z <sub>0</sub> - ΔZ			
					$\tan^{-1} \frac{\bar{v}}{\bar{u}}$ Deg. u			
1	0	4.71	-0.0102	99.93	3.136	7.716	0.12384	
2	+2	4.69	-0.098	99.50	-2.079	3.382	7.711	-1.19699
3	+4	4.67	-0.096	99.08	-2.036	3.629	7.699	-1.1772
4	+6	4.66	-0.106	98.86	-2.24	3.875	7.677	-1.2980
5	+8	4.66	-0.118	98.86	-2.50	4.119	7.647	-1.4486
6	+10	4.67	-0.128	99.08	-2.716	4.363	7.608	-1.5702
7	-2	4.80	-0.154	101.83	-3.267	2.889	7.711	-1.83758
8	-4	4.88	-0.200	103.53	-4.24	2.643	7.699	-2.34519
9	-6	4.94	-0.248	104.80	-5.26	3.397	7.677	-2.8733
10	-8	4.97	-0.298	105.44	-6.32	2.153	7.647	-3.43016
11	-10	4.97	-0.320	106.44	-6.789	1.909	7.608	-3.64469

Table XXI  
Rotation in Pitch

Re. No.: 14.54 (200 ft/sec)							$\bar{v}$	$x_0 + \Delta x$	$z_0 - \Delta z$	$\tan^{-1} \frac{\bar{v}}{\bar{u}}$	Deg
Run No.	Rotation $\theta$ Deg	$\Delta x$ ins	$\Delta z$ ins	DC Voltmeter (A+B)	DC Voltmeter (A-B)	ft/sec	ft/sec	ft/sec	ft/sec		
1	0.0	0.0	0.0	9.436	0.00	200.198	0.00	3.136	7.715	0.00	
2	+2	0.2466	-0.0043	9.435	-0.090	200.176	-1.909	3.382	7.711	-0.5463	
3	+4	0.493	-0.0172	9.425	-0.108	199.964	-2.291	3.629	7.699	-0.6564	
4	+6	0.739	-0.0387	9.455	-0.125	200.60	-2.652	3.875	7.677	-0.7574	
5	+8	0.983	-0.0688	9.483	-0.149	201.195	-3.161	4.119	7.647	-0.9001	
6	+10	1.227	-0.1074	9.514	-0.172	201.85	-3.649	4.363	7.608	-1.03565	
7	-2	-0.2466	-0.0043	9.484	-0.072	201.216	-1.527	2.889	7.711	-0.43146	
8	-4	-0.493	-0.0172	9.592	-0.090	203.50	-1.909	2.643	7.699	-0.53746	
9	-6	-0.739	-0.0387	9.693	-0.169	205.65	-2.312	2.397	7.677	-0.64411	
10	-8	-0.983	-0.0688	9.802	-0.145	207.96	-3.076	2.153	7.647	-0.84741	
11	-10	-1.227	-0.1074	10.00	-0.228	212.16	-4.837	1.909	7.608	-1.3060	

Table XXII  
Rotation in Pitch

Region: Potential Core						Sensor Location: 1 cm				
Run No.	Rotation $\theta$ Deg	$\Delta X$ ins	$\Delta Z$ ins	DC Voltmeter- (A+B)	Volt (A-B)	$\bar{U}$ ft/sec	$\bar{V}$ ft/sec	$X_0 + \Delta X$ ins	$Z_0 + \Delta Z$ ins	$\tan^{-1} \frac{\bar{v}}{\bar{u}}$ Deg
1	-5	0	0	14.146	0.0	300.12	0.00	3.136	7.716	0.00
2	+2	0.2466	-0.0043	14.13	-0.004	299.78	-0.0848	3.382	7.711	-0.0162
3	+4	0.493	-0.0172	14.13	-0.052	299.78	-i.10	3.629	7.699	-0.21023
4	+6	0.739	-0.0387	14.148	-0.072	300.16	-1.527	3.875	7.677	-0.291477
5	+8	0.983	-0.0688	14.189	-0.093	301.039	-1.973	4.119	7.647	-0.3755
6	+10	1.227	-0.1074	14.25	-0.108	302.54	-2.291	4.363	7.608	-0.4338
7	-2	-0.2466	-0.0043	14.22	-0.005	301.697	-0.106	2.899	7.711	-0.0201
8	-4	-0.493	-0.0172	14.33	-0.01	304.03	-0.212	2.643	7.699	-0.03995
9	-6	-0.739	-0.0387	14.504	-0.024	307.72	-0.509	2.397	7.677	-0.09477
10	-8	-0.983	-0.0688	14.70	-0.088	311.88	-1.867	2.153	7.647	-0.34298
11	-10	-1.227	-0.1074	14.82	-0.185	314.427	-3.925	1.909	7.608	-0.71518

Table XXXIII  
Rotation in Yaw

Sensor Type: X T1.5  
Region: Potential Core  
Re. No.: 7.2 (100 ft/sec)  
Slopes:  $K_1 = K_2 = 30 \text{ ft/sec/volt}$   
Fluid Temperature: 75.5°F

Probe Model: 1241  
Cathodometer:  $X_0 = 7.518 \text{ ins}$   
 $Y_0 = 9.124 \text{ cm}$   
 $Z_0 = 6.65 \text{ in}$

Run No.	Rotation Deg	Digital Voltmeter-Volt		RMS Voltmeter-Volt		$\bar{u}$ ft/sec	$\bar{w}$ ft/sec	$\tan^{-1} \frac{\bar{w}}{\bar{u}}$ Deg	$u'$ ft/sec	$w'$ ft/sec
		(A+B)	(A-B)	$\sqrt{(A+B)^2}$	$\sqrt{(A-B)^2}$					
1	0.0	4.72	0.00	.016	.016	100.00	0.00	0.00	.339	.339
2	-1	4.74	-.072	.014	.015	100.56	+1.527	+.870	.297	.318
3	-2	4.74	-.140	.013	.015	100.56	+2.97	+1.691	.276	.318
4	-4	4.75	-.281	.013	.015	100.99	+5.96	+3.378	.276	.318
5	-6	4.77	-.420	.013	.017	101.20	+8.91	+5.032	.276	.360
6	-8	4.79	-.560	.014	.017	101.62	+11.88	+6.668	.297	.360
7	-10	4.80	-.689	.015	.018	101.83	+14.618	+8.169	.318	.381
8	+1	4.73	+.065	.012	.012	100.35	-1.378	-.787	0.254	.254
9	+2	4.730	+.140	.011	.012	100.35	-2.970	-1.695	.233	.254
10	+4	4.725	+.260	.012	.012	100.24	-5.516	-3.143	.254	.254
11	+6	4.72	+.362	.012	.011	100.14	-7.680	-4.385	.254	.233
12	+8	4.715	+.476	.012	.011	100.03	-10.099	-5.765	.254	.233
13	+10	4.710	+.585	.012	.011	99.929	-12.411	-7.08	.254	.233

Table XXXIV  
Rotation in Yaw

Sensor Type: X T1.5  
Region: Potential Core  
Re. No.: 14.54 (200 ft/sec)  
Slopes:  $K_1 = K_2 = 30$  ft/sec/volt  
Fluid Temperature: 75.5°F

Probe Model: 1241  
Cathodometer:  $X_0 = 7.518$  ins  
 $Y_0 = 9.124$  cm  
 $Z_0 = 6.65$  in

Run No.	Rotation Deg.	Digital Voltmeter-Volt (A+B)	RMS Voltmeter-Volt $\sqrt{(A+B)^2 + (A-E)^2}$	$\bar{u}$ ft/sec	$\bar{w}$ ft/sec	$\tan^{-1} \frac{\bar{w}}{\bar{u}}$ Deg.	$\frac{u'}{ft}$ sec	$\frac{w'}{ft}$ sec
1	0.0	9.43	0.00	.028	200.07	0.0	0.0	.594
2	-1	9.44	-9.120	.029	200.28	+2.54	+0.728	.615
3	-2	9.44	-.260	.032	200.28	+5.516	+1.577	.636
4	-4	9.45	-.534	.028	.030	200.49	+11.323	+3.23
5	-6	9.46	-.791	0.03	0.05	200.70	+16.78	+4.78
6	-8	9.46	-1.08	.042	.035	200.70	+22.91	+6.513
7	-10	9.45	-1.302	0.041	.04	200.49	+27.62	+7.84
8	+1	9.37	+1.158	.028	.027	198.79	-3.35	-.966
9	+2	9.36	+.304	.028	.024	198.58	-6.449	-1.860
10	+4	9.33	+.616	.03	.025	197.94	-13.069	-3.776
11	+6	9.32	+.873	.03	.024	197.73	-18.52	-5.35
12	+8	9.31	+1.132	.03	.024	197.52	-24.016	-6.932
13	+10	9.30	+1.370	.03	.024	197.31	-29.066	-8.38

Table XXV  
Rotation in Yaw

Sensor Type: X T1.5  
Region: Potential Core  
Re. No.: 21.8 (300 ft/sec)  
Slopes:  $K_1 = K_2 = 30 \text{ ft/sec/volt}$   
Fluid Temperature: 76.5°F

Run No.	Rotation in Yaw Deg.	Digital Voltmeter-Volt		RMS Voltmeter-Volt		$\bar{u}$ ft/sec	$\bar{w}$ ft/sec	$\tan^{-1} \frac{\bar{w}}{\bar{u}}$	$\bar{u}'$ ft/sec	$\bar{w}'$ ft/sec
		(A+B)	(A-B)	$\sqrt{(A+B)^2 + (A-B)^2}$	$\sqrt{(A-B)^2}$					
1	0.0	14.14	0.0	0.055	0.055	300.0	0.00	0.00	1.166	1.166
2	-1	14.12	-112	.065	.065	299.57	2.376	+0.454	1.379	1.379
3	-2	14.14	-0.238	0.055	.055	300.0	5.049	+0.964	1.166	1.166
4	-4	14.128	-0.640	.057	.055	299.74	13.578	+2.593	1.209	1.209
5	-6	14.14	-0.968	.057	.057	300.0	20.537	+3.916	1.209	1.209
6	-8	14.12	-1.30	.068	.068	299.57	27.58	+5.260	1.443	1.443
7	-10	14.10	-1.603	.068	.062	299.15	34.00	+6.484	1.443	1.315
8	+1	14.14	+.238	.048	.048	300.0	-5.049	-0.964	1.018	1.018
9	+2	14.14	+.439	.040	.045	300.0	-9.314	-1.778	.848	.954
10	+4	14.15	+.771	.048	.046	300.23	-16.357	-3.114	1.018	.9759
11	+6	14.16	1.122	.048	.047	300.4	-23.80	-4.529	1.018	.997
12	+8	14.17	1.458	.048	.045	300.6	-30.933	-5.874	1.018	.954
13	+10	14.188	1.769	.048	.047	301.018	-37.53	-7.1067	1.018	.997

Table XXVI  
Rotation in Pitch

**Sensor Type:** X T1.5  
**Region:** Potential Core  
**Re. No.:** 7.2 (100 ft/sec)  
**Slopes:**  $K_1 = K_2 = 30$  ft/sec/volt  
**Fluid Temperature:** 70°F

Run No.	Rotation Deg	$\Delta Y$ ins	$\Delta X$ ins	Digital Voltmeter			RMS Voltmeter Volt	$\bar{u}$ ft/sec	$\bar{w}$ ft/sec	$\tan^{-1} \frac{\bar{w}}{\bar{u}}$ Deg. $\bar{u}$
				(A+B)	(A-B)	$\sqrt{(A+B)Z}$				
1	0.0	0.0	0.00	4.72	0.00	0.008	0.008	100.14	0.00	0.00
2	+1	-.19039	-0.00065	4.73	-0.060	0.008	0.008	100.35	-1.272	-0.726
3	+2	-.3807	-.002615	4.75	-0.128	0.008	0.008	100.77	-2.7326	-1.553
4	+4	-.76099	-.01045	4.78	-0.255	0.008	0.008	101.44	-5.410	-3.053
5	+6	-1.1403	-.02352	4.81	-0.384	0.008	0.008	102.05	-8.147	-4.564
6	+8	-1.5182	-.04173	4.83	-0.503	0.008	0.008	102.47	-10.6718	-5.945
7	+10	-1.89438	-.06525	4.86	-0.630	0.008	0.008	103.111	-13.366	-7.386
8	-1	+.19039	-0.00065	4.72	+.060	0.008	0.008	100.14	+1.272	0.727
9	-2	+.3807	-.002615	4.716	+.118	0.008	0.008	100.056	+2.503	1.433
10	-4	+.76099	-.01045	4.70	+.242	0.008	0.008	99.717	+5.134	2.947
11	-6	+1.1403	-.02352	4.70	+.357	0.008	0.008	99.717	+7.574	4.343
12	-8	+1.5182	-.04173	4.70	+.483	0.008	0.008	99.717	+10.247	5.867
13	-10	+1.89438	-.06525	4.70	+.593	0.008	0.008	99.717	+12.581	7.1908

Table XXVII  
Rotation in Pitch

Sensor Type: X T1.5  
Region: Potential Core  
Re. No.: 14.54 (200 ft/sec)  
Slopes:  $K_1 = K_2 = 30 \text{ ft/sec/volt}$   
Fluid Temperature: 68.5°F

Run No.	Rotation Deg.	$\Delta Y$ ins	$\Delta X$ ins	Digital Voltmeter-Volt		RMS Voltmeter-Volt		$\bar{u}$ ft/sec	$\bar{w}$ ft/sec	$\tan^{-1} \frac{\bar{w}}{\bar{u}}$ Deg
				(A+B)	(A-B)	(A+B)Z	(A-B)Z			
1	0.0	0.00	0.00	9.43	0.00	0.036	0.030	200.07	0.0	0.0
2	+1	-0.19039	-0.00065	9.43	-0.128	0.036	0.030	200.07	-2.7157	-7.7776
3	+2	-0.3807	-0.002615	9.44	-0.242	0.036	0.03	200.28	-5.134	-1.4684
4	+4	-0.76099	-0.01045	9.50	-0.501	0.036	0.03	201.55	-10.629	-3.0187
5	+6	-1.1.1403	-0.02352	9.53	-0.75	0.036	0.03	202.19	-15.912	-4.4998
6	+8	-1.5182	-0.04173	9.58	-0.976	0.036	0.03	203.25	-20.707	-5.817
7	+10	-1.89438	-0.06525	9.64	-1.21	0.036	0.03	204.52	-25.67	-7.1538
8	-1	+0.19039	-0.00065	9.41	+0.109	0.036	0.03	199.646	2.3125	0.6636
9	-2	+0.3807	-0.002615	9.39	+0.228	0.036	0.03	199.22	4.837	1.3908
10	-4	+0.76099	-0.01045	9.37	+0.463	0.036	0.03	198.79	9.823	2.8289
11	-5	+1.1.1403	-0.02352	9.35	+0.688	0.036	0.03	198.37	14.586	4.2053
12	-8	+1.5182	-0.04179	9.35	+0.925	0.036	0.03	198.37	19.625	5.6499
13	-10	+1.89438	-0.06525	9.35	+1.11	0.036	0.03	198.37	23.55	6.77032

Table XXVIII  
Rotation in Pitch

Run No.	Rotation Deg.	$\Delta Y$ cm	$\Delta X$ ins	Digital Voltmeter-Volt		RMS Voltmeter-Volt	$\bar{u}$ ft/sec	$\bar{w}$ ft/sec	$\tan^{-1} \frac{\bar{w}}{\bar{u}}$ Deg
				(A+B)	(A-B)				
1	0.0	0.00	0.00	14.14	0.00	0.06	300.0	0.00	0.00
2	+1	-0.19039	-0.00065	14.1	-0.16	0.06	300.0	-3.394	-0.648
3	+2	-0.3807	-0.002615	14.	-0.312	0.06	300.2	-6.619	-1.2639
4	+4	-0.76099	-0.01045	14.20	-0.653	0.06	301.27	-13.854	-2.6329
5	+6	-1.1403	-0.02352	14.230	-0.968	0.06	301.90	-20.537	-3.891
6	+8	-1.5182	-0.04173	14.29	-1.26	0.06	303.18	-26.73	-5.038
7	+10	-1.89438	-0.06525	14.34	-1.55	0.06	304.24	-32.88	-6.168
8	-1	+0.19039	-0.00065	14.09	+0.110	0.06	298.94	+2.333	0.4474
9	-2	+.3807	-0.002615	14.08	+0.282	0.06	298.72	+5.983	1.147
10	-4	+.76099	-0.01045	14.06	+0.584	0.06	298.30	12.39	2.378
11	-6	+1.1403	-0.02352	14.06	+0.904	0.06	298.30	19.179	3.678
12	-8	+1.5182	-0.04173	14.06	+1.188	0.06	298.30	25.205	4.8297
13	-10	+1.89438	-0.06525	14.06	1.480	0.06	298.30	31.400	6.009

## Appendix B

### Influence of Air Temperature Variations on Linearized Sensor Response

The energy balance between the power supplied to the heaters and heat gained by the air moving past it gives:

$$\frac{E_1^2}{R_1} + \frac{E_2^2}{R_2} = \dot{m}_a c_{pair} (T_{T_2} - T_{T_1}) \quad (14)$$

Where  $T_{T_1}$ ,  $T_{T_2}$  are the bulk fluid temperatures and  $R_1$ ,  $R_2$  are the resistances of the heating elements.

In the present case,

$$E_1 = E_2 = E$$

$$R_1 = 8.5 \Omega$$

$$R_2 = 8.0 \Omega$$

$$\therefore E^2 = \frac{\dot{m}_a \times 0.24 \times \Delta T_a \times 10^4}{9.481 \times 0.24 \times 26470588}$$

$$\text{or } E^2 = 32.29914542 \sqrt{\dot{m}_a \Delta T_a} \quad (15)$$

$$\text{Now } \dot{m}_a = \sqrt{\frac{k g_c}{R}} \frac{P_{T_e}}{\sqrt{T_{T_e}}} A e \frac{M_e}{(1 + \frac{k-1}{2} M_e^2) \frac{(k+1)}{2(k-1)}} \quad (16)$$

But  $A_e = 10$  sq cm

$$\therefore m_a = 0.0098991618 \frac{P_{Te}}{\sqrt{\frac{T}{T_e}}} \frac{M_e}{(1 + 0.2 M_e^2)^{3.0}} \quad (17)$$

For a given  $m_a$  and  $\Delta T$ , equation (14) gives the value of Voltage setting required on the variac. The calculations are tabulated in Table XXVI.

Table XXIX  
Variation in Fluid Temperature

		25	50	100	150	200	250	300
$V_e$ ft/sec	$M_e$	0.022	0.045	0.09	0.13	0.17	0.22	0.26
$P_T$ PSFA		2076.52	2082.719	2091.6658	2105.2437	2124.955	2150.296	2181.269
$\dot{m}_a$ lbm/sec	$\Delta T = 4^{\circ}F$	.019438	.0398765	.0798045	0.11541199	0.1512485	0.195781	0.23205297
$\dot{m}_a$ lbm/sec	$\Delta T = 8^{\circ}F$	9.0063	12.899698	18.248817	21.94555	25.122714	28.5829	31.1820
$\dot{m}_a$ lbm/sec	$\Delta T = 12^{\circ}F$	0.0193843	0.0397236	0.07951	0.1149869	0.1506914	0.195060	0.2311982
$\dot{m}_a$ lbm/sec	$\Delta T = 16^{\circ}F$	12.719237	18.209294	25.7600	30.97848	35.46339	40.3478	43.92666
$\dot{m}_a$ lbm/sec	$\Delta T = 20^{\circ}F$	0.019331099	0.0395833	0.0792198	0.114566	0.15014027	0.19434698	0.23035293
$\dot{m}_a$ lbm/sec	$\Delta T = 24^{\circ}F$	15.556429	22.260640	31.49187	37.87124	43.354	49.32539	53.70052
$\dot{m}_a$ lbm/sec	$\Delta T = 28^{\circ}F$	0.0192259	0.039440	0.078932	0.114150	0.149594	0.193641	0.22951
$\dot{m}_a$ lbm/sec	$\Delta T = 32^{\circ}F$	17.9141739	36.29757	43.65047	49.96985	56.8525	61.894467	
$\dot{m}_a$ lbm/sec	$\Delta T = 36^{\circ}F$	0.01915678	0.039298	0.078145	0.113739269	0.1490364	0.1979437	0.2286891
$\dot{m}_a$ lbm/sec	$\Delta T = 40^{\circ}F$	12.57250	40.379	48.71483	55.76378	63.44849	69.07625	

## Appendix C

### Calibration--Set Up

For the purposes of illustration, the set up procedure for the single sensor T1.5 Model 1214 is explained below:

$$P_a = 29.241 \text{ ins Hg} = 2069.3630 \text{ P.S.F.O.}$$

$$T_a = 68^{\circ}\text{F} = 528^{\circ}\text{R}$$

$$P_a = \frac{P_a}{RT_a} = \frac{2069.363}{53.3 \times 528 \times 32.2} = 0.0022835982 \text{ slug/ft}^3$$

$$V_a = \sqrt{\frac{2 \times 1.94 \times 32.2 \times \Delta h}{12 \times 0.0022835982}}$$

or

$$V_a = 67.52 \sqrt{\Delta h} \text{ ft per sec}$$

where

$\Delta h$  is in inches of water.

$$R_{\text{Sensor}} + R_{\text{Probe}} + R_{\text{Holder}} = 5.74 + 0.18 + 0.02 = 5.94 \Omega$$

$$R_{\text{Sensor}} + R_{\text{Probe}} + R_{\text{Holder measured}} = 6.33 \Omega$$

$$R_{\text{Sensor alone}} = 6.33 - 0.2 = 6.13 \Omega$$

$$\text{Overheat Ratio} = 1.5$$

$$\therefore \text{Operating Resistance} = 1.5 \times 6.13 = 0.195 \Omega$$

### Temperature Correction

For small variations in fluid temperature, the temperature correction recommended by Ref 25 for non linear bridge output is given by:

$$\left[ \frac{t_s - t_{e2}}{t_s - t_{e1}} \right]^{1/2}$$

where  $t_s$  is the sensor operating temperature,  $t_{e1}$  and  $t_{e2}$  are the calibration temperature and new environment temperature respectively.

$$T_{e1} = 528^{\circ}\text{R}$$

$$T_{e2} = 530^{\circ}\text{R}$$

$$R_H = R_e [1 + a_R(t_s - t_e)]$$

$$9.195 = 6.13 [1 + 0.0023 (t_s - 528)]$$

$$t_s = 745.39^{\circ}\text{R}$$

$$\begin{aligned} \text{Temperature Correction} &= \left[ \frac{745.39 - 528}{745.39 - 530} \right]^{1/2} \\ &= 1.0046320 \end{aligned}$$

(

Table XXX  
Calibration Curve Set Up Table

		Probe Model: 1214		
		Range: 0-300 ft/sec		
		Start = 68°F      Finish = 70°F		
Observation No.	Ins Water Δh	Bridge Output E Volt	Bridge Output ETC Volt	Bridge Output EZC Volt
1	20.0	3.418	3.4338	1.8525
2	18.0	3.389	3.40469	1.8234
3	16.0	3.357	3.37259	1.79130
4	14.0	3.318	3.3333	1.75201
5	12.0	3.280	3.29519	1.7139
6	10.0	3.232	3.2469	1.66561
7	9.0	3.201	3.2158	1.63451
8	8.0	3.169	3.18367	1.60238
9	7.0	3.140	3.15454	1.57325
10	6.0	3.102	3.1163 <sup>f</sup> n	1.53509
11	5.0	3.057	3.07116	1.48987
12	4.5	3.030	3.04403	1.46274
13	4.0	3.001	3.01490	1.43361
14	3.5	2.972	2.98576	1.40447
15	3.0	2.936	2.9495	1.36821
16	2.0	2.841	2.85416	1.272869
17	1.8	2.811	2.82402	1.24273
18	1.6	2.784	2.79689	1.21560
19	1.4	2.756	2.76876	1.18747
20	1.2	2.724	2.73660	1.15531
21	1.0	2.685	2.69740	1.116110

Table XXX (continued)

Observation No.	In <sub>s</sub> Water Δh	Bridge Output E Volt	Bridge Output E <sub>TG</sub> Volt	Bridge Output E <sub>ZC</sub> Volt	ft/sec v
22	0.9	2.664	2.676339	1.09504	64.055
23	0.8	2.640	2.65222	1.07093	60.9917
24	0.7	2.612	2.62409	1.04280	56.491
25	0.6	2.582	2.59390	1.01261	52.300
26	0.4	2.504	2.81559	0.93430	42.703
27	0.2	2.386	2.39705	0.81576	30.1958
28	0.0	1.574	1.58129	0.0	0.0

Polynomial CoefficientsComputerNormalized

$$C_0 = -0.055233006 \quad A_y = 0.654833076$$

$$C_1 = 11.245301 \quad B_y^2 = 0.723280$$

$$C_2 = 6.5029972 \quad C_y^3 = 4.7590467$$

$$C_3 = 22.402357 \quad D_y^4 = 3.866119$$

$$C_4 = 9.5283042$$

Table XXXI  
Calibration Curve Set Up Table

Sensor Type: T1.5 Overheat Ratio: 1.2		Probe Model: 1210 Range: 0-300 ft/sec			
Observation No.	Iris Water Δh	Bridge Output E Volt	Bridge Output FTC Volt	Bridge Output EZC Volt	ft/sec v
1	20.0	2.441	2.441	1.341	305.0
2	18.0	2.421	2.421	1.321	289.85
3	16.0	2.396	2.396	1.296	272.80
4	14.0	2.367	2.367	1.261	255.18
5	12.0	2.337	2.337	1.237	236.25
6	10.0	2.301	2.301	1.201	215.66
7	9.0	2.277	2.277	1.177	204.60
8	8.0	2.255	2.255	1.155	192.90
9	7.0	2.232	2.232	1.132	180.44
10	6.0	2.204	2.204	1.104	167.05
11	5.0	2.170	2.170	1.070	152.50
12	4.0	2.131	2.131	1.031	136.40
13	3.5	2.107	2.107	1.007	127.53
14	3.0	2.082	2.082	0.982	118.12
15	2.5	2.052	2.052	0.952	107.80
16	2.0	2.016	2.016	0.916	96.45
17	1.8	1.999	1.999	0.899	91.50
18	1.6	1.980	1.980	0.88	86.26
19	1.4	1.957	1.957	0.857	80.69
20	1.2	1.933	1.933	0.833	74.71

Table XXXI (continued)

Observation No.	Ins Water Ah	Bridge Output E Volt	Bridge Output ETC Volt	Bridge Output EZC Volt	ft/sec v
21	1.0	1.907	1.907	0.807	68.20
22	0.9	1.879	1.879	0.779	64.70
23	0.8	1.862	1.862	0.762	61.00
24	0.7	1.841	1.841	0.741	57.00
25	0.6	1.818	1.818	0.718	52.80
26	0.5	1.790	1.790	0.690	48.20
27	0.4	1.758	1.758	0.658	43.10
28	0.3	1.716	1.716	0.616	37.30
29	0.2	1.656	1.656	0.556	30.5
30	0.1	1.550	1.550	0.450	21.56
31	0.0	1.100	1.100	0.00	0.00

Polynomial CoefficientsComputerNormalized

$C_0 = -0.016019$

$A_y = 1.141577$

$C_1 = 25.653432$

$B_y^2 = 1.72947$

$C_2 = 29.112053$

$C_y^3 = 0.899031$

$C_3 = 11.335806$

$D_y^4 = 6.231245$

$C_4 = 58.853327$

Table XXXII  
Calibration Curve Set Up Table

Sensor Type: T1.5 Overheat Ratio: 1.5		Probe Model: 1210 Range: 0-300 ft/sec		
Data:		1. Bridge voltage output at zero flow = 1.588 volts. 2. Bridge voltage output at full scale flow = 3.443 volts. 3. Ambient Temperature: Start = 72° F Finish = 72° F		
Observation No.	Ins Water Δh	Bridge Output E Volt	Bridge Output ETC Volt	Bridge Output EZC Volt
1	20.0	3.452	3.452	1.864
2	18.0	3.423	3.423	1.835
3	16.0	3.389	3.389	1.801
4	14.0	3.349	3.349	1.761
5	12.0	3.310	3.310	1.722
6	10.0	3.260	3.260	1.672
7	9.0	3.229	3.229	1.641
8	8.0	3.197	3.197	1.609
9	7.0	3.166	3.166	1.578
10	6.0	3.127	3.127	1.539
11	5.0	3.080	3.080	1.492
12	4.0	3.026	3.026	1.438
13	3.5	2.995	2.995	1.407
14	3.0	2.960	2.960	1.372
15	2.5	2.918	2.918	1.330
16	2.0	2.867	2.867	1.279
17	1.8	2.843	2.843	1.255
18	1.6	2.817	2.817	1.229
19	1.4	2.778	2.778	1.200
20	1.2	2.755	2.755	1.167

Table XXXII (continued)

Observation No.	Ins Water Ah	Bridge Output E Volt	Bridge Output ETC Volt	Bridge Output EZC Volt	ft/sec v
21	1.0	2.719	2.719	1.131	68.00
22	0.9	2.680	2.680	1.092	64.00
23	0.8	2.656	2.656	1.068	60.60
24	0.7	2.628	2.628	1.040	56.68
25	0.6	2.598	2.598	1.010	52.47
26	0.5	2.561	2.561	0.973	48.00
27	0.4	2.517	2.517	0.929	43.00
28	0.3	2.460	2.460	0.872	37.00
29	0.2	2.389	2.389	0.801	30.00
30	0.1	2.258	2.258	0.670	21.40
31	0.0	1.588	1.588	0.0	0.00

<u>Polynomial Coefficients</u>	
<u>Computer</u>	<u>Normalized</u>
$C_0 = -0.022885466$	$A_y = 0.50659$
$C_1 = 8.1929307$	$B^2_y = 3.50875$
$C_2 = 30.590485$	$C^3_y = -1.49164$
$C_3 = -7.0105798$	$D^4_y = 7.47761$
$C_4 = 18.945607$	

**Table XXXIII**  
Calibration Curve Set Up Table

**Sensor Type: T1.5  
Overheat Ratio: 1.8**

Data:

1. Bridge voltage output at zero flow condition = 1.918 volts.
2. Bridge voltage output at full scale flow = 4.063 volts.
3. Ambient Temperature: Start = 77°F Finish = 77°F.

Observation No.	Ins Water Δh	Bridge Output		Bridge Output ETC Volt	Bridge Output EZC Volt	fit/sec v
		E Volt	ETC Volt			
1	20.0	4.074	4.074	2.156	305.00	
2	18.0	4.040	4.040	2.122	289.35	
3	16.0	4.001	4.001	2.083	272.80	
4	14.0	3.956	3.956	2.038	255.18	
5	12.0	3.910	3.910	1.992	236.25	
6	10.0	3.853	3.853	1.935	215.66	
7	9.0	3.817	3.817	1.899	204.60	
8	8.0	3.780	3.780	1.862	192.90	
9	7.0	3.745	3.745	1.827	180.44	
10	6.0	3.699	3.699	1.781	167.05	
11	5.0	3.646	3.646	1.728	152.50	
12	4.0	3.585	3.585	1.667	136.40	
13	3.5	3.548	3.548	1.630	127.59	
14	3.0	3.505	3.505	1.587	118.12	
15	2.5	3.458	3.458	1.540	107.80	
16	2.0	3.400	3.400	1.484	96.45	
17	1.8	3.373	3.373	1.455	91.50	
18	1.6	3.342	3.342	1.424	86.26	
19	1.4	3.308	3.308	1.390	80.69	
20	1.2	3.271	3.271	1.353	74.71	

Table XXXIII (continued)

Observation No.	Ins Water Δh	Bridge Output E Volt	Bridge Output E <sub>T</sub> C Volt	Bridge Output E <sub>ZC</sub> Volt	ft/sec v
21	1.0	3.228	3.228	1.310	68.20
22	0.9	3.188	3.188	1.270	64.70
23	0.8	3.160	3.160	1.242	61.00
24	0.7	3.130	3.130	1.212	57.00
25	0.6	3.090	3.090	1.172	52.80
26	0.5	3.047	3.047	1.129	48.20
27	0.4	3.002	3.002	1.084	43.10
28	0.3	2.936	2.936	1.018	37.30
29	0.2	2.873	2.873	0.955	30.50
30	0.1	2.706	2.706	0.783	21.56
31	0.0	1.918	1.918	0.00	0.00

Polynomial Coefficients

Computer

Normalized

$$\begin{aligned}
 C_0 &= 0.095813887 & A_y &= 0.807857 \\
 C_1 &= 11.298702 & B_y^2 &= 0.2999639 \\
 C_2 &= 1.9558507 & C_y^3 &= 5.1803627 \\
 C_3 &= 1.9558507 & D_y^4 &= 3.7090679 \\
 C_4 &= 5.2562602
 \end{aligned}$$

**Table XXXIV**  
**Calibration Curve Set Up Table**

**Sensor Type:** X Tl.5  
**Overheat Ratio:** 1.5  
**Sensor No:** 1 (outer)  
**Data:**

1. Bridge output at zero flow = 1.563 volts.
2. Bridge output at full scale flow = 3.408 volts.
3. Ambient Temperature: Start = 74°F Finish = 74°F

Observation No.	In <sub>s</sub> Water Δh	Bridge Output E Volt	Bridge Output ETC Volt	Bridge Output EZC Volt	ft/sec v
1	20.0	3.418	3.418	1.855	304.15
2	18.0	3.388	3.388	1.825	288.54
3	16.0	3.356	3.356	1.793	272.04
4	14.0	3.318	3.318	1.755	254.47
5	12.0	3.277	3.277	1.714	235.59
6	10.0	3.228	3.228	1.665	215.06
7	9.0	3.200	3.200	1.637	204.03
8	8.0	3.169	3.169	1.606	192.36
9	7.0	3.135	3.135	1.572	179.93
10	6.0	3.096	3.096	1.533	166.589
11	5.0	3.052	3.052	1.489	152.07
12	4.0	2.998	2.998	1.435	--
13	3.5	2.966	2.966	1.403	127.23
14	3.0	2.930	2.930	1.367	117.79
15	2.5	2.888	2.888	1.325	107.53
16	2.0	2.835	2.835	1.272	96.18
17	1.8	2.805	2.805	1.242	91.24
18	1.6	2.779	2.779	1.216	86.02

Table XXXIV (continued)

Observation No.	Ins Water Δh	Bridge Output E Volt	Bridge Output E <sub>TC</sub> Volt	Bridge Output E <sub>ZC</sub> Volt	ft/sec v
19	1.4	2.749	2.749	1.186	80.47
20	1.2	2.716	2.716	1.153	74.50
21	1.0	2.677	2.677	1.114	68.01
22	0.9	2.655	2.655	1.092	64.52
23	0.8	2.630	2.630	1.067	60.83
24	0.7	2.603	2.603	1.040	56.90
25	0.6	2.572	2.572	1.009	52.68
26	0.5	2.537	2.537	0.974	48.09
27	0.4	2.493	2.493	0.930	43.01
28	0.3	2.439	2.439	0.873	37.25
29	0.2	2.366	2.366	0.803	30.41
30	0.1	2.250	2.250	0.687	21.50
31	c.0	1.563	1.563	0.0	0.00

Polynomial Coefficients

Computer

$$\begin{aligned}
 C_0 &= 0.051602129 \\
 C_1 &= 5.3437508 \\
 C_2 &= 27.313379 \\
 C_3 &= 3.6060702 \\
 C_4 &= 15.056535
 \end{aligned}$$

Normalized

$$\begin{aligned}
 A_y &= 0.32953 \\
 B^2 &= 3.11600 \\
 C^3 &= 0.7610761 \\
 D^4 &= 5.878827 \\
 Y &
 \end{aligned}$$

Table XXXV  
Calibration Curve Set Up Table

Sensor Type: X T1.5	Probe Model: I240				
Overheat Ratio: 1.5	Range: 0-300 ft/sec				
Sensor No. 1 (Outer)	Orientation: 45 deg.				
Data:					
1. Bridge output at zero flow = 1. 569 volts.					
2. Bridge output at full scale flow = 3.189 volts.					
3. Ambient Temperature: Start = 69°F Finish = 70°F					
Observation No.	Ins Water Δh	Bridge Output E Volt	Bridge Output ETC Volt	Bridge Output EZC Volt	Bridge Output ft/sec v
1	20.0	3.189	1.396	1.6264	302.95
2	18.0	3.160	3.167	1.5974	287.41
3	16.0	3.130	3.137	1.5674	270.97
4	14.0	3.097	3.104	1.5344	253.47
5	12.0	3.057	3.064	1.4944	234.66
6	10.0	3.011	3.018	1.4484	214.22
7	9.0	2.984	2.990	1.4204	203.22
8	8.0	2.956	9.963	1.3934	191.60
9	7.0	2.920	2.926	1.3564	179.23
10	6.0	2.886	2.892	1.3224	165.93
11	5.0	2.847	2.853	1.2834	151.47
12	4.5	2.825	2.831	1.2614	143.70
13	4.0	2.7960	2.802	1.2324	135.48
14	3.5	2.770	2.776	1.2064	126.73
15	3.0	2.737	2.743	1.1734	117.33
16	2.5	2.694	2.700	1.1304	107.110
17	2.0	2.640	2.646	1.0764	95.80
18	1.8	2.622	2.630	1.0604	91.00
19	1.6	2.600	2.606	1.0364	86.00

Table XXXV (continued)

Observation No.	Ins Water Δh	Bridge Output E Volt	Bridge Output ETC Volt	Bridge Output EZC Volt	ft/sec v
20	1.4	2.576	2.582	1.0124	80.00
21	1.2	2.552	2.557	0.9874	74.50
22	1.0	2.520	2.525	0.9554	68.00
23	0.9	2.494	2.500	0.9304	64.20
24	0.8	2.472	2.477	0.9081	60.59
25	0.7	2.448	2.453	0.8834	56.68
26	0.6	2.420	2.425	0.8554	52.47
27	0.5	2.389	2.394	0.8244	47.90
28	0.4	2.350	2.355	0.7854	42.84
29	0.3	2.290	2.295	0.7254	37.10
30	0.2	2.270	2.275	0.7054	30.29
31	0.1	2.131	2.136	0.5664	21.42
32	0.0	1.566	1.5696	0.00	0.00

## Polynomial Coefficients

Normalized Computer

$$c_0 = 0.00643259$$

$$B_w^2 = 1.103675$$

$$c_3 = 5.0280$$

二二

$$D_y^z = 2.946466$$

Table XXXVI  
Calibration Curve Set Up Table

**Sensor Type:** X T1.5  
**Overheat Ratio:** 1.5  
**Sensor No.:** 2 (Lower)

Data:

1. Bridge output at zero flow = 1.471 volts.

2. Bridge output at full scale flow = 3.073 volts.

3. Ambient Temperature: Start = 70°F Finish = 700°F

Probe Model: 1240  
Range: 0-300 ft/sec  
Orientation: Normal

Observation No.	Ins Water Δh	Bridge Output E Volt	Bridge Output E <sub>TC</sub> Volt	Bridge Output EZC Volt	ft/sec v
1	20.0	3.0760	3.0760	1.605	303.0
2	18.0	3.051	3.051	1.580	287.5
3	16.0	3.026	3.026	1.555	271.0
4	14.0	2.994	2.994	1.523	253.57
5	12.0	2.954	2.954	1.483	234.70
6	10.0	2.907	2.907	1.436	214.30
7	9.0	2.880	2.880	1.409	203.30
8	8.0	2.850	2.850	1.379	191.68
9	7.0	2.815	2.815	1.344	179.30
10	6.0	2.780	2.780	1.309	166.00
11	5.0	2.740	2.740	1.269	151.50
12	4.0	2.680	2.680	1.209	135.50
13	3.5	2.650	2.650	1.179	126.78
14	3.0	2.620	2.620	1.149	117.38
15	2.5	2.570	2.570	1.099	107.15
16	2.0	2.520	2.520	1.049	95.80
17	1.8	2.490	2.490	1.019	90.90
18	1.6	2.470	2.470	0.999	86.00
19	1.4	2.440	2.440	0.969	80.00

Table XXXVI (continued)

Observation No.	Ins Water $\Delta h$	Bridge Output E Volt	Bridge Output ETC Volt	Bridge Output EZC Volt	ft/sec v
20	1.2	2.410	2.410	0.939	74.00
21	1.0	2.380	2.380	0.909	68.00
22	0.9	2.360	2.360	0.889	64.00
23	0.8	2.335	2.335	0.864	60.60
24	0.7	2.310	2.310	0.839	56.68
25	0.6	2.280	2.280	0.809	52.47
26	0.5	2.250	2.250	0.779	48.00
27	0.4	2.210	2.210	0.739	43.00
28	0.3	2.150	2.150	0.679	37.00
29	0.2	2.080	2.080	0.609	30.00
30	0.1	1.978	1.978	0.507	21.40
31	0.0	1.471	1.471	0.00	0.00

Polynomial CoefficientsComputerNormalized

$$C_0 = -0.057862554$$

$$A_y = 1.536835$$

$$C_1 = 28.725888$$

$$B_y^2 = 0.62946$$

$$C_2 = 7.3306004$$

$$C_y^3 = 4.304947$$

$$C_3 = 31.236617$$

$$D_y^4 = 3.526199$$

$$C_4 = 15.941458$$

$$0.00$$

Table XXXVII  
Calibration Curve Set Up Table

**Sensor Type:** X T1.5

**Overheat Ratio:** 1.5

**Sensor No.** 2 (Lower)

Data:

1. Bridge output at zero flow = 1.465 volts.

2. Bridge output at full scale flow = 3.055 volts.

3. Ambient Temperature: Start = 71°F Finish = 71°F

Observation No.	Ins Water Δh	Bridge Output E Volt	Bridge Output ETC Volt	Bridge Output EZC Volt	ft/sec v
1	20.0	3.060	3.030	1.595	302.95
2	18.0	3.033	3.033	1.568	287.41
3	16.0	3.004	3.004	1.539	270.97
4	14.0	2.970	2.970	1.505	253.47
5	12.0	2.932	2.932	1.467	234.66
6	10.0	2.888	2.888	1.423	214.22
7	9.0	2.863	2.863	1.398	203.22
8	8.0	2.835	2.835	1.370	191.60
9	7.0	2.802	2.802	1.337	179.23
10	6.0	2.769	2.769	1.304	165.03
11	5.0	2.791	2.791	1.266	151.47
12	4.0	2.682	2.682	1.217	135.48
13	3.5	2.655	2.655	1.190	126.73
14	3.0	2.625	2.625	1.160	117.33
15	2.5	2.585	2.585	1.120	107.11
16	2.0	2.541	2.541	1.076	95.80
17	1.8	2.522	2.522	1.057	91.00
18	1.6	2.501	2.501	1.036	86.00
19	1.4	2.477	2.477	1.012	80.00
20	1.2	2.452	2.452	0.987	74.20

Table XXXVII (continued)

Observation No.	Ins Water $\Delta h$	Bridge Output E Volt	Bridge Output ETC Volt	Bridge Output EZC Volt	ft/sec v
21	1.0	2.420	2.420	0.955	68.00
22	0.9	2.388	2.388	0.932	64.20
23	0.8	2.368	2.368	0.903	60.59
24	0.7	2.344	2.344	0.879	56.68
25	0.6	2.316	2.316	0.851	52.47
26	0.5	2.285	2.285	0.820	47.90
27	0.4	2.247	2.247	0.782	42.84
28	0.3	2.184	2.184	0.719	37.10
29	0.2	2.128	2.128	0.6653	30.29
30	0.1	2.027	2.027	0.562	21.42
31	0.0	1.465	1.465	0.00	0.00

Polynomial Coefficients

Computer

$$\begin{aligned}
 C_0 &= -0.046256791 & A_y &= 0.898468 \\
 C_1 &= 16.952233 & B_y^2 &= 1.437102 \\
 C_2 &= 17.053544 & C_y^3 &= 3.4395 \\
 C_3 &= 25.669975 & D_y^4 &= 4.227338 \\
 C_4 &= 19.842657
 \end{aligned}$$

Table XXXVIII  
Rotation in Yaw

Run No.	Yaw Angle $\phi$ Deg	Rotation Deg	DC Voltmeter-Volt	$(A+B)$	$(A-B)$	$\sqrt{(A+B)^2}$	$\sqrt{(A-B)^2}$	RMS Voltmeter-Volt		$\bar{u}$ ft/sec	$\bar{v}$ ft/sec	$u'$ ft/sec	$v'$ ft/sec	$\tan^{-1} \frac{\bar{v}}{\bar{u}}$ Deg
								Region: Shear Flow	Reference Orientation: $48^\circ$					
1	48	0	3.412	0.00	0.5	0.45	72.390	0.00	10.608	9.547	0.00			
2	49	+1	3.38	-0.025	0.5	0.45	71.7114	-0.5304	10.608	9.547	-0.36196			
3	50	+2	3.36	-0.066	0.5	0.45	71.287	-1.400	10.608	9.547	-1.1250			
4	51	+3	3.34	-0.098	0.5	0.45	70.8628	-2.079	10.608	9.547	-1.68049			
5	52	+4	3.33	-0.146	0.5	0.45	70.6506	-3.0975	10.608	9.547	-2.51038			
6	54	+6	3.30	-0.238	0.5	0.45	70.014	-5.0495	10.608	9.547	-4.12510			
7	56	+8	3.28	-0.308	0.5	0.45	69.5890	-6.5346	10.608	9.547	-5.36444			
8	58	+10	3.20	-0.394	0.5	0.45	67.8925	-8.359	10.608	9.547	-7.01899			
9	60	+12	3.16	-0.465	0.5	0.45	67.0438	-9.8656	10.608	9.547	-8.37108			
10	62	+14	3.04	-0.520	0.5	0.4	64.4978	-11.0325	10.608	9.547	-9.70663			
11	64	+16	3.00	-0.601	0.45	0.45	63.6449	-12.75	9.547	9.547	-11.327259			
12	66	+18	2.99	-0.683	0.45	0.45	63.437	-14.490	9.547	9.547	-12.8665			
13	68	+20	2.94	-0.740	0.40	0.425	62.376	-15.700	8.486	9.0169	-14.1278			
14	70	+22	2.90	-0.798	0.42	0.42	61.527	-16.9306	8.91	8.91	-15.38549			
15	72	+24	2.88	-0.895	0.42	0.425	61.103	-18.988	8.91	9.0169	-17.2628			
16	74	+26	2.83	-0.966	0.42	0.425	60.042	-20.495	8.91	9.0169	-18.8470			
17	76	+28	2.75	-1.00	0.40	0.40	58.345	-21.2154	8.486	8.486	-19.983138			
18	78	+30	2.69	-1.05	0.41	0.40	57.072	-22.277	8.486	8.486	-21.32226			

Table XXXIX  
Rotation in Yaw

Run No.	Yaw Angle $\phi$ Deg	Rotation Deg	DC Voltmeter-Volt	RMS Voltmeter-Volt		$\bar{u}$ ft/sec	$\bar{v}$ ft/sec	$u'$ ft/sec	$v'$ ft/sec	$\tan^{-1} \frac{\bar{v}}{\bar{u}}$
				(A+B)	$\sqrt{(A+B)^2 - (A-B)^2}$					
1	48	0	3.412	0.00	0.45	72.390	0.09	9.547	9.457	0.0
2	47	-1	3.40	0.068	0.45	72.1357	1.4427	9.457	9.457	1.14575
3	46	-2	3.39	+0.118	0.45	71.9236	2.5035	9.457	9.457	1.99353
4	45	-3	3.38	+0.174	0.425	71.71145	3.6916	9.0169	9.0169	2.94690
5	44	-4	3.36	+0.205	0.425	71.287	4.34936	9.0169	9.0169	3.4914
6	42	-6	3.32	+ 300	0.420	70.4384	6.3649	8.910	8.910	5.09140
7	40	-8	3.30	+0.401	0.420	70.014	8.5077	8.910	9.0169	6.92828
8	38	-10	3.28	+0.483	0.42	69.5898	10.2475	8.910	8.910	8.37693
9	36	-12	3.26	+0.564	0.42	69.165	11.9660	8.910	8.910	9.81538
10	34	-14	3.24	+.668	0.42	68.7411	14.1725	8.910	8.910	11.6495
11	32	-16	3.22	+0.774	0.42	68.3168	16.4214	8.910	8.910	13.5158
12	30	-18	3.20	+0.836	0.42	67.892	17.7369	8.910	8.910	14.64137
13	28	-20	3.20	+0.914	0.42	67.892	19.3917	8.910	8.910	15.9407
14	26	-22	3.17	1.021	0.42	67.256	21.66195	8.910	8.910	17.8528
15	24	-24	3.19	1.087	0.42	67.680	23.0622	8.910	8.910	18.8167
16	22	-26	3.17	1.20	0.42	67.256	25.4596	8.910	8.910	20.7340
17	20	-28	3.15	1.265	0.40	66.831	26.8387	8.486	8.486	21.475
18	18	-30	3.10	1.356	0.40	65.7708	28.7624	8.486	8.486	23.6254

Table XL  
Rotation in Yaw

Run No.	Yaw Angle $\phi$ Deg	Rotation Deg	DC Voltmeter-Volt	RMS Voltmeter-Volt		$\bar{u}$ ft/sec	$\bar{v}$ ft/sec	$u'$ ft/sec	$v'$ ft/sec	$\tan^{-1} \frac{v'}{u'}$ Deg
				(A+B)	$\sqrt{(A-B)^2}$					
1	48	0	6.45	0.00	1.0	0.75	136.845	0.00	21.216	15.912
2	49	+1	6.43	-0.05	1.0	0.75	136.421	-1.0608	21.216	15.912
3	50	+2	6.40	-0.131	1.0	0.75	135.785	-2.779	21.216	15.912
4	51	+3	6.38	-0.233	1.0	0.75	135.36	-4.943	21.216	15.912
5	52	+4	6.33	-0.318	1.0	0.75	134.299	-6.747	21.216	15.912
6	54	+6	6.30	-0.480	1.0	0.75	133.66	-10.184	21.216	15.912
7	56	+8	6.28	-0.660	1.0	0.75	133.239	-14.00	21.216	15.912
8	58	+10	6.20	-0.805	1.0	0.75	131.54	-17.079	21.216	15.912
9	60	+12	6.13	-0.941	1.0	0.75	130.056	-19.964	21.216	15.912
10	62	+14	6.06	-1.14	0.95	0.70	128.57	-24.186	20.155	14.85
11	64	+16	5.96	-1.268	0.95	0.70	126.449	-26.90	20.155	14.85
12	66	+18	5.86	-1.38	0.95	0.70	124.328	-29.278	20.155	14.85
13	68	+20	5.72	-1.52	0.95	0.70	121.357	-32.25	20.155	14.85
14	70	+22	5.68	-1.64	0.95	0.70	120.051	-34.795	20.155	14.85
15	72	+24	5.50	-1.81	0.95	0.70	116.690	-38.40	20.155	14.85
16	74	+26	5.42	-1.92	0.90	0.70	114.99	-40.735	19.09	14.85
17	76	+28	5.35	-2.06	0.90	0.70	113.50	-43.70	19.09	14.85
18	78	+30	5.28	-2.15	0.90	0.70	112.022	-45.61	19.09	14.85

Table XLI  
Rotation in Yaw

Fluid Temperature: 75°F  
Sensor Location: 25 cm  
Sensor Type: X T1.5  
Zero Reading of Cathodometer:  $X_0 = 12.584$  ins  
 $Y_0 = 8.871$  cm  
 $Z_0 = 7.716$  ins

Region: Shear Flow  
Reference Orientation: 48°  
Probe Model: 1240  
 $K_1 = 30$  ft/sec/volt  
 $K_2 = 30$  ft/sec/volt  
Re. No.: 14.54 (200 ft/sec)

Run No.	Yaw Angle $\phi$ Deg	Rotation Deg	DC Voltmeter-Volt	RMS Voltmeter-Volt		$\bar{u}$ ft/sec	$\bar{v}$ ft/sec	$u'$ ft/sec	$v'$ ft/sec	$\tan^{-1} \frac{\bar{v}}{\bar{u}}$
				(A+B)	(A-B)					
1	48	0	6.45	0.00	1.0	0.75	136.845	0.00	21.216	15.912
2	47	-1	6.43	+0.135	1.0	0.70	136.421	2.864	21.216	14.85
3	46	-2	6.42	+0.208	1.0	0.70	136.209	4.413	21.216	14.85
4	45	-3	6.43	+0.298	1.0	0.70	136.421	6.3224	21.216	14.85
5	44	-4	6.45	+0.418	1.0	0.70	136.845	8.868	21.216	14.85
6	42	-6	6.45	+0.586	1.0	0.70	136.845	12.433	21.216	14.85
7	40	-8	6.42	+0.765	0.95	0.70	136.209	16.230	20.155	14.85
8	38	-10	6.38	+0.964	0.95	0.70	135.360	20.452	20.155	14.85
9	36	-12	6.36	+1.13	0.95	0.70	134.935	23.974	20.155	14.85
10	34	-14	6.34	+1.29	0.95	0.70	134.512	27.369	20.155	14.85
11	32	-16	6.32	+1.47	0.95	0.70	134.087	31.188	20.155	14.85
12	30	-18	6.30	+1.69	0.95	0.70	133.66	35.855	20.155	14.85
13	28	-20	6.28	+1.85	0.95	0.70	133.239	39.25	20.155	14.85
14	26	-22	6.24	+2.04	0.95	0.70	132.390	43.28	20.155	14.85
15	24	-24	6.17	+2.16	0.95	0.70	130.905	45.827	20.155	14.85
16	22	-26	6.10	+2.38	0.95	0.70	129.42	50.495	20.155	14.85
17	20	-28	6.04	+2.55	0.95	0.70	128.147	54.1018	20.155	14.85
18	18	-30	5.98	+2.71	0.85	0.70	126.874	57.496	20.155	14.85

Table XLII  
Rotation in Yaw

				Region: Shear Flow			
				Reference Orientation: 48°			
				Probe Model: 1240			
Zero Reading of Cathodometer: $X_0 = 12.584$ ins				$K_1 = 30$ ft/sec/volt			
$Y_0 = 8.871$ cm				$K_2 = 30$ ft/sec/volt			
$Z_0 = 7.716$ ins				Re. No.: 21.8 (300 ft/sec)			
Run No.	Yaw Angle $\phi$ Deg	Rotation Deg	DC Voltmeter-Volt	RMS Voltmeter-Volt	$\bar{u}$ ft/sec	$\bar{v}$ ft/sec	$\tan^{-1} \frac{\bar{v}}{\bar{u}}$ Deg
			(A+B)	(A-B) $\sqrt{(A+B)^2 - (A-B)^2}$			
1	48	0	9.46	0.00	1.20	200.70	0.00
2	49	+1	9.46	-0.10	1.20	200.70	-2.12
3	50	+2	9.40	-0.241	1.20	199.43	-5.11
4	51	+3	9.38	-0.350	1.20	199.00	-7.425
5	52	+4	9.36	-0.501	1.20	198.58	-10.629
6	54	+6	9.28	-0.750	1.20	196.88	-15.91
7	56	+8	9.22	-1.02	1.15	195.61	-21.64
8	58	+10	9.04	-1.24	1.10	191.73	-26.30
9	60	+12	8.92	-1.51	1.10	189.25	-32.036
10	62	+14	8.83	-1.72	1.10	187.34	-36.49
11	64	+16	8.76	-1.92	1.10	185.85	-40.73
12	66	+18	8.58	-2.14	1.10	182.03	-45.40
13	68	+20	8.46	-2.34	1.10	179.49	-49.64
14	70	+22	8.30	-2.56	1.05	176.036	-54.31
15	72	+24	8.17	-2.73	1.00	173.33	-57.92
16	74	+26	7.98	-2.91	1.00	169.30	-61.73
17	76	+28	7.81	-3.10	1.05	165.70	-65.77
18	78	+30	7.68	-3.24	1.25	162.94	-68.74

Table XLIII  
Rotation in Yaw

Fluid Temperature: 73°F							Region: Shear Flow						
Sensor Type: X TI.5							Reference Orientation: 48°						
Sensor Location: 25 cm							Probe Model: 1240						
Zero Reading of Cathodomometer: $X_0 = 12.584$ ins							$K_1 = 30 \text{ ft/sec/volt}$						
$Y_0 = 8.871$ cm							$K_2 = 30 \text{ ft/sec/volt}$						
$Z_0 = 7.716$ ins							Re. No.: 21.80 (300 ft/sec)						
Run No.	Yaw Angle Deg	Rotation Deg	DC Voltmeter-Volt	DC Voltmeter-Volt	(A+B)	(A-B)	RMS Voltmeter-Volt	$\sqrt{(A+B)^2 - (A-B)^2}$	$\bar{u}$ ft/sec	$\bar{v}$ ft/sec	$u'$ ft/sec	$v'$ ft/sec	$\tan^{-1} \frac{\bar{v}}{\bar{u}}$ Deg
1	48	0	9.46	0.00	1.50	1.20	200.70	0.00	31.82	25.45	0.00		
2	47	-1	9.45	+0.125	1.50	1.20	200.70	2.65	31.82	25.45	0.757		
3	46	-2	9.44	+0.296	1.50	1.20	200.70	6.28	31.82	25.45	1.796		
4	45	-3	9.46	+0.415	1.50	1.20	200.70	8.80	31.82	25.45	2.510		
5	44	-4	9.46	+0.573	1.50	1.25	200.70	12.157	31.82	26.52	3.466		
6	42	-6	9.43	+0.834	1.50	1.25	200.70	17.69	31.82	26.52	5.0528		
7	40	-8	9.40	+1.120	1.50	1.25	199.43	23.76	31.82	26.52	6.794		
8	38	-10	9.41	+1.138	1.50	1.25	199.64	29.27	31.82	26.52	8.340		
9	36	-12	9.36	+1.63	1.50	1.25	198.58	34.58	31.82	26.52	9.878		
10	34	-14	9.34	+1.90	1.50	1.25	198.16	40.31	31.82	26.52	11.498		
11	32	-16	9.30	+2.18	1.50	1.30	197.31	46.25	31.82	27.58	13.192		
12	30	-18	9.25	+2.44	1.50	1.30	196.25	51.76	31.82	27.58	14.775		
13	28	-20	9.18	+2.71	1.45	1.30	194.76	57.49	30.76	27.58	16.445		
14	26	-22	9.13	+2.98	1.40	1.30	193.70	63.22	29.70	27.58	18.0756		
15	24	-24	9.02	+3.16	1.40	1.30	191.37	67.04	29.70	27.58	19.306		
16	22	-26	8.96	+3.45	1.40	1.30	190.1	73.196	29.70	27.58	21.0586		
17	20	-28	8.86	+3.68	1.40	1.30	187.97	78.07	29.70	27.58	22.554		
18	18	-30	8.75	+3.88	1.35	1.30	185.64	82.31	28.64	27.58	23.9117		

Table XLIV  
Rotation in Pitch

Sensor Type: X T1.5		Region: Shear Flow (25 cm)		Re. No.: 7.2 (100 ft/sec)		Slopes: K <sub>1</sub> = K <sub>2</sub> = 30 ft/sec/volt		Fluid Temperature: 71°F		Probe Model: 1240		Reference Orientation: 48°		Cathodometer: X <sub>0</sub> = 12.584 ins		Y <sub>0</sub> = 8.871 cm		Z <sub>0</sub> = 7.716 ins	
Run No.	Rotation Deg	ΔX ins	ΔZ ins	(A+B)	Volt	(A+B)	Digital Voltmeter-Volt	(A-B)	RMS Voltmeter-Volt	(A+B) <sup>2</sup>	(A-B) <sup>2</sup>	X = Z <sub>0+</sub> ΔX	Z = Z <sub>0+</sub> ΔZ	U-bar ft/sec	V-bar ft/sec	W-bar ft/sec	tan <sup>-1</sup> V-bar / U-bar Deg		
1	0	0.00	0.00	3.412	0.00	0.425	0.35	12.584	7.716	72.330	0.00	0.00	0.00	0.00	0.00	0.00			
2	+2	0.2466	-0.0043	3.352	0.00	0.425	0.35	12.830	7.711	71.1174	0.00	0.00	0.00	0.00	0.00	0.00			
3	+4	0.493	-0.0172	3.352	0.00	0.425	0.35	13.077	7.699	71.1174	0.00	0.00	0.00	0.00	0.00	0.00			
4	+6	0.739	-0.0387	3.352	0.00	0.425	0.35	13.323	7.677	71.1174	0.00	0.00	0.00	0.00	0.00	0.00			
5	+8	0.983	-0.0688	3.332	0.00	0.425	0.35	13.567	7.647	70.693	0.00	0.00	0.00	0.00	0.00	0.00			
6	+10	1.227	-0.1074	3.322	0.00	0.425	0.35	13.811	7.608	70.4809	0.00	0.00	0.00	0.00	0.00	0.00			
7	+12	1.469	-0.154	3.392	0.00	0.425	0.35	14.053	7.561	71.9660	0.00	0.00	0.00	0.00	0.00	0.00			
8	+14	1.7099	-0.2099	3.402	0.00	0.425	0.35	14.294	7.506	72.178	0.00	0.00	0.00	0.00	0.00	0.00			
9	+16	1.948	-0.2738	3.392	0.00	0.425	0.35	14.532	7.442	71.966	0.00	0.00	0.00	0.00	0.00	0.00			
10	-2	-0.2466	-0.0043	3.352	0.00	0.425	0.35	12.3374	7.711	71.1173	0.00	0.00	0.00	0.00	0.00	0.00			
11	-4	-0.493	-0.0172	3.352	0.00	0.425	0.35	12.091	7.699	71.1173	0.00	0.00	0.00	0.00	0.00	0.00			
12	-6	-0.739	-0.0387	3.352	0.00	0.425	0.325	11.845	7.677	71.1173	0.00	0.00	0.00	0.00	0.00	0.00			
13	-8	-0.983	-0.0688	3.362	0.00	0.425	0.30	11.601	7.647	71.329	0.00	0.00	0.00	0.00	0.00	0.00			
14	-10	-1.227	-0.1074	3.425	+0.00	0.425	0.30	11.357	7.608	72.666	0.00	0.00	0.00	0.00	0.00	0.00			
15	-12	-1.469	-0.1544	3.422	+0.00	0.425	0.30	11.115	7.561	72.6025	0.00	0.00	0.00	0.00	0.00	0.00			
16	-14	-1.7099	-0.2099	3.482	+0.00	0.425	0.30	10.874	7.506	73.875	0.00	0.00	0.00	0.00	0.00	0.00			
17	-16	-1.948	-0.2738	3.502	+0.00	0.425	0.30	10.636	7.442	74.299	0.00	0.00	0.00	0.00	0.00	0.00			

Table XLV  
Rotation in Pitch

Run No.	Rotation Deg	$\Delta X$ ins	$\Delta Z$ ins	Digital Voltmeter Volt	$(A+B)$	$(A-B)$	RMS Voltmeter Volt	$X_0^+ \Delta X$	$Z_0^+ \Delta Z$	$\bar{u}$ ft/sec	$\bar{v}$ ft/sec	$\tan^{-1} \frac{\bar{v}}{\bar{u}}$ Deg
								$\sqrt{(A+B)Z}$	$\sqrt{(A-B)^2}$			
1	0	0.0	0.0	6.45	0.00	1.0	0.75	12.584	7.716	136.845	0.00	0.00
2	+2	0.2466	-0.0043	6.36	0.00	1.0	0.75	12.830	7.711	134.936	0.00	0.00
3	+4	0.493	-0.0172	6.34	0.00	1.0	0.75	13.077	7.699	134.512	0.00	0.00
4	+6	0.739	-0.0387	6.34	0.00	1.0	0.75	13.323	7.677	134.512	0.00	0.00
5	+8	0.983	-0.0688	6.30	-0.03	1.0	0.75	13.567	7.647	133.663	-0.63649	-0.2728
6	+10	1.227	-0.1074	6.30	-0.03	1.0	0.75	13.811	7.608	133.663	-0.63643	-0.2728
7	+12	1.469	-0.1544	6.36	-0.05	1.0	0.75	14.053	7.561	134.936	-1.0608	-0.4504
8	+14	1.7099	-0.2099	6.46	-0.08	1.0	0.75	14.294	7.506	137.057	-1.6973	-0.70950
9	+16	1.948	-0.2738	6.48	-0.095	1.0	0.75	14.532	7.442	137.48	-2.0155	-0.8399
10	-2	-0.2466	-0.0043	6.38	0.00	1.0	0.75	12.3374	7.711	135.36	0.00	0.00
11	-4	-0.493	-0.0172	6.34	0.00	1.0	0.75	12.091	7.699	134.512	0.00	0.00
12	-6	-0.739	-0.0387	6.48	0.00	1.0	0.75	11.845	7.677	137.48	0.00	0.00
13	-8	-0.983	-0.0688	6.52	+0.0	1.0	0.75	11.601	7.647	138.33	0.00	0.00
14	-10	-1.227	-0.1074	6.60	+0.0	1.0	0.75	11.357	7.608	140.028	0.00	0.00
15	-12	-1.469	-0.1544	6.60	+0.0	1.0	0.75	11.115	7.561	140.028	0.00	0.00
16	-14	-1.7099	-0.2099	6.60	+0.0	1.0	0.75	10.874	7.506	140.028	0.00	0.00
17	-16	-1.948	-0.2738	6.60	0.0	1.0	0.75	10.636	7.442	140.028	0.00	0.00

Table XLVI  
Rotation in Pitch

Run No.	Rota-tion Deg	$\Delta X$ ins	$\Delta Z$ ins	Digital Volt-meter-Volt		RMS Voltmeter-Volt	$X = \frac{X_0 +}{\Delta X}$	$Z = \frac{Z_0}{\Delta X}$	$\bar{u}$ ft/sec	$\bar{v}$ ft/sec	$u'$ ft/sec	$v'$ ft/sec	$\tan^{-1} \frac{\bar{v}}{\bar{u}}$ Deg u	
				(A+B)	(A-B)									
1	0	0.0	0.00	9.46	0.00	1.50	1.20	12.584	7.716	200.707	0.00	31.8	25.45	0.00
2	+2	0.2466	-0.0043	9.48	0.00	1.50	1.20	12.830	7.711	201.131	0.00	31.8	25.45	0.00
3	+4	0.493	-0.0172	9.50	-0.03	1.50	1.20	13.077	7.699	201.55	-0.6364	31.8	25.45	-0.1809
4	+6	0.739	-0.0387	9.52	-0.04	1.5	1.20	13.323	7.677	201.98	-0.8486	31.8	25.45	-0.2407
5	+8	0.983	-0.0688	9.54	-0.06	1.5	1.20	13.567	7.647	202.404	-1.27298	31.8	25.45	-0.36034
6	+10	1.227	-0.1074	9.58	-0.07	1.5	1.20	13.811	7.608	203.253	-1.485	31.8	25.45	-0.4186
7	+12	1.469	-0.1544	9.61	-0.09	1.5	1.20	14.053	7.561	203.89	-1.909	31.8	25.45	-0.5364
8	+14	1.7099	-0.2099	9.63	-0.10	1.5	1.2	14.294	7.506	204.314	-2.1216	31.8	25.45	-0.5949
9	+16	1.948	-0.2738	9.65	-0.125	1.5	1.2	14.532	7.442	204.738	-2.652	31.8	25.45	-0.742118
10	-2	-0.2466	-0.0043	9.55	+0.00	1.5	1.2	12.3374	7.711	202.616	0.00	31.8	25.45	0.00
11	-4	-0.493	-0.0172	9.64	+0.00	1.5	1.2	12.091	7.699	204.526	0.00	31.8	25.45	0.00
12	-6	-0.739	-0.0387	9.66	+0.00	1.5	1.2	11.845	7.677	204.95	0.00	31.8	25.45	0.00
13	-8	-0.983	-0.0688	9.70	+0.00	1.5	1.2	11.601	7.647	205.799	0.00	31.8	25.45	0.00
14	-10	-1.227	-0.1074	9.72	+0.00	1.5	1.2	11.357	7.608	206.223	0.00	31.8	25.45	0.00
15	-12	-1.469	-0.1544	9.78	+0.00	1.50	1.2	11.115	7.561	207.496	0.00	31.8	25.45	0.00
16	-14	-1.7099	-0.2099	9.80	+0.00	1.50	1.2	10.874	7.506	207.920	0.00	31.8	25.45	0.00
17	-16	-1.948	-0.2738	9.82	+0.00	1.50	1.2	10.636	7.442	208.345	0.00	31.8	25.45	0.00

Table XLVII  
Rotation in Yaw

Run No.	Yaw Angle $\phi$ Deg	Rotation Deg	(A+B) volts	(A-B) volts	Region: Shear Flow		
					$\sqrt{(A+B)^2}$	$\sqrt{(A-B)^2}$	Reference Orientation: 135°
1	135	0	3.41	0.00	0.425	0.425	Probe Model: 1240
2	136	+1	3.38	0.04	0.425	0.425	$K_1 = 30 \text{ ft/sec/volt}$
3	137	+2	3.36	+0.086	0.420	0.420	$K_2 = 30 \text{ ft/sec/volt}$
4	138	+3	3.30	+0.122	0.420	0.420	Re. No.: 7.20 (based upon wire diameter)
5	140	+5	3.28	+0.201	0.420	0.420	(100 ft/sec)
6	142	+7	3.30	+0.300	0.42	0.42	
7	144	+9	3.32	+0.403	0.425	0.425	
8	146	+11	3.34	+0.500	0.425	0.425	
9	148	+13	3.27	+0.584	0.425	0.425	
10	150	+15	3.28	+0.664	0.420	0.420	
11	152	+17	3.30	+0.776	0.420	0.420	
12	154	+19	3.25	+0.877	0.420	0.420	
13	156	+21	3.24	+0.960	0.420	0.420	
14	158	+23	3.25	+1.030	0.420	0.420	
15	160	+25	3.20	1.150	0.420	0.420	
16	162	+27	3.18	1.202	0.400	0.400	
17	165	+30	3.14	1.316	0.400	0.400	
					0.0	0.0	0.00
					72.3479	72.3479	0.0169
					ft/sec	ft/sec	ft/sec
					$\bar{u}$	$\bar{v}$	$u'$
					ft/sec	ft/sec	ft/sec
					$\tan^{-1} \frac{\bar{v}}{\bar{u}}$		
					Deg		

Table XLVIII  
Rotation in Yaw

Fluid Temperature: 72°F  
Sensor Type: X T1.5  
Zero Reading of Cathodometer:  $X_0 = 12.584$  ins  
 $Y_0 = 8.871$  cm  
 $Z_0 = 7.716$  ins  
Re. No.: 7.2 (based upon wire diameter) (100 ft/sec)

Run No.	Yaw Angle $\phi$ Deg	Rotation Deg	DC Voltmeter-Volt		RMS Voltmeter-Volt		$\bar{u}$ ft/sec	$\bar{v}$ ft/sec	$u'$ ft/sec	$v'$ ft/sec	$\tan^{-1} \frac{\bar{v}}{\bar{u}}$	Deg
			(A+B)	(A-B)	$\sqrt{(A+B)Z}$	$\sqrt{(A-B)Z}$						
1	135	0	3.41	0.00	0.425	72.3479	0.00	9.0169	9.0169	0.00	0.00	0.00
2	134	-1	3.40	-0.046	0.425	72.1357	-0.9759	9.0169	9.0169	-0.7750		
3	133	-2	3.38	-0.108	0.425	71.7114	-2.29137	9.0169	9.0169	-1.830129		
4	132	-3	3.34	-0.157	0.425	70.8628	-3.33097	9.0169	9.0169	-2.69126		
5	130	-5	3.30	-0.234	0.425	70.0141	-4.9646	9.0169	9.0169	-4.0559		
6	128	-7	3.25	-0.315	0.425	68.953	-6.683	9.0169	9.0169	-5.5558		
7	126	-9	3.20	-0.396	0.425	67.8925	-8.4016	9.0169	9.0169	-7.05440		
8	124	-11	3.17	-0.474	0.420	67.256	-10.0565	8.9109	8.9109	-8.504185		
9	122	-13	3.07	-0.540	0.420	65.134	-11.4568	8.9109	8.9109	-9.97604		
10	120	-15	3.02	-0.610	0.420	64.0735	-12.942	8.9109	8.9109	-11.41934		
11	118	-17	3.00	-0.701	0.420	63.649	-14.8727	8.9109	8.9109	-13.152176		
12	116	-19	2.98	-0.775	0.400	63.22489	16.4427	8.486	8.486	-14.5778		
13	114	-21	2.90	-0.808	0.410	61.527	-17.1428	8.698	8.698	-15.5690		
14	112	-23	2.86	-0.880	0.400	60.6789	-18.670	8.486	8.486	-17.10235		
15	110	-25	2.80	-0.938	0.400	59.4059	-19.900	8.486	8.486	-18.5200		
16	108	-27	2.76	-1.002	0.400	58.557	-21.2164	8.486	8.486	-19.91648		
17	105	-30	2.66	-1.08	0.400	56.4356	-22.9187	8.486	8.486	-22.0978		

Table XLIX  
Rotation in Yaw

Re. No.: 14.54 (200 ft/sec)							Region: Shear Flow			
Run No.	Yaw Angle $\phi$ Deg	Rotation Deg	DC Voltmeter-Volt	RMS Voltmeter-Volt	$\bar{U}$ ft/sec	$\bar{V}$ ft/sec	$u'$ ft/sec	$v'$ ft/sec	$\tan^{-1} \frac{\bar{v}}{\bar{u}}$ Deg	
1	135	0	6.45	0.00	1.00	136.845	0.00	21.2164	0.00	
2	134	-1	6.39	-0.02	0.95	135.572	-0.424	20.1558	-0.17919	
3	133	-2	6.36	-0.147	0.95	134.936	-3.1188	20.1558	-1.3240	
4	132	-3	6.34	-0.218	0.95	134.512	-4.625	20.1558	-1.816080	
5	131	-4	6.30	-0.335	0.95	133.663	-7.10749	20.1558	-3.04381	
6	129	-6	6.27	-0.489	0.95	133.026	-10.3748	20.1558	-4.4595	
7	127	-8	6.21	-0.643	0.95	131.753	-13.6421	20.1558	-5.911510	
8	125	-10	6.18	-0.798	0.95	131.1173	-16.9306	20.1558	-7.3576	
9	123	-12	6.10	-0.975	0.95	129.420	-20.686	20.1558	-9.081125	
10	121	-14	6.00	-1.140	0.95	127.298	-24.1867	20.1558	-10.7580	
11	119	-16	5.95	-1.270	0.90	126.237	-26.9448	19.094	-12.0487	
12	117	-18	5.86	-1.398	0.90	124.328	-29.660	19.094	-13.41783	
13	115	-20	5.78	-1.570	0.90	122.630	-33.3097	19.094	-15.1964	
14	113	-22	5.72	-1.701	0.90	121.387	-36.089	19.094	-16.5613	
15	111	-24	5.64	-1.830	0.85	119.660	-38.826	18.033	-17.97665	
16	109	-26	5.55	-1.980	0.85	117.751	-42.00	18.033	-19.63054	
17	107	-28	5.48	-2.086	0.85	116.2659	-44.257	18.033	-20.8394	
18	105	-30	5.35	-2.187	0.85	113.5077	-46.400	18.033	-22.25159	

Table L  
Rotation in Yaw

Fluid Temperature: 720F  
 Sensor Type: X T1.5  
 Zero Reading of Cathetometer:  $X_0 = 12.584$  ins  
 $Y_0 = 8.871$  cm  
 $Z_0 = 7.716$

Re. No.: 14.54 (200 ft/sec)

Run No.	Yaw Angle $\phi$ Deg	Rotation Deg	DC Voltmeter Volt	RMS Voltmeter Volt		$\bar{u}$ ft/sec	$\bar{v}$ ft/sec	$u'$ ft/sec	$v'$ ft/sec	$\tan^{-1} \frac{v}{u}$
				(A+B)	(A-B)					
1	135	0	6.45	0.00	1.00	136.8458	0.00	21.2164	21.764	0.00
2	136	+1	6.40	+0.106	0.950	1.00	135.785	2.2489	20.1558	21.2164
3	137	+2	6.39	0.213	0.950	1.00	135.572	4.900	20.1558	21.2164
4	138	+3	6.36	0.320	0.950	0.950	134.936	6.78925	20.1558	20.1558
5	139	+4	6.34	0.401	0.950	0.950	134.512	8.50777	20.1558	20.1558
6	141	+6	6.35	0.594	0.950	0.950	134.724	12.60254	20.1558	20.1558
7	143	+8	6.34	0.787	0.950	0.950	134.512	16.6973	20.1558	20.1558
8	145	+10	6.29	0.960	0.950	0.950	133.4512	20.3677	20.1558	20.1558
9	147	+12	6.25	1.130	0.950	0.950	132.6025	23.9745	20.1558	20.1558
10	149	+14	6.23	1.315	0.950	0.950	132.1782	27.8995	20.1558	20.1558
11	151	+16	6.20	1.516	0.950	0.950	131.5417	32.1640	20.1558	20.1558
12	153	+18	6.18	1.676	0.950	0.950	131.11739	35.558	20.1558	20.1558
13	155	+20	6.10	1.843	0.95	0.95	129.420	39.1018	20.1558	20.1558
14	157	+22	6.04	2.00	0.95	0.95	128.147	42.4328	20.1558	20.1558
15	159	+24	6.00	2.21	0.90	0.90	127.298	46.888	19.094	19.094
16	161	+26	5.95	2.38	0.90	0.90	126.2376	50.495	19.094	19.094
17	163	+28	5.86	2.44	0.90	0.90	124.328	51.768	19.094	19.094
18	165	+30	5.83	2.670	0.90	0.90	123.691	56.6478	19.094	19.094

Table LI  
Rotation in Yaw

Run No.	Yaw Angle φ Deg	Rotation Deg	DC Voltmeter Volt	RMS Voltmeter - Volt		$\bar{u}$ ft/sec	$\bar{v}$ ft/sec	$u'$ ft/sec	$v'$ ft/sec	$\tan^{-1} \frac{v}{u}$ Deg
				(A+B)	(A-B)					
1	135	0.0	9.46	0.00	1.5	1.15	200.46	0.00	31.819	24.39
2	136	+1	9.45	0.03	1.5	1.15	200.67	0.63639	31.819	24.39
3	137	+2	9.48	+0.18	1.5	1.20	201.10	3.818	31.819	25.459
4	138	+3	9.50	+0.34	1.5	1.20	201.50	7.2124	31.819	25.459
5	140	+4	9.50	+0.48	1.5	1.20	201.50	10.18	31.819	25.459
6	142	+6	9.35	+0.794	1.5	1.20	198.34	16.84	31.819	25.459
7	144	+8	9.30	+1.04	1.5	1.20	197.28	22.06	31.819	25.459
8	146	+10	9.28	+1.35	1.5	1.20	196.85	28.637	31.819	25.459
9	148	+12	9.17	+1.61	1.5	1.20	194.52	34.153	31.819	25.459
10	150	+14	9.08	+1.92	1.5	1.20	192.61	40.729	31.819	25.459
11	152	+16	9.00	+2.21	1.5	1.20	190.92	46.88	31.819	25.459
12	154	+18	8.89	+2.48	1.45	1.20	188.58	52.608	30.759	25.459
13	156	+20	8.78	+2.71	1.45	1.20	186.25	57.487	30.759	25.459
14	158	+22	8.68	+2.92	1.40	1.15	184.13	61.942	29.698	24.395
15	160	+24	8.56	+3.19	1.40	1.15	181.58	67.67	29.698	24.395
16	162	+26	8.48	+3.40	1.35	1.15	179.88	72.125	29.698	24.395
17	164	+28	8.31	+3.61	1.30	1.10	176.28	76.579	23.33	23.34
18	166	+30	8.20	+3.81	1.30	1.10	173.95	80.822	23.33	23.34

Table LII  
Rotation in Yaw

Fluid Temperature: 78°F							Region: Shear Flow			
Sensor Location: 25 c.n							Reference Orientation: 135°			
Sensor Type: X%1.5							Probe Model: 1240			
Zero Reading of Cathodometer: $X_0 = 12.584$ ins							$K_1 = 30 \text{ ft/sec/volt}$			
$Y_0 = 6.871$ cm							$K_2 = 30 \text{ ft/sec/volt}$			
$Z_0 = 7.716$ ins							Re. No.: 21.8 (300 ft/sec)			
Run No.	Yaw Angle $\phi$ Deg	Rotation Deg	DC Voltmeter Volt	RMS Voltmeter Volt	$\bar{u}$ ft/sec	$\bar{v}$ ft/sec	$\bar{u}'$ ft/sec	$v'$ ft/sec	$\tan^{-1} \frac{\bar{v}}{\bar{u}}$ Deg	
			(A+B)	$\sqrt{(A+B)^2 - (A-B)^2}$						
1	134	1	9.46	-0.20	1.50	1.20	200.67	-4.24	31.819	25.459
2	133	2	9.50	-0.360	1.50	1.20	201.527	-7.63	31.819	25.459
3	132	3	9.50	-0.491	1.50	1.20	201.527	-10.417	31.819	25.459
4	130	4	9.49	-0.630	1.50	1.20	201.315	-13.36	31.819	25.459
5	128	5	9.48	-0.890	1.50	1.15	201.10	-18.88	31.819	24.398
6	126	9	9.46	-1.140	1.50	1.15	200.678	-24.186	31.819	24.398
7	124	11	9.39	-1.410	1.50	1.15	199.19	-29.91	31.819	24.398
8	122	13	9.38	-1.68	1.50	1.15	198.98	-35.64	31.819	24.398
9	120	15	9.28	-1.89	1.50	1.15	196.86	-40.1	31.819	24.398
10	118	17	9.18	-2.15	1.45	1.10	194.739	-45.61	30.763	23.338
11	116	19	9.04	-2.32	1.45	1.10	191.769	-49.22	30.763	23.338
12	114	21	8.90	-2.53	1.45	1.10	188.799	-53.67	30.763	23.338
13	112	23	8.76	-2.78	1.40	1.10	185.829	-58.98	29.703	23.338
14	110	25	8.68	-2.93	1.40	1.10	184.13	-62.164	29.703	23.338
15	108	27	8.57	-3.14	1.35	1.10	181.79	-66.619	28.642	23.338
16	106	29	8.46	-3.36	1.35	1.15	179.46	-71.287	28.642	24.398
17	104	31	8.31	-3.55	1.40	1.15	176.28	-75.318	29.703	24.398

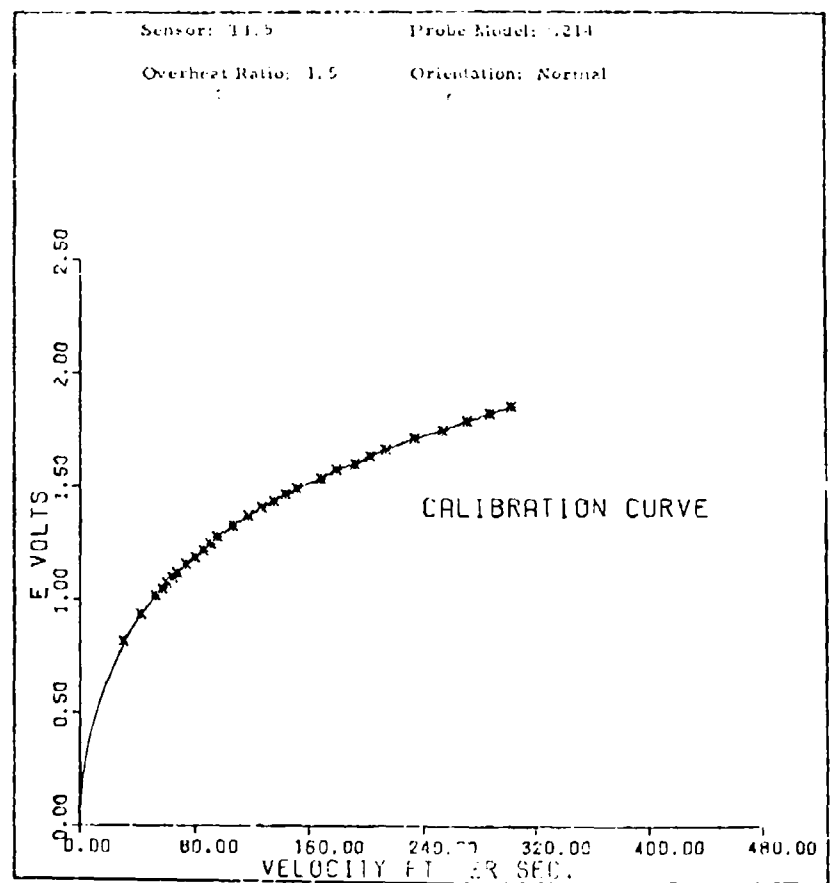


Fig. 47. Non Linear Bias - Output Variations With Velocity

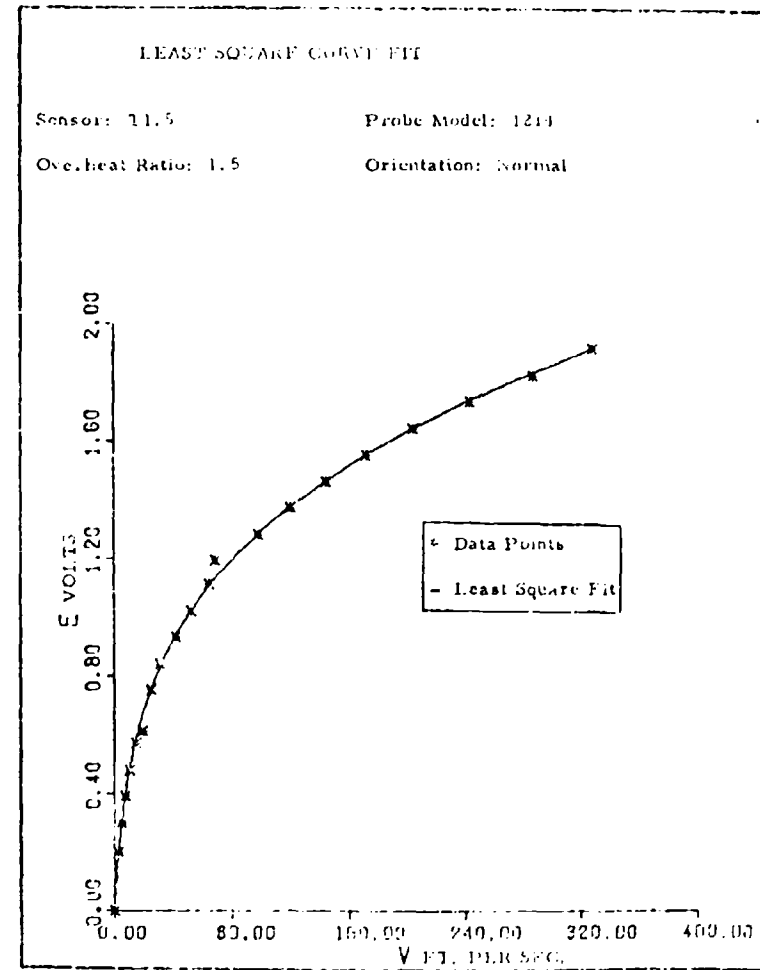


Fig. 48 Fourth Order Least Square Polynomial Curve Fit for Evaluation of Linearizer Coefficients

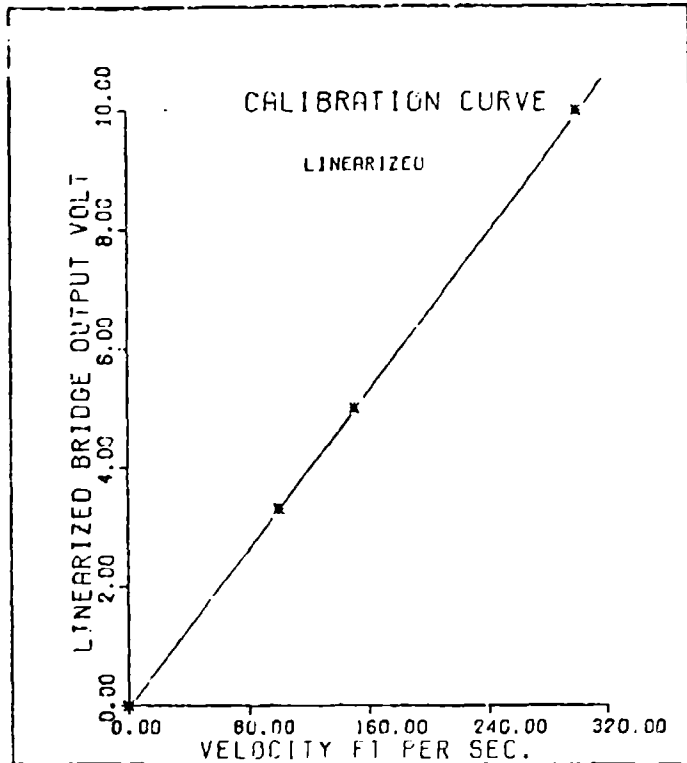


Fig. 49. Linearized Bridge Voltage Output for a  
0.00015 Inch (0.000381 cm) Dia. Hot Wire Sensor  
in Atmospheric Air

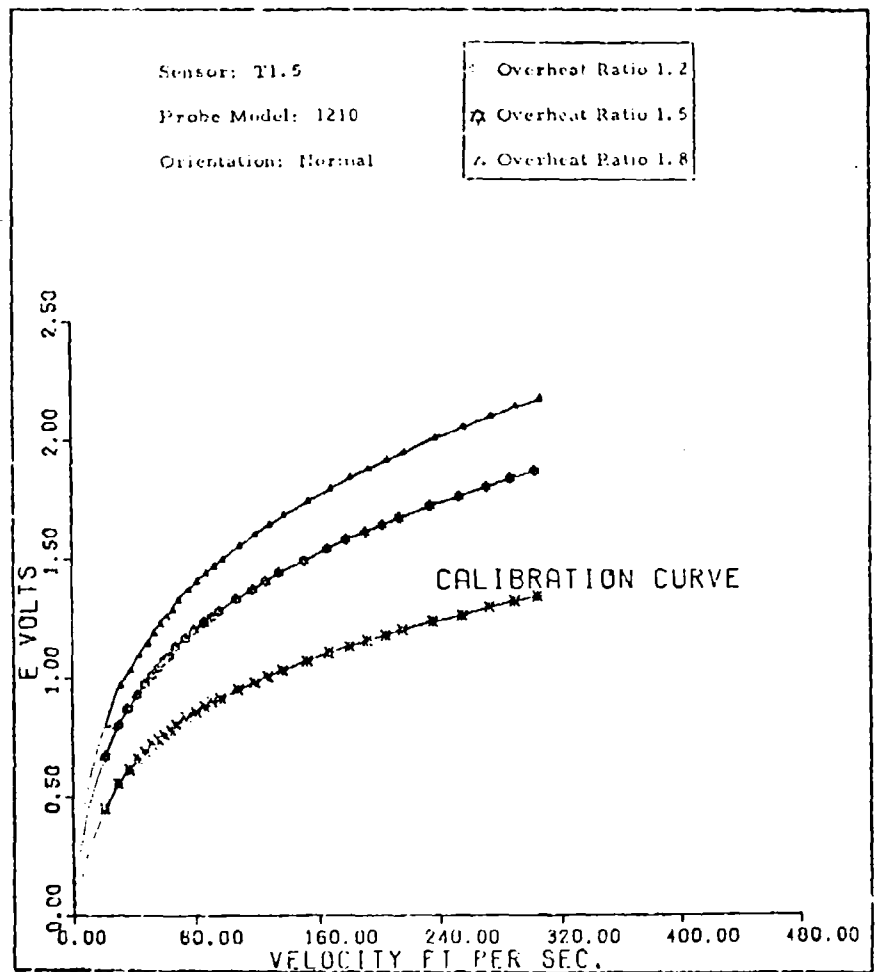


Fig. 50. Influence of Overheat Ratio on Non-Linear Sensor Response

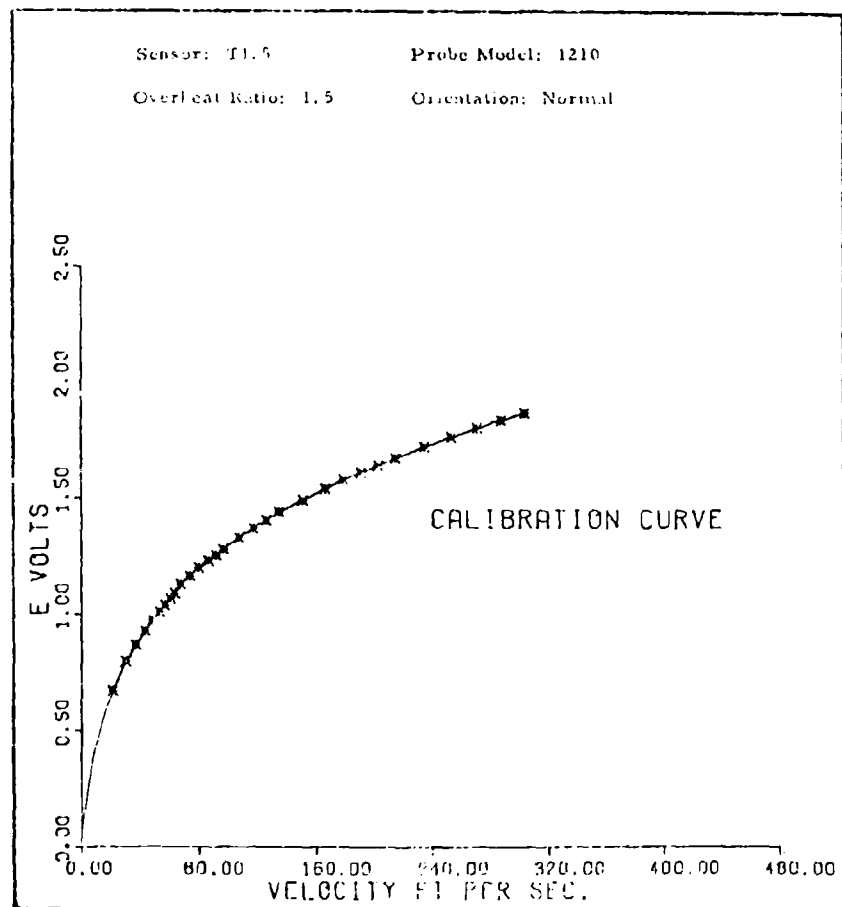


Fig. 51. Non Linear Bridge Output Variations With Velocity

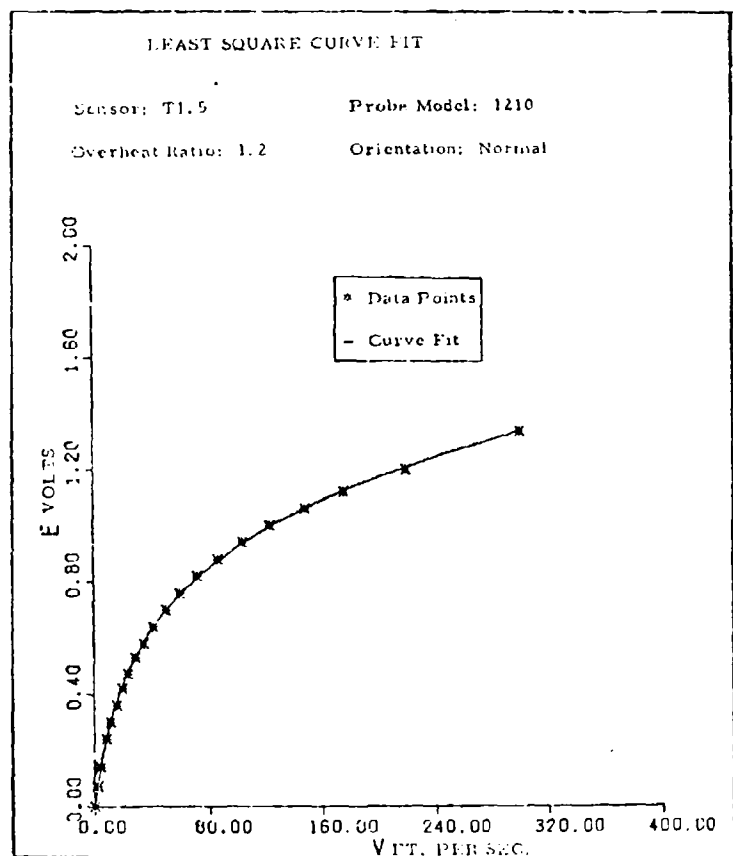


Fig. 52. Fourth Order Least Square Polynomial Curve Fit for Evaluation of Linearizer Coefficients

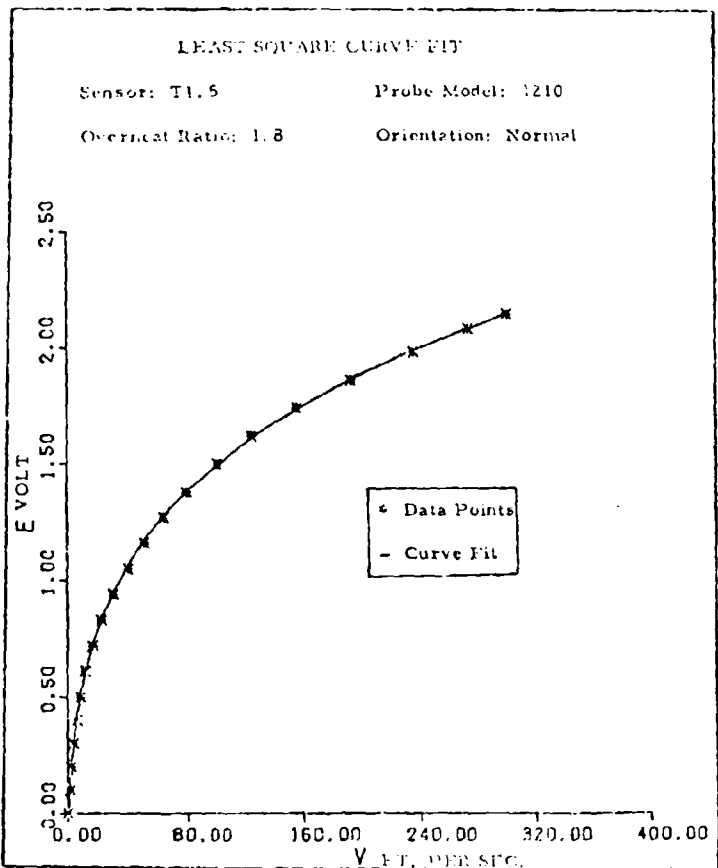


Fig. 53. Fourth Order Least Square Polynomial Curve Fit for Evaluation of Linearized Coefficients

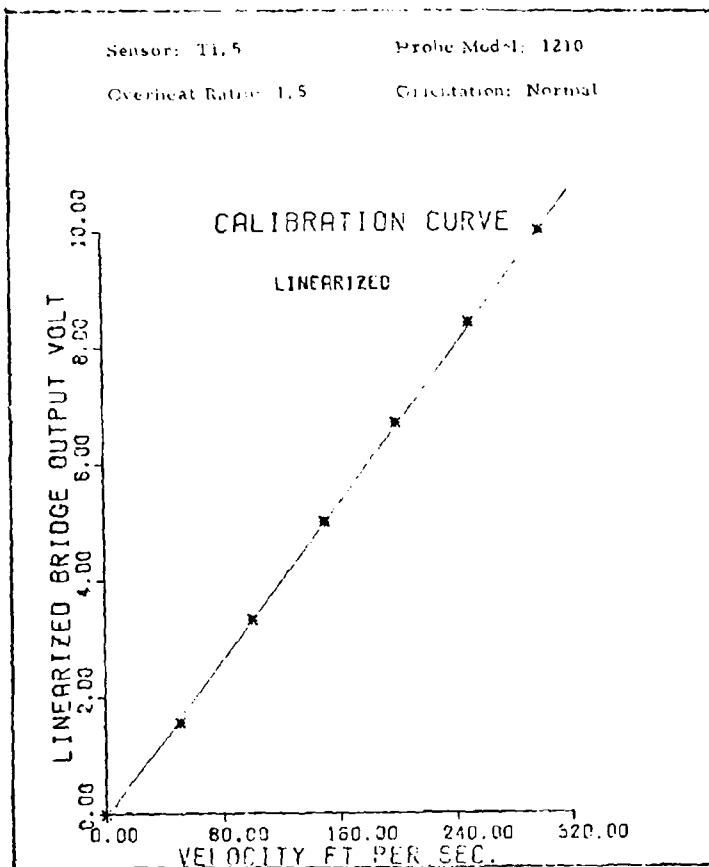


Fig. 95. Linearized Bridge Output for 3.0.00015 Inch (0.000381 cm)  
Dia. Hot Wire Sensor in Atmospheric Air

Sensor: T1.5                  Probe Model: 1210  
Overheat Ratio: 1.2                  Orientation: Normal

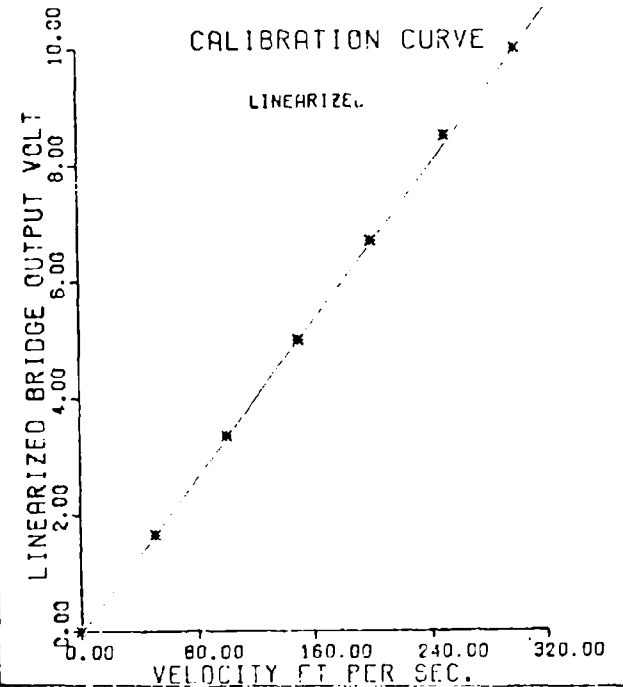


Fig. 56. Linearized Bridge Output for a 0.00015 Inch  
(0.000381 cm) Dia. Hot Wire Sensor in Atmospheric  
Air

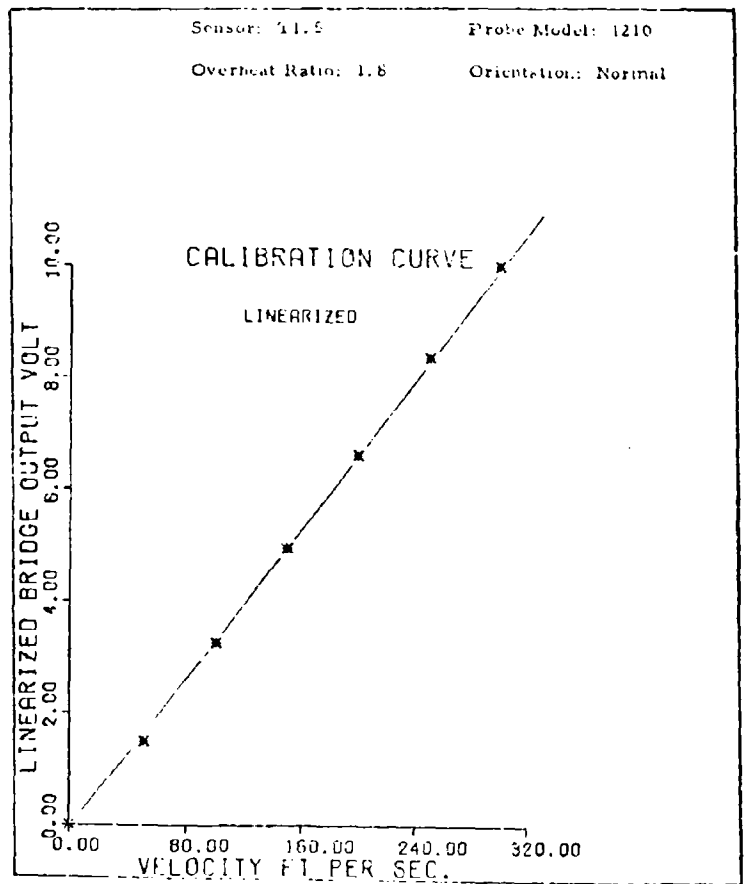


Fig. 57. Linearized Bridge Output for a 0.00015 inch Dia.  
(0.000381 cm) Hot Wire Sensor in Atmospheric Air.

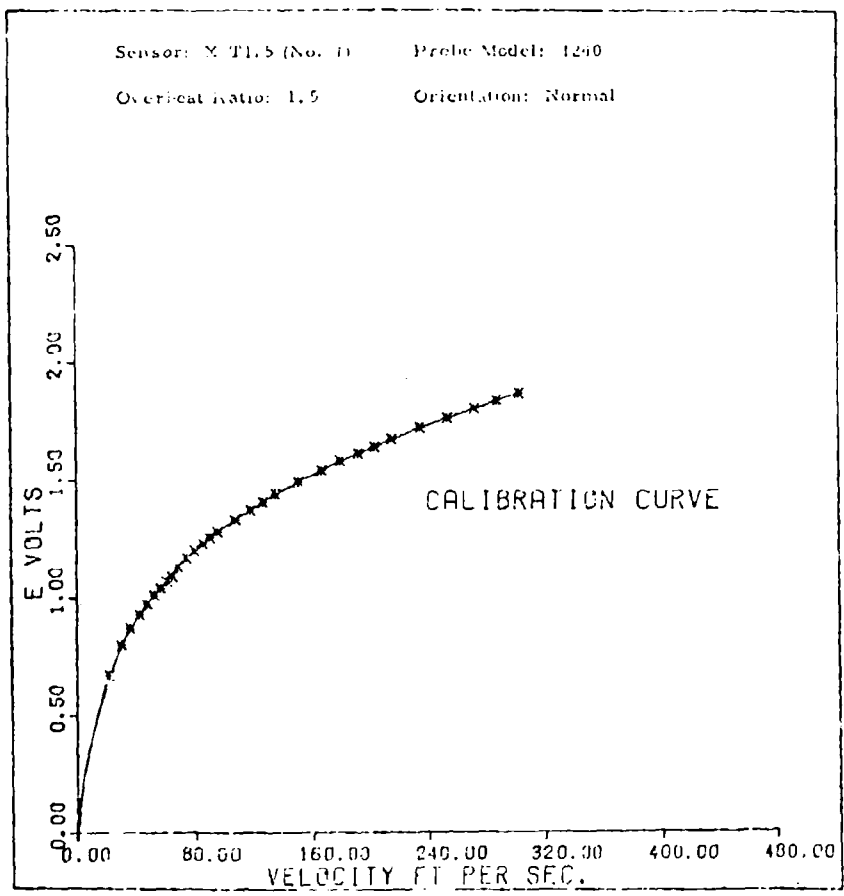


Fig. 59. Non Linear Bridge Output Variations With Velocity

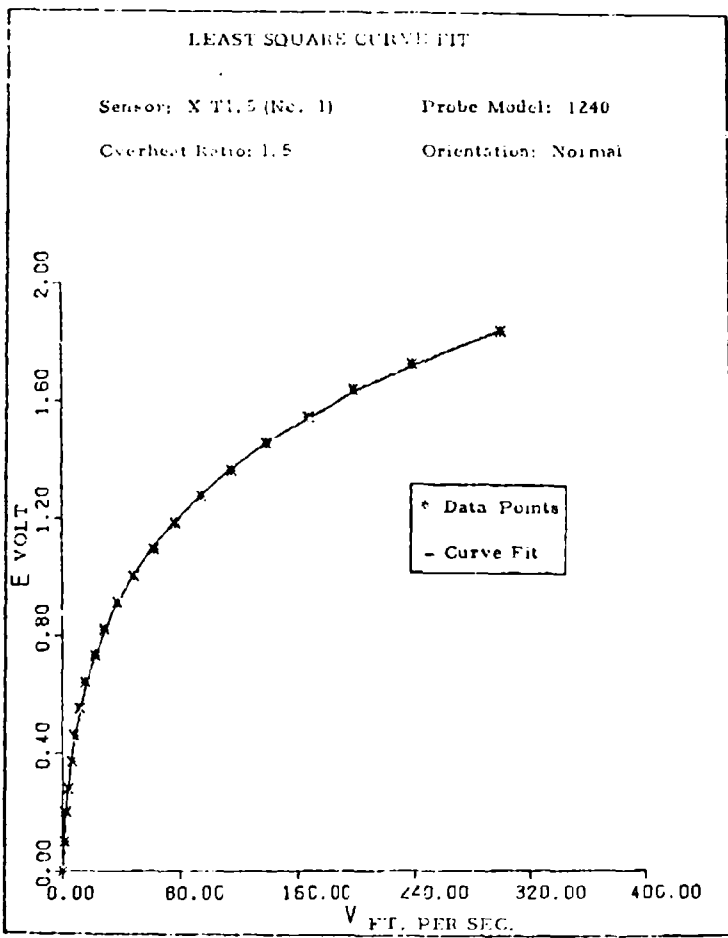


Fig. 59. Fourth Order Least Square Polynomial Curve Fit for Evaluation of Linearizer Coefficients

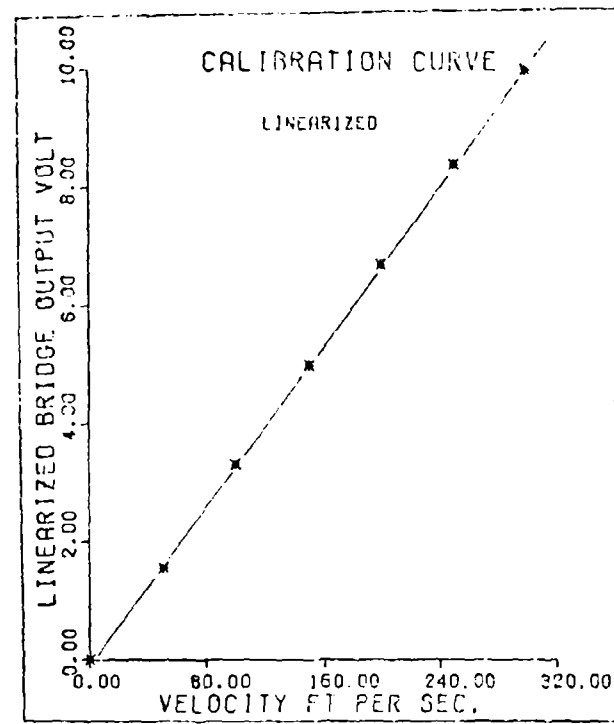


Fig. 60. Linearized Bridge Output for a 0.00015 Inch Dia.  
(0.000381 cm) Hot Wire Sensor in Atmospheric Air

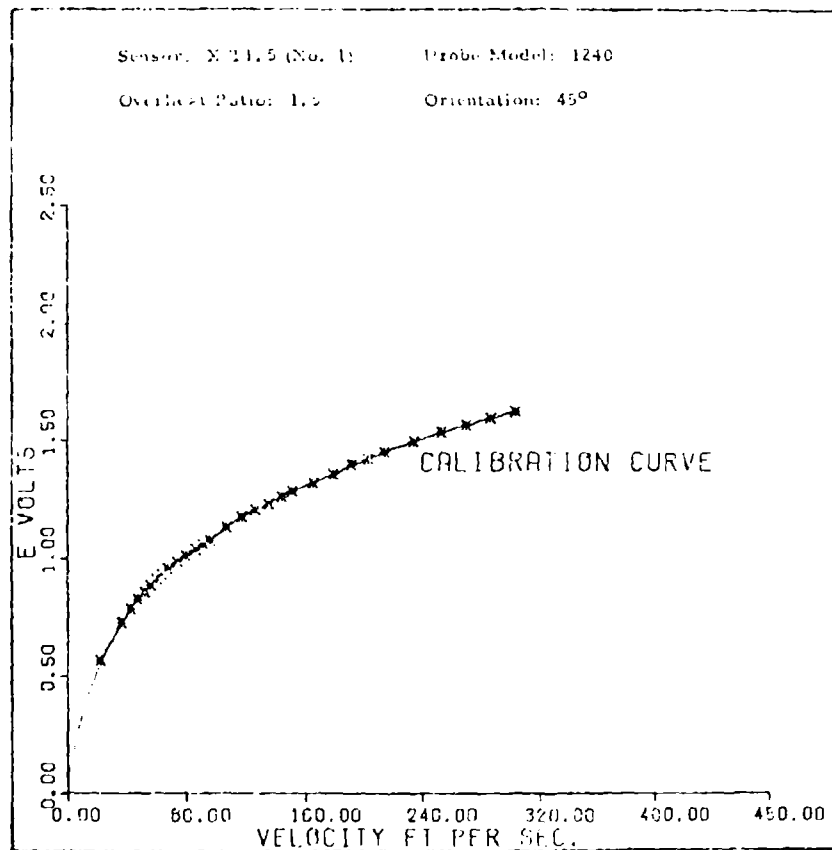


Fig. 61. Non Linear Bridge Output Variations With Velocity

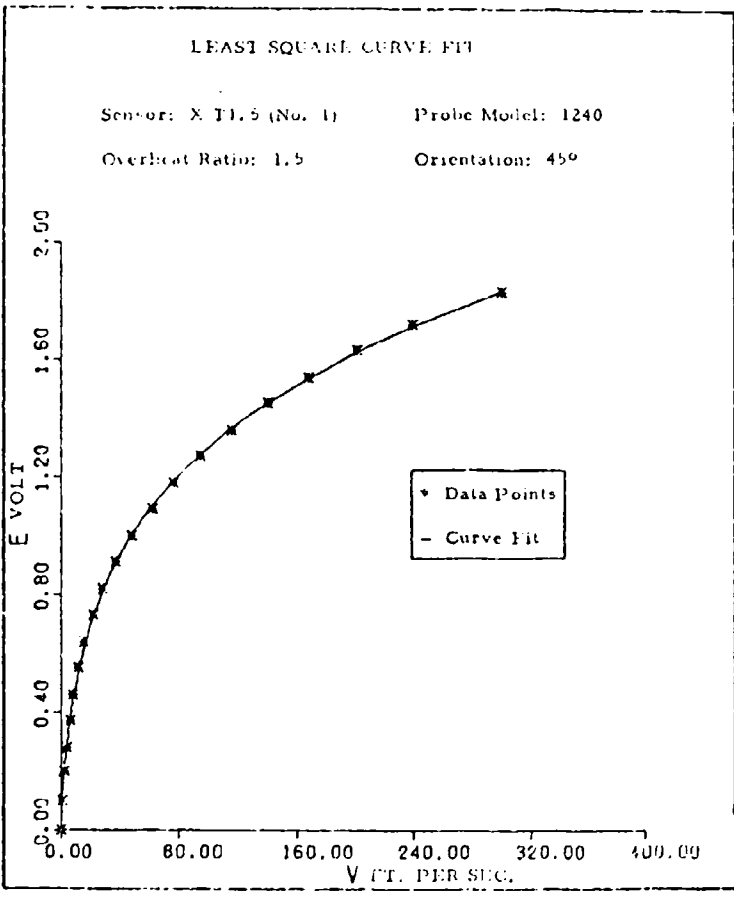


Fig. 62. Fourth Order Least Square Curve Fit for Evaluation of Linearizer Coefficients

Sensor: X 11.5 (No. 1)      Probe Model: 1240  
Overheat Ratio: 1.5      Orientation: 45°

CALIBRATION CURVE

LINARIZED

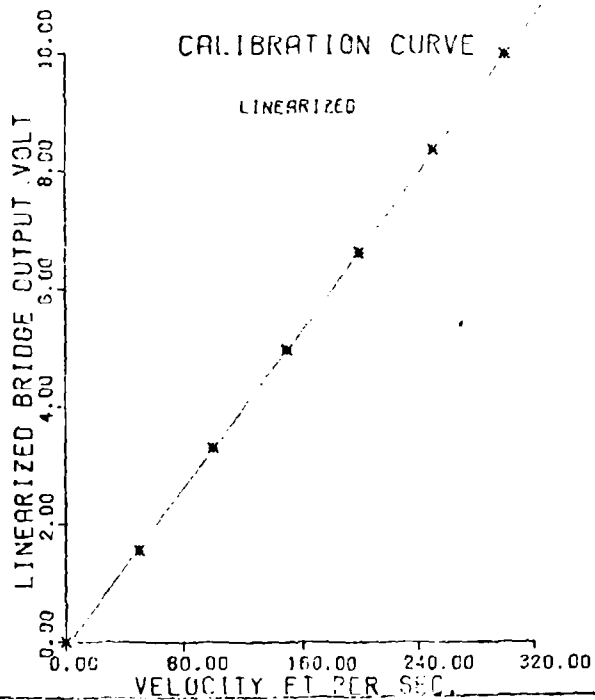


Fig. 63. Linearized Bridge Output for a 0.00015 inch Dia.  
(0.000381 cm) Hot Wire Sensor in Atmospheric Air

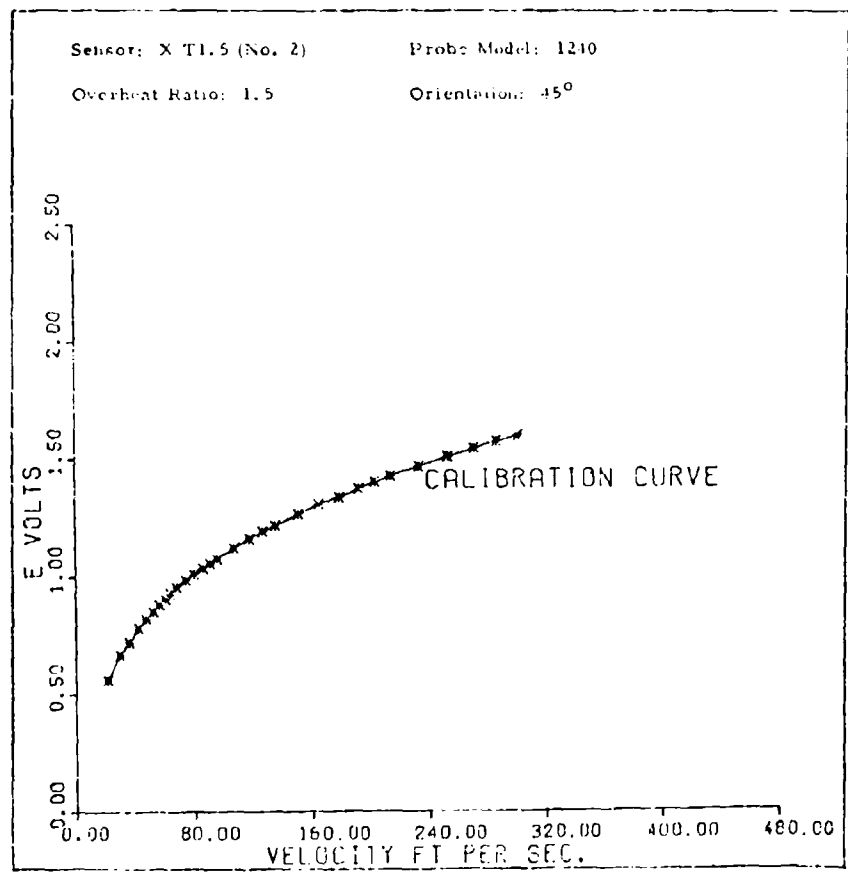


Fig. 64. Non Linear Bridge Output Variations With Velocity

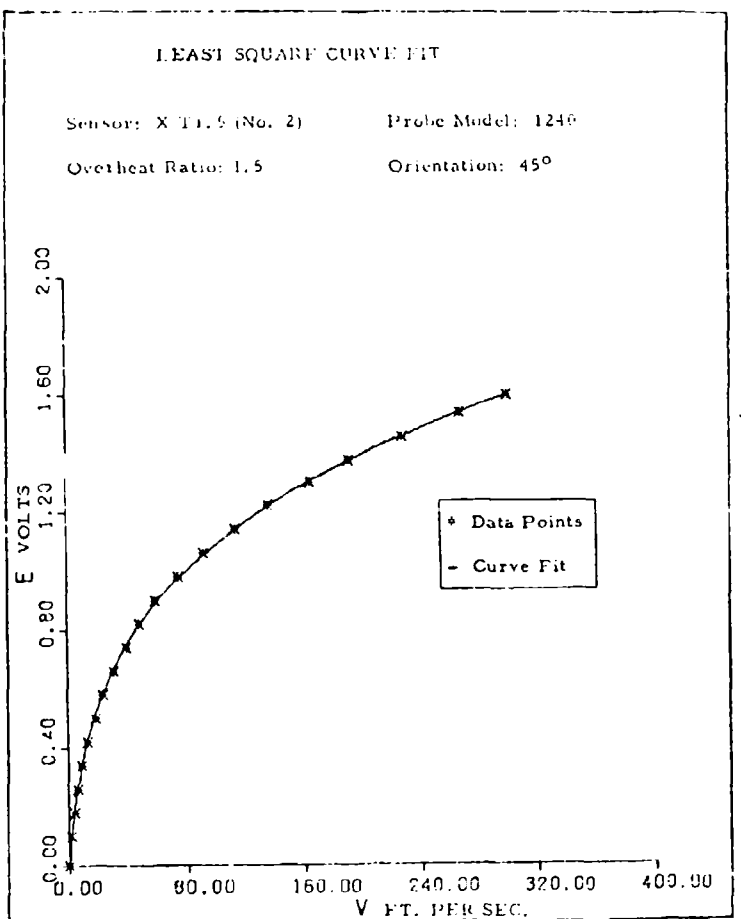


Fig. 65. Fourth Order Least Square Polynomial Curve Fit for Evaluation of Linearizer Coefficients

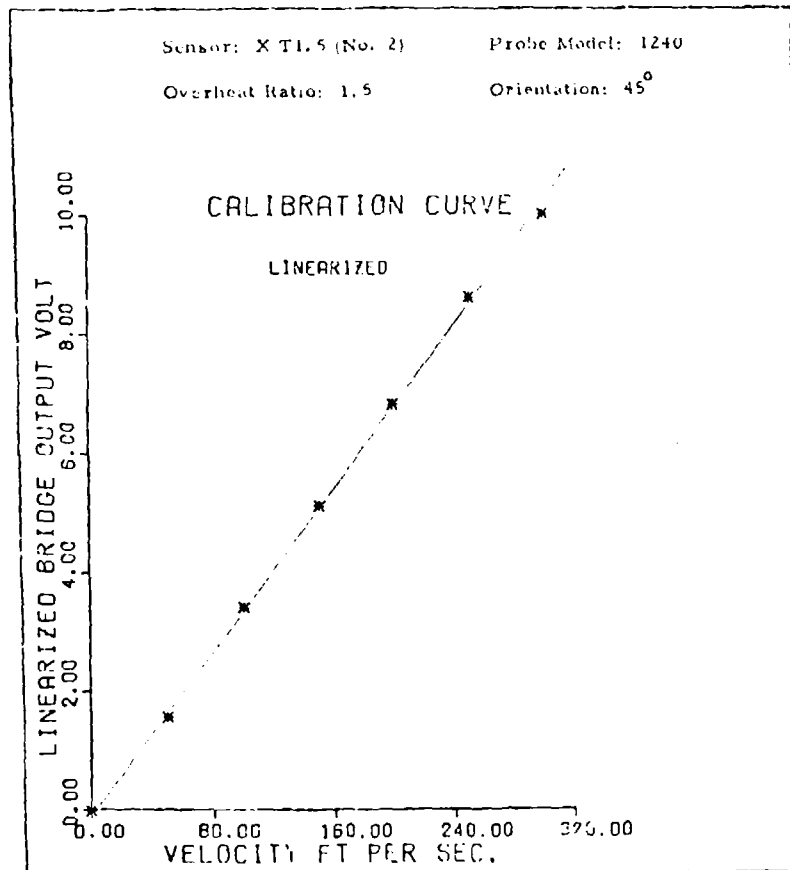


Fig. 66. Linearized Bridge Output for a 0.00015 Inch Dia. (0.000381 cm)  
Hot Wire Sensor in Atmospheric Air

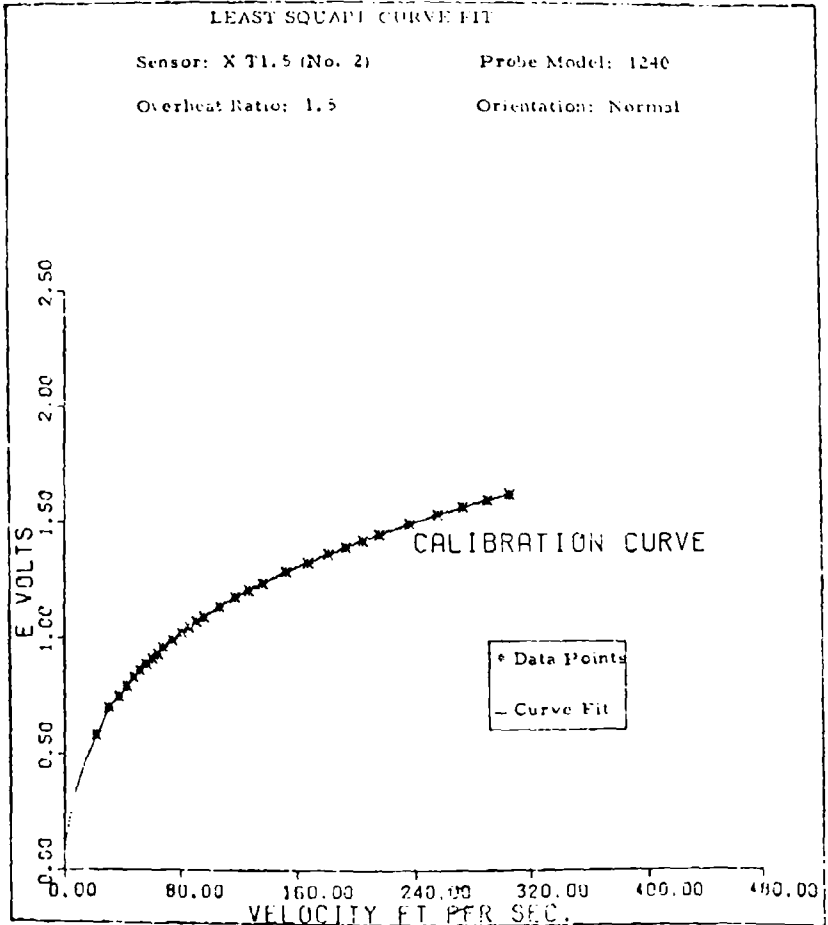


Fig. 67. Fourth Order Least Square Polynomial Curve Fit  
for Evaluation of Linearizer Coefficients

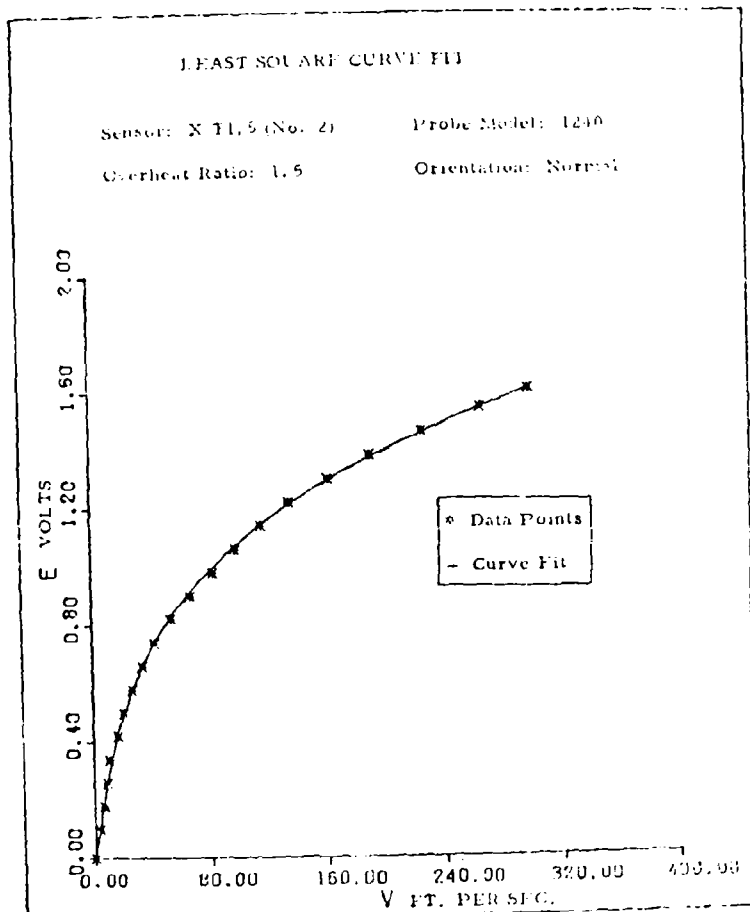


Fig. 68. Fourth Order Least Square Polynomial Curve Fit  
 for Evaluation of Linearizer Coefficients

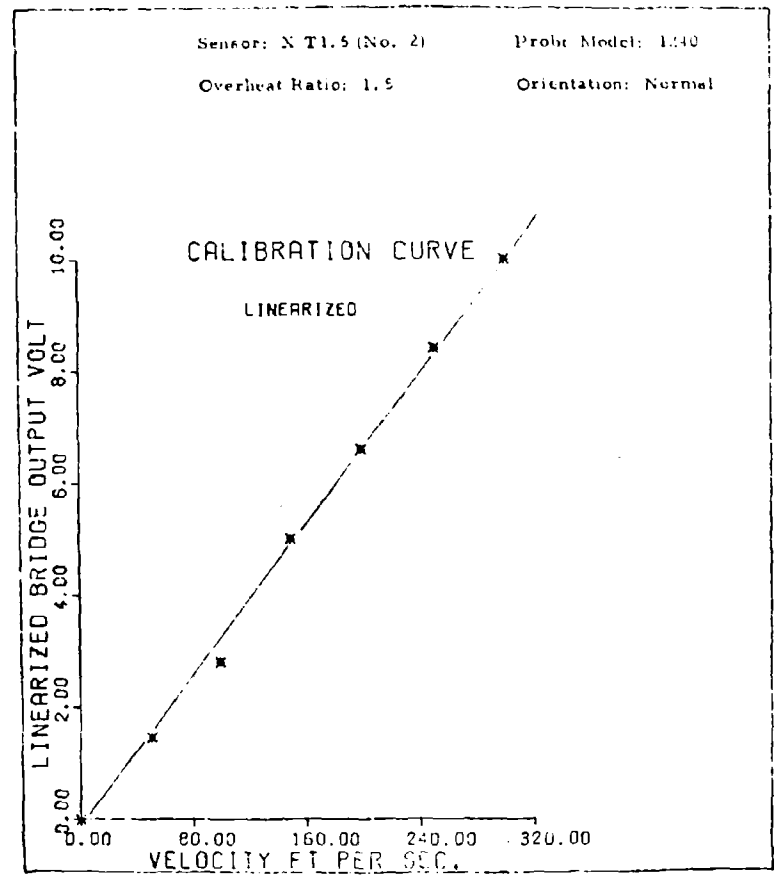


Fig. 49. Linearized Bridge Output for a 0.00015 Inch  
(0.000381 cm) Dia. Hot Wire Sensor in Atmospheric Air

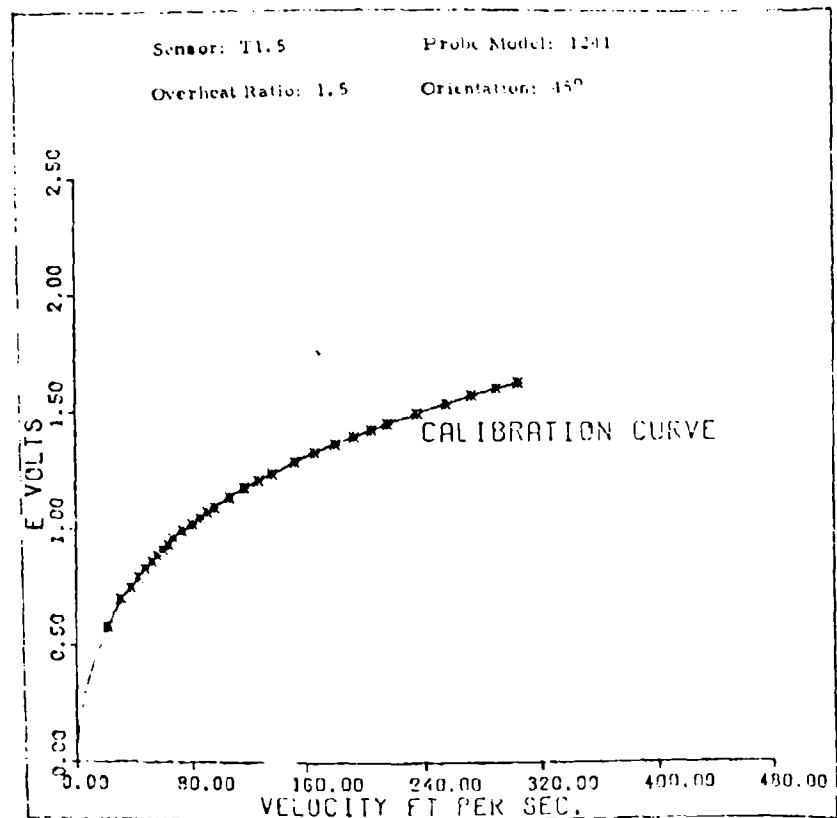


Fig. 70. Non Linear Bridge Output Variations with Velocity

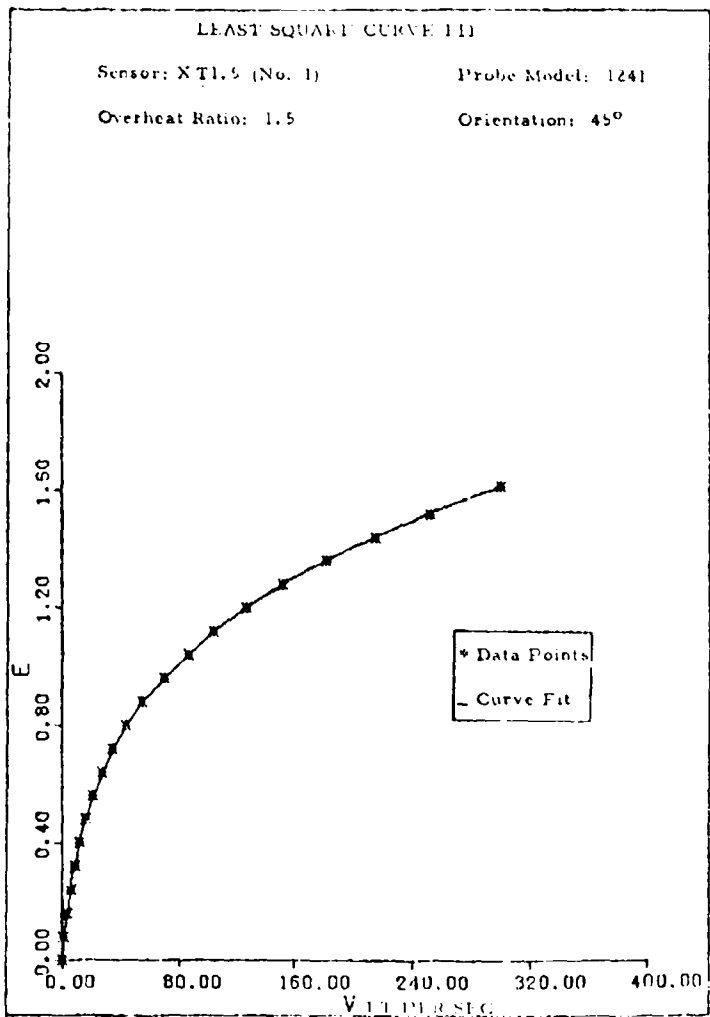


Fig. 7i. Fourth Order Least Square Polynomial Curve Fit  
 for Evaluation of Linearizer Coefficients

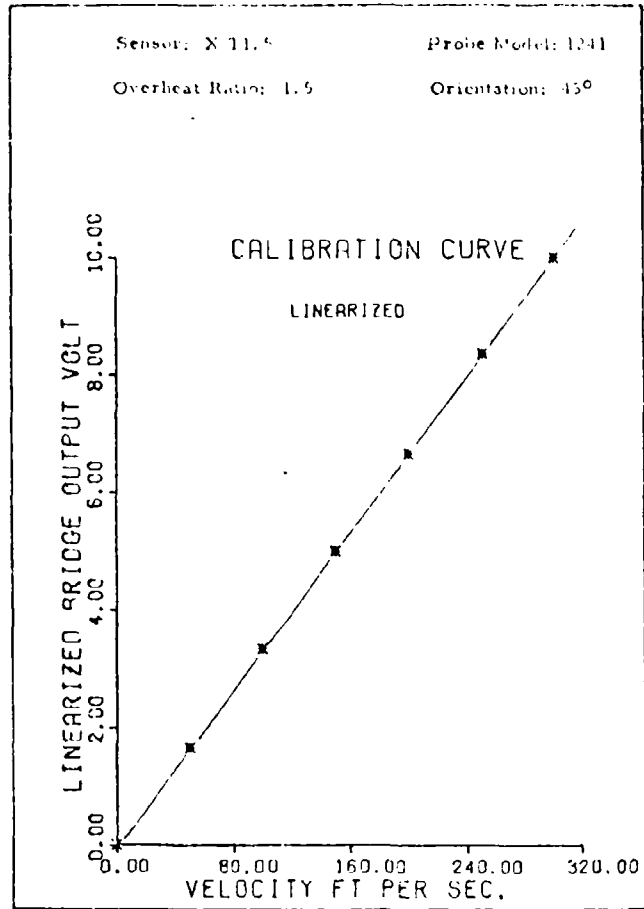


Fig. 72. Linearized Bridge Output for a 0.00015 Inch (0.000381 cm) Dia. Hot Wire Sensor in Atmospheric Air

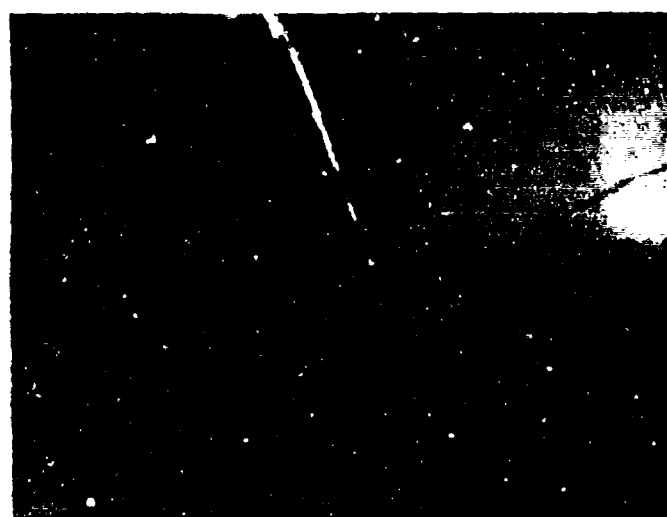


Fig. 7J. The Cross Wire Arrangement of  
Model 1240 Sensor Viewed Under  
Microscope (Magnification 50:1)

Appendix D

Computer Programs

# Best Available Copy

## Program for Evaluating Polynomial Coefficients

```
      SUBROUTINE EVALUATE(X,Y,N)
      DIMENSION X(10),Y(10)
      DATA N/10/
      DO 10 I=1,N
      Y(I)=X(I)
 10    CONTINUE
      CALL EVAL(X,Y,N)
      DO 20 I=1,N
      Y(I)=X(I)
 20    CONTINUE
      RETURN
      END
      SUBROUTINE EVAL(X,Y,N)
      DIMENSION X(10),Y(10)
      DATA N/10/
      DO 10 I=1,N
      Y(I)=X(I)
 10    CONTINUE
      DO 20 I=1,N
      DO 30 J=1,I
      Y(I)=Y(I)+X(J)
 30    CONTINUE
 20    CONTINUE
      RETURN
      END
```

```

12C76,24P055=INPUT,TAPES=1,2,3,4,5,6,7,8,9,10,11,12,13,14,15,16,17,18,19,20,21,22,23,24,25,26,27,28,29,30,31,32,33,34,35,36,37,38,39,40,41,42,43,44,45,46,47,48,49,50,51,52,53,54,55,56,57,58,59,60,61,62,63,64,65,66,67,68,69,70,71,72,73,74,75,76,77,78,79,80,81,82,83,84,85,86,87,88,89,90,91,92,93,94,95,96,97,98,99,100,101,102,103,104,105,106,107,108,109,110,111,112,113,114,115,116,117,118,119,120,121,122,123,124,125,126,127,128,129,130,131,132,133,134,135,136,137,138,139,140,141,142,143,144,145,146,147,148,149,150,151,152,153,154,155,156,157,158,159,160,161,162,163,164,165,166,167,168,169,170,171,172,173,174,175,176,177,178,179,180,181,182,183,184,185,186,187,188,189,190,191,192,193,194,195,196,197,198,199,200,201,202,203,204,205,206,207,208,209,210,211,212,213,214,215,216,217,218,219,220,221,222,223,224,225,226,227,228,229,230,231,232,233,234,235,236,237,238,239,240,241,242,243,244,245,246,247,248,249,250,251,252,253,254,255,256,257,258,259,260,261,262,263,264,265,266,267,268,269,270,271,272,273,274,275,276,277,278,279,280,281,282,283,284,285,286,287,288,289,290,291,292,293,294,295,296,297,298,299,299,300,301,302,303,304,305,306,307,308,309,309,310,311,312,313,314,315,316,317,318,319,319,320,321,322,323,324,325,326,327,328,329,329,330,331,332,333,334,335,336,337,338,339,339,340,341,342,343,344,345,346,347,348,349,349,350,351,352,353,354,355,356,357,358,359,359,360,361,362,363,364,365,366,367,368,369,369,370,371,372,373,374,375,376,377,378,379,379,380,381,382,383,384,385,386,387,388,389,389,390,391,392,393,394,395,396,397,398,399,399,400,401,402,403,404,405,406,407,408,409,409,410,411,412,413,414,415,416,417,418,419,419,420,421,422,423,424,425,426,427,428,429,429,430,431,432,433,434,435,436,437,438,439,439,440,441,442,443,444,445,446,447,448,449,449,450,451,452,453,454,455,456,457,458,459,459,460,461,462,463,464,465,466,467,468,469,469,470,471,472,473,474,475,476,477,478,479,479,480,481,482,483,484,485,486,487,488,489,489,490,491,492,493,494,495,496,497,498,499,499,500,501,502,503,504,505,506,507,508,509,509,510,511,512,513,514,515,516,517,518,519,519,520,521,522,523,524,525,526,527,528,529,529,530,531,532,533,534,535,536,537,538,539,539,540,541,542,543,544,545,546,547,548,549,549,550,551,552,553,554,555,556,557,558,559,559,560,561,562,563,564,565,566,567,568,569,569,570,571,572,573,574,575,576,577,578,579,579,580,581,582,583,584,585,586,587,588,589,589,590,591,592,593,594,595,596,597,598,599,599,600,601,602,603,604,605,606,607,608,609,609,610,611,612,613,614,615,616,617,618,619,619,620,621,622,623,624,625,626,627,628,629,629,630,631,632,633,634,635,636,637,638,639,639,640,641,642,643,644,645,646,647,648,649,649,650,651,652,653,654,655,656,657,658,659,659,660,661,662,663,664,665,666,667,668,669,669,670,671,672,673,674,675,676,677,678,679,679,680,681,682,683,684,685,686,687,688,689,689,690,691,692,693,694,695,696,697,698,699,699,700,701,702,703,704,705,706,707,708,709,709,710,711,712,713,714,715,716,717,718,719,719,720,721,722,723,724,725,726,727,728,729,729,730,731,732,733,734,735,736,737,738,739,739,740,741,742,743,744,745,746,747,748,749,749,750,751,752,753,754,755,756,757,758,759,759,760,761,762,763,764,765,766,767,768,769,769,770,771,772,773,774,775,776,777,778,779,779,780,781,782,783,784,785,786,787,788,789,789,790,791,792,793,794,795,796,797,798,799,799,800,801,802,803,804,805,806,807,808,809,809,810,811,812,813,814,815,816,817,818,819,819,820,821,822,823,824,825,826,827,828,829,829,830,831,832,833,834,835,836,837,838,839,839,840,841,842,843,844,845,846,847,848,849,849,850,851,852,853,854,855,856,857,858,859,859,860,861,862,863,864,865,866,867,868,869,869,870,871,872,873,874,875,876,877,878,879,879,880,881,882,883,884,885,886,887,888,889,889,890,891,892,893,894,895,896,897,898,899,899,900,901,902,903,904,905,906,907,908,909,909,910,911,912,913,914,915,916,917,918,919,919,920,921,922,923,924,925,926,927,928,929,929,930,931,932,933,934,935,936,937,938,939,939,940,941,942,943,944,945,946,947,948,949,949,950,951,952,953,954,955,956,957,958,959,959,960,961,962,963,964,965,966,967,968,969,969,970,971,972,973,974,975,976,977,978,979,979,980,981,982,983,984,985,986,987,988,989,989,990,991,992,993,994,995,996,997,998,999,999,1000,1001,1002,1003,1004,1005,1006,1007,1008,1009,1009,1010,1011,1012,1013,1014,1015,1016,1017,1018,1019,1019,1020,1021,1022,1023,1024,1025,1026,1027,1028,1029,1029,1030,1031,1032,1033,1034,1035,1036,1037,1038,1039,1039,1040,1041,1042,1043,1044,1045,1046,1047,1048,1049,1049,1050,1051,1052,1053,1054,1055,1056,1057,1058,1059,1059,1060,1061,1062,1063,1064,1065,1066,1067,1068,1069,1069,1070,1071,1072,1073,1074,1075,1076,1077,1078,1079,1079,1080,1081,1082,1083,1084,1085,1086,1087,1088,1089,1089,1090,1091,1092,1093,1094,1095,1096,1097,1098,1099,1099,1100,1101,1102,1103,1104,1105,1106,1107,1108,1109,1109,1110,1111,1112,1113,1114,1115,1116,1117,1118,1119,1119,1120,1121,1122,1123,1124,1125,1126,1127,1128,1129,1129,1130,1131,1132,1133,1134,1135,1136,1137,1138,1139,1139,1140,1141,1142,1143,1144,1145,1146,1147,1148,1149,1149,1150,1151,1152,1153,1154,1155,1156,1157,1158,1159,1159,1160,1161,1162,1163,1164,1165,1166,1167,1168,1169,1169,1170,1171,1172,1173,1174,1175,1176,1177,1178,1179,1179,1180,1181,1182,1183,1184,1185,1186,1187,1188,1189,1189,1190,1191,1192,1193,1194,1195,1196,1197,1198,1198,1199,1200,1201,1202,1203,1204,1205,1206,1207,1208,1209,1209,1210,1211,1212,1213,1214,1215,1216,1217,1218,1219,1219,1220,1221,1222,1223,1224,1225,1226,1227,1228,1229,1229,1230,1231,1232,1233,1234,1235,1236,1237,1238,1239,1239,1240,1241,1242,1243,1244,1245,1246,1247,1248,1249,1249,1250,1251,1252,1253,1254,1255,1256,1257,1258,1259,1259,1260,1261,1262,1263,1264,1265,1266,1267,1268,1269,1269,1270,1271,1272,1273,1274,1275,1276,1277,1278,1279,1279,1280,1281,1282,1283,1284,1285,1286,1287,1288,1289,1289,1290,1291,1292,1293,1294,1295,1296,1297,1298,1298,1299,1300,1301,1302,1303,1304,1305,1306,1307,1308,1309,1309,1310,1311,1312,1313,1314,1315,1316,1317,1318,1319,1319,1320,1321,1322,1323,1324,1325,1326,1327,1328,1329,1329,1330,1331,1332,1333,1334,1335,1336,1337,1338,1339,1339,1340,1341,1342,1343,1344,1345,1346,1347,1348,1349,1349,1350,1351,1352,1353,1354,1355,1356,1357,1358,1359,1359,1360,1361,1362,1363,1364,1365,1366,1367,1368,1369,1369,1370,1371,1372,1373,1374,1375,1376,1377,1378,1379,1379,1380,1381,1382,1383,1384,1385,1386,1387,1388,1389,1389,1390,1391,1392,1393,1394,1395,1396,1397,1398,1398,1399,1400,1401,1402,1403,1404,1405,1406,1407,1408,1409,1409,1410,1411,1412,1413,1414,1415,1416,1417,1418,1419,1419,1420,1421,1422,1423,1424,1425,1426,1427,1428,1429,1429,1430,1431,1432,1433,1434,1435,1436,1437,1438,1439,1439,1440,1441,1442,1443,1444,1445,1446,1447,1448,1449,1449,1450,1451,1452,1453,1454,1455,1456,1457,1458,1459,1459,1460,1461,1462,1463,1464,1465,1466,1467,1468,1469,1469,1470,1471,1472,1473,1474,1475,1476,1477,1478,1479,1479,1480,1481,1482,1483,1484,1485,1486,1487,1488,1489,1489,1490,1491,1492,1493,1494,1495,1496,1497,1498,1498,1499,1500,1501,1502,1503,1504,1505,1506,1507,1508,1509,1509,1510,1511,1512,1513,1514,1515,1516,1517,1518,1519,1519,1520,1521,1522,1523,1524,1525,1526,1527,1528,1529,1529,1530,1531,1532,1533,1534,1535,1536,1537,1538,1539,1539,1540,1541,1542,1543,1544,1545,1546,1547,1548,1549,1549,1550,1551,1552,1553,1554,1555,1556,1557,1558,1559,1559,1560,1561,1562,1563,1564,1565,1566,1567,1568,1569,1569,1570,1571,1572,1573,1574,1575,1576,1577,1578,1579,1579,1580,1581,1582,1583,1584,1585,1586,1587,1588,1589,1589,1590,1591,1592,1593,1594,1595,1596,1597,1598,1598,1599,1600,1601,1602,1603,1604,1605,1606,1607,1608,1609,1609,1610,1611,1612,1613,1614,1615,1616,1617,1618,1619,1619,1620,1621,1622,1623,1624,1625,1626,1627,1628,1629,1629,1630,1631,1632,1633,1634,1635,1636,1637,1638,1639,1639,1640,1641,1642,1643,1644,1645,1646,1647,1648,1649,1649,1650,1651,1652,1653,1654,1655,1656,1657,1658,1659,1659,1660,1661,1662,1663,1664,1665,1666,1667,1668,1669,1669,1670,1671,1672,1673,1674,1675,1676,1677,1678,1679,1679,1680,1681,1682,1683,1684,1685,1686,1687,1688,1689,1689,1690,1691,1692,1693,1694,1695,1696,1697,1698,1698,1699,1700,1701,1702,1703,1704,1705,1706,1707,1708,1709,1709,1710,1711,1712,1713,1714,1715,1716,1717,1718,1719,1719,1720,1721,1722,1723,1724,1725,1726,1727,1728,1729,1729,1730,1731,1732,1733,1734,1735,1736,1737,1738,1739,1739,1740,1741,1742,1743,1744,1745,1746,1747,1748,1749,1749,1750,1751,1752,1753,1754,1755,1756,1757,1758,1759,1759,1760,1761,1762,1763,1764,1765,1766,1767,1768,1769,1769,1770,1771,1772,1773,1774,1775,1776,1777,1778,1779,1779,1780,1781,1782,1783,1784,1785,1786,1787,1788,1789,1789,1790,1791,1792,1793,1794,1795,1796,1797,1798,1798,1799,1800,1801,1802,1803,1804,1805,1806,1807,1808,1809,1809,1810,1811,1812,1813,1814,1815,1816,1817,1818,1819,1819,1820,1821,1822,1823,1824,1825,1826,1827,1828,1829,1829,1830,1831,1832,1833,1834,1835,1836,1837,1838,1839,1839,1840,1841,1842,1843,1844,1845,1846,1847,1848,1849,1849,1850,1851,1852,1853,1854,1855,1856,1857,1858,1859,1859,1860,1861,1862,1863,1864,1865,1866,1867,1868,1869,1869,1870,1871,1872,1873,1874,1875,1876,1877,1878,1879,1879,1880,1881,1882,1883,1884,1885,1886,1887,1888,1889,1889,1890,1891,1892,1893,1894,1895,1896,1897,1898,1898,1899,1900,1901,1902,1903,1904,1905,1906,1907,1908,1909,1909,1910,1911,1912,1913,1914,1915,1916,1917,1918,1919,1919,1920,1921,1922,1923,1924,1925,1926,1927,1928,1929,1929,1930,1931,1932,1933,1934,1935,1936,1937,1938,1939,1939,1940,1941,1942,1943,1944,1945,1946,1947,1948,1949,1949,1950,1951,1952,1953,1954,1955,1956,1957,1958,1959,1959,1960,1961,1962,1963,1964,1965,1966,1967,1968,1969,1969,1970,1971,1972,1973,1974,1975,1976,1977,1978,1979,1979,1980,1981,1982,1983,1984,1985,1986,1987,1988,1989,1989,1990,1991,1992,1993,1994,1995,1996,1997,1998,1998,1999,2000,2001,2002,2003,2004,2005,2006,2007,2008,2009,2009,2010,2011,2012,2013,2014,2015,2016,2017,2018,2019,2019,2020,2021,2022,2023,2024,2025,2026,2027,2028,2029,2029,2030,2031,2032,2033,2034,2035,2036,2037,2038,2039,2039,2040,2041,2042,2043,2044,2045,2046,2047,2048,2049,2049,2050,2051,2052,2053,2054,2055,2056,2057,2058,2059,2059,2060,2061,2062,2063,2064,2065,2066,2067,2068,2069,2069,2070,2071,2072,2073,2074,2075,2076,2077,2078,2079,2079,2080,2081,2082,2083,2084,2085,2086,2087,2088,2089,2089,2090,2091,2092,2093,2094,2095,2096,2097,2098,2098,2099,2100,2101,2102,2103,2104,2105,2106,2107,2108,2109,2109,2110,2111,2112,2113,2114,2115,2116,2117,2118,2119,2119,2120,2121,2122,2123,2124,2125,2126,2127,2128,2129,2129,2130,2131,2132,2133,2134,2135,2136,2137,2138,2139,2139,2140,2141,2142,2143,2144,2145,2146,2147,2148,2149,2149,
```

```

V(T) = C(B)
DO 1 J=1,4
1   V(T) = T**2 + V(T) + C(L)
      CALL PLOT(V,T)
      V1=Y(HQ)
      CALL PLOT((5/2,1/2,0),V1,1/4,1/4)
      CALL SCAL(V,1,-1/2)
      CALL SCAL(V,1/2,1/2)
      CALL SCAL(V,1,1)
      X(2,2)=(-1,0)
      X(2,3)=(0,1)
      Y(2,2)=V(1,1)
      Y(2,3)=V(1,2)
      CALL ATYS(Y(1,1),Y(1,2),0.0,1.4,V)
      CALL ATYS(Y(2,1),Y(2,2),0.0,1.4,V)
      CALL LINP(V,X,21,1,1)
      CALL PLOT(V)
      STOP
      END

```

## Program for Fourth Order Least Square Curve Fit to the Data Points

Vita

Flight Lieutenant Kauser was born on 15 November 1943 at Multan, Pakistan. He graduated from Emerson College, Multan in 1961. In 1962, he joined Loughborough University of Technology, Loughborough, U.K. from where he obtained his Bachelor Degree in Aeronautical Engineering with Honours in 1966. He joined Pakistan Air Force in 1966 and was assigned to Pakistan Air Force College of Aeronautical Engineering (P.A.F. C.A.E.). After teaching at the school for nine years, he was selected to go to the United States to do M.S. in Aeronautical Engineering from the Air Force Institute of Technology and entered the Graduate Aeronautical Engineering program in June, 1975.

Permanent address: PAF Base Korangi Creek  
Karachi-20 Pakistan

This thesis was typed by Mrs. Joyce Clark.

## UNCLASSIFIED

SECURITY CLASSIFICATION OF THIS PAGE (When Data Entered)

REPORT DOCUMENTATION PAGE		READ INSTRUCTIONS BEFORE COMPLETING FORM
1. REPORT NUMBER <u>14 GAE/AE/76D-4</u>	2. GOVT ACCESSION NO. <u>(6)</u>	3. RECIPIENT'S CATALOG NUMBER
4. TITLE (and Subtitle) <u>PERFORMANCE AND EVALUATION OF AN X HOT WIRE SENSOR IN A TWO DIMENSIONAL FREE JET IN THE PRESENCE OF CROSS FLOW COMPONENT.</u>		5. TYPE OF REPORT & PERIOD COVERED MS Thesis
7. AUTHOR(s) <u>Fazal B. Kauser</u> Flight Lieutenant, PAF		6. PERFORMING ORG. REPORT NUMBER <u>(9) Master's thesis</u>
9. PERFORMING ORGANIZATION NAME AND ADDRESS <u>Air Force Institute of Technology (AFIT-EN) Wright-Patterson AFB, Ohio 45433</u>		10. PROGRAM ELEMENT, PROJECT, TASK AREA & WORK UNIT NUMBERS
11. CONTROLLING OFFICE NAME AND ADDRESS		12. REPORT DATE <u>11 December 1976</u>
14. MONITORING AGENCY NAME & ADDRESS (if different from Controlling Office)		13. NUMBER OF PAGES <u>187 (12)2126</u>
		15. SECURITY CLASS. (of this report) UNCLASSIFIED
		15a. DECLASSIFICATION/DOWNGRADING SCHEDULE
16. DISTRIBUTION STATEMENT (of this Report)  Approved for public release; distribution unlimited.		
17. DISTRIBUTION STATEMENT (of the abstract entered in Block 20, if different from Report)		
18. SUPPLEMENTARY NOTES  <u>Approved for public release; IAW AFR 190-17</u>  <u>JERRAL F. GUESS, Captain, USAF</u> <u>Director of Information</u>		
19. KEY WORDS (Continue on reverse side if necessary and identify by block number)  Anemometer Hot Wire X Sensor		
20. ABSTRACT (Continue on reverse side if necessary and identify by block number)  This thesis reports the results of an experimental investigation of rotation tests conducted with two X wire sensor arrangements in the potential core of a free jet and the influence of small temperature variations on the linearized response of a hot wire sensor. The tests were performed in the free jet issuing from a 10 cm x 1 cm nozzle having turbulence intensity of 0.3 per cent at the exit plane. The two X wire sensors used were TSI Model 1240 and TSI Model 1214. Each sensor arrangement consisted of two platinum coated,		

12-225

UNCLASSIFIED

SECURITY CLASSIFICATION OF THIS PAGE(When Data Entered)

tungsten wires, having 3.81 micron diameter, active sensor length 1.25 mm millimeter and separated by 1 millimeter apart. The X sensor Model 1240 was yawed and pitched through  $\pm 30$  degrees and  $\pm 10$  degrees respectively. The size of the potential core, however, limited the movement in yaw and pitch of the Model 1241 to  $\pm 10$  degrees. The tests were conducted at three values of Reynolds Number 7.2, 14.54 and 21.8 based upon the wire diameter. The investigation showed that both the X sensors had a strong preference for the direction of mean motion, and the error due to misalignment in yaw was largest at very small misalignment angles. The Model 1240 showed insensitivity to misalignment in pitch in the upper range of Reynolds Number but the Model 1241 was highly sensitive to the misalignment in pitch. In the second part of the study, the air temperature was increased from  $4^{\circ}\text{F}$  to  $20^{\circ}\text{F}$  above the reference and its influence on the linearized response of the upstream sensor of Model 1240 was observed. The test results showed a strong influence of the variations in air temperature on the linearized sensor response at velocities below approximately 100 feet per second.

3971 313

UNCLASSIFIED

SECURITY CLASSIFICATION OF THIS PAGE(When Data Entered)